PONTIFICIA UNIVERSIDAD CATÓLICA DE CHILE

SCHOOL OF ENGINEERING

CRUSTAL FAULTS IN THE CHILEAN ANDES: SEISMOTECTONIC CONSTRAINTS FROM A COMBINED GEOLOGICAL AND GEOPHYSICAL APPROACH.

ISABEL V. SANTIBÁÑEZ BORIĆ

Thesis submitted to the Office of Graduate Studies in partial fulfillment of the requirements for the Degree of Doctor of Engineering Sciences

Advisor:

JOSÉ CEMBRANO P.

Santiago de Chile (Sept. 2019)

PONTIFICIA UNIVERSIDAD CATÓLICA DE CHILE

SCHOOL OF ENGINEEERING

CRUSTAL FAULTS IN THE CHILEAN ANDES: SEISMOTECTONIC CONSTRAINTS FROM A COMBINED GEOLOGICAL AND GEOPHYSICAL APPROACH.

ISABEL VERÓNICA SANTIBÁÑEZ BORIĆ

Members of the Committee

JOSÉ CEMBRANO

GONZALO YÁÑEZ

GABRIEL GONZÁLEZ

RAFAEL RIDDELL

CARLOS COSTA

GUSTAVO LAGOS

Thesis submitted to the Office of Graduate Studies in partial fulfillment of the requirements for the Degree of Doctor in Engineering Sciences

Santiago de Chile, September 2019

The human understanding is no dry light, but receives an infusion from the will and affections; whence proceed sciences which may be called “sciences as one would.” For what a man had rather were true he more readily believes. Therefore he rejects difficult things from impatience of research; sober things, because they narrow hope; the deeper things of nature, from superstition; the light of experience, from arrogance and pride, lest his mind should seem to be occupied with things mean and transitory; things not commonly believed, out of deference to the opinion of the vulgar. Numberless in short are the ways, and sometimes imperceptible, in which the affections colour and infect the understanding.

Francis Bacon, Novum Organon (1620)

A mis amados hijos Seba y Emi, fuentes inagotables de inspiración y cambio

ACKNOWLEDGEMENTS

Esta Tesis es el resultado de un largo trabajo desarrollado gracias al apoyo de muchas personas, amigos y científicos, y diversos proyectos e instituciones. A todos ellos les debo agradecimiento incalculable por confiar en mí y en que este propósito y deseo fuese logrado.

La Comisión Nacional de Ciencia y Tecnología (CONICYT) a través de la Beca de Doctorado Nacional, el Proyecto FONDECYT Regular 1140846, el Proyecto FONDEF +Andes D10I1027, el Proyecto FONDAP CEGA 15090013, y el Proyecto FONDAP CIGIDEN 15110017 financiaron directa e indirectamente esta Tesis, además de ser la plataforma para reunir a destacados geólogos e ingenieros. El proyecto SARA-GEM fue un pilar fundamental en el desarrollo de la metodología y la posibilidad de aprender de científicos relevantes a nivel mundial en la temática.

El científico que me apoyó y entusiasmó a seguir este doctorado, fue mi profesor supervisor José Cembrano. Su pasión por la enseñanza de la ciencia y sus desafíos éticos, han sido una sorpresa y un tremendo regalo de este camino. Esta aventura comenzó a poco de que formaran el grupo de Geociencias de la Pontificia Universidad Católica junto a los profesores Gloria Arancibia y Gonzalo Yáñez, al que se integraron mi compañera Pamela Pérez-Flores y la invaluable Mariel Castillo. A todos ellos mis más profundas gracias, por su ayuda, paciencia y amistad. Mis agradecimientos también al resto que fue incorporándose al grupo de geociencias y nuestra especial dinámica: Rodrigo, Tiaren, Nico, Gerd, Rocío, Gert, Tomás, Pablo I., Ashley, Elias, Álvaro, Javi. Así también los "de afuera": Pablo S., Joaquín CA, Ian, Angelo, Camilo, José G.

Numerosos profesores y sus conocimientos están reflejados en este documento y merecen un especial reconocimiento: Carlos Costa por considerarme en el proyecto SARA-GEM y apoyarme en el desarrollo del mismo y mi Tesis. A Gabriel González por incluirme en su proyecto y por los numerosos terrenos en el norte y sus enseñanzas. A Rafael Riddell por incorporarnos al panel de trabajo de Espectro de Diseño del IChC. Constantino Mpodozis, Carlos Marquardt, Felipe Aron, Andrés Veloso y Jorge Crempien

de la PUC y Felipe Leyton, R. Allmendinger, Pablo Salazar, han tenido recomendaciones y opiniones sumamente valiosas. A todos los del Departamento de Ingeniería Estructural y Geotecnia, y en especial a Josefina, Jenny, Carlitos (QEPD), Luis y Priscilla. A las señoras del café y Marina.

A mis amigos: Marcela, Fernanda, Luis A., Sandra, Robin, Chigua, Igor, y a las chicas-hidro; Clau, Caro, Gi, Ire, Su, Kerstin, Pili, Vivi y Virgi, por su apoyo especial.

Y finalmente a mi familia. A mis abuelos Luis, Berta y Magdalena, que me regalonearon y estimularon la curiosidad por la ciencia y la tierra con sus historias y paseos. A mis padres Marcelo y María Angélica, por enseñarme el valor de la educación y de ser una persona involucrada socialmente, y por permitirme soñar e imaginar que todo es posible. A mis hermanos Pablo, Titi, Mona, Mari, Javi, Dani y Pipe, por su mantenerme siempre preparada para los altibajos de la vida y enseñarme que nada es tan grave que no nos podamos reír. Y muchísimas gracias a mis hijos por comprender como es su madre y enseñarme que siempre se puede aprender.

CONTENTS

Page

TABLE INDEX

Page

FIGURE INDEX

Page

ABSTRACT

The Chilean Andes, as a characteristic tectonic and geomorphological region, is a perfect location to unravel the geological nature of seismic hazards. The Chilean segment of the Nazca–South American subduction zone has experienced mega-earthquakes with moment magnitudes (Mw) >8.5 (e.g., Mw 9.5 Valdivia, 1960; Mw 8.8 Maule, 2010) and many large earthquakes with Mw >7.5, both with recurrence times of tens to hundreds of years. By contrast, crustal faults within the overriding South American plate commonly have longer recurrence times (thousands of years) and are known to produce earthquakes with a maximum Mw of 7.0–7.5. Subduction-type earthquakes are considered to be the principal seismic hazard in Chile, and have the potential to cause significant damage to its population and economy. However, crustal (non-subduction) earthquakes can also cause great destruction at a local scale due to their shallower hypocentral depth. Nevertheless, the nature, timing, and slip rates of crustal seismic sources in the Chilean Andes remain poorly constrained. This work aims to address the seismic potential of crustal faults in Chile, and to contribute to the estimation of key fault parameters for the assessment of seismic hazard. In this thesis, the main parameters that determine the magnitude of an earthquake, including length, width and mean displacement of some case studies crustal faults and their morphotectonic settings, exposing the parametrical similarities in longitudinal domains (N-S stripes) and disparity from W to E, across latitudinal domains.

Faults lying on each of the margin-parallel domains share some first-order geometric, kinematic, and seismogenic potential properties. The maximum hypocentral depths for crustal earthquakes vary across margin-parallel tectonic domains, from 25–30 km depth in the outer forearc to 8–12 km depth in the volcanic arc, thus allowing a first-order assessment of seismic potential. Current structural, paleoseismological, and geodetic data, although sparse and limited, suggest that slip rates of Chilean crustal faults range from 0.2 mm/yr (in the forearc region) to up to ~10.0 mm/yr (in the intra-arc region).

Faults in the outer forearc region have the potential to generate Mw 7 earthquakes every few thousand years. One key characteristic of these faults is that they can be reactivated as the result of Mw ~8.5+ subduction earthquakes. An example of this is the Pichilemu fault, which generated two Mw 6.9+ earthquakes in 2010, only a few days after the Maule earthquake. Larger earthquakes can be generated by outer-forearc faults since the cold thick crust of the outer forearc region allows the nucleation of earthquakes with depths of up to 30 km. Typical faults in the inner forearc, such as the San Ramón fault east of Santiago, have been shown to generate Mw ~7–7.5 earthquakes with similar or slightly longer recurrence times than those of faults in the outer forearc. Moreover, intra-arc faults, such as 40 km long segments of the Liquiñe–Ofqui fault system in Southern Chile, are capable of producing Mw 6–7 earthquakes every few hundred years; however, the maximum size of these earthquakes is limited by a relatively thin seismogenic crust (8–12 km in thickness), which prevents the propagation of earthquakes at depths greater than 12 km.

The existence of different tectonic modes for crustal fault reactivation and their wide range of slip rates complicates the estimation of seismic hazard. A rigorous seismic hazard assessment must therefore consider the different tectonic settings, timing of activation, and slip rates of Andean crustal faults. Understanding the nature of these faults will allow a better evaluation of the associated seismic hazard and allow better constraints to be placed on the relationship between these faults and the subduction seismic cycle.

RESUMEN

FALLAS CORTICALES EN LOS ANDES CHILENOS: UNA APROXIMACIÓN GEOLÓGICA Y GEOFÍSICA COMBINADA

Los Andes chilenos, entendidos como una región tectónica y geomorfológica característica, son un lugar perfecto para revelar la naturaleza geológica del peligro sísmico. El segmento chileno de la zona de subducción Nazca-Sudamericana ha experimentado mega-terremotos de Magnitud de Momento (Mw) >8,5 (e.g., Mw 9,5 Valdivia, 1960; Mw 8,8 Maule, 2010) y numerosos terremotos de Mw >7,5, ambos tipos con tasas de recurrencia de decenas a cientos de años. En contraste, las fallas corticales en la placa superior sudamericana comúnmente tienen tasas de recurrencia mayores (miles de años) y son conocidas por producir terremotos con magnitud Mw máximas 7,0 a 7,5. Los terremotos del tipo subducción han sido considerados como el principal peligro sísmico en Chile, con el potencial de causar daño importante a la población y economía, pero los terremotos corticales también tienen la capacidad de causar gran destrucción a escala local, debido a la menor profundidad de sus hipocentros. Sin embargo, la naturaleza, las tasas de recurrencia y el deslizamiento de las fallas corticales en Chile están pobremente delimitadas. Este trabajo tiene como objetivo investigar el potencial sismogénico de las fallas corticales en Chile, y contribuir en la estimación de los principales parámetros de las fallas para la evaluación del peligro sísmico. Se examinaron los parámetros principales involucrados en la magnitud de un terremoto, incluyendo largo, ancho y desplazamiento medio de las fallas corticales y su disposición morfotectónica, revelando las similitudes en los parámetros en cada dominio longitudinal (franjas N-S) y una mayor disparidad de W a E (dominios latitudinales).

Las fallas en cada uno de los dominios paralelos al margen comparten algunas características geométricas, cinemáticas y de potencial sismogénico de primer orden. Las máximas profundidades de hipocentros corticales cambian en los dominios tectónicos paralelos al margen continental desde 25-30 km en el antearco externo a 8-12 km en el

arco volcánico, lo que permite una primera aproximación a la evaluación del potencial sísmico. Aunque dispersos y limitados, los datos estructurales, paleosismológicos y geodésicos actuales sugieren tasas de deslizamiento de las fallas corticales en Chile entre 0,2 mm/a (dominio antearco) y 10,0 mm/a (dominio intraarco).

Las fallas de la región del antearco externo tienen el potencial de generar terremotos Mw 7 cada pocos miles de años. Una característica clave de estas fallas es que pueden reactivarse como resultado de los terremotos de subducción de Mw >8,5, como el caso de la falla Pichilemu en 2010, que generó dos terremotos, solo unos días después del terremoto de Maule. Son factibles terremotos más grandes, porque la corteza gruesa y fría de la región del antearco externo permite la nucleación de terremotos con profundidades de hasta 30 km. Las fallas típicas del antearco interno, como la falla de San Ramón al este de Santiago, han demostrado generar terremotos de Mw ~7−7,5 con tiempos de recurrencia similares o ligeramente más largos que los del antearco externo. Por último, las fallas en el arco volcánico, como los segmentos de 40 km de longitud del sistema de fallas Liquiñe-Ofqui en el sur de Chile, son capaces de producir terremotos Mw 6-7 cada pocos cientos de años; sin embargo, su tamaño máximo está limitado por una corteza sismogénica relativamente delgada (8 a 12 km) que evita la propagación de los terremotos más profundo.

Las diferentes condiciones tectónicas de reactivación de las fallas corticales junto al amplio rango de tasas de deslizamiento complican la estimación del peligro sísmico. La investigación rigurosa del peligro sísmico debe considerar los diferentes escenarios tectónicos, las tasas de recurrencia naturaleza de estas fallas nos ayudará no solo a entender mejor el peligro sísmico asociado, sino que también a precisar la conexión con el ciclo sísmico de subducción.

1 INTRODUCTION

1.1 Organization of this Thesis

This thesis contains an introductory chapter, two self-supporting chapters prepared to be presented as papers in scientific journals, and a final conclusion chapter.

Chapter l contains the statement of the addressed scientific problem along with the geological and tectonic background.

Chapter 2 is a manuscript entitled, “Crustal faults in the Chilean Andes: geological constraints and seismic potential”, which has been published in the journal *Andean Geology*. This manuscript addresses the nature and significance of crustal faults along the Chilean Andes margin. Its main objective is to investigate the common characteristics of crustal faults and estimate key crustal-fault parameters and general conditions related to the faults’ tectonic and geomorphological setting, while introducing a first approximation for the seismic hazard assessment (SHA) of crustal faults in Chile. Despite the large epistemic uncertainties involved in most fault data, basic fault-condition parameters were constrained in order to better understand the influence of geological structures in SHA and to provide guidance for further research on this topic.

Chapter 3 explores the use of different geophysical methodologies to characterize geometries of potentially seismogenic crustal faults, which are themselves directly involved in their seismogenic potential. Specifically, we attempted to describe the geometric and kinematic features of the Aeropuerto Fault. Another aim of this work is to study the relationships between sediments, rocks, and faults in order to shed light on basin shape and on the rate and age of normal-slip displacement.

Chapter 4 includes a discussion and the main conclusions of this thesis.

1.2 Theoretical Background

Chile is located on a continental margin where the Nazca and South American plates converge obliquely to the margin (plate convergence vector with a N78°E strike) at rate of 66–79 mm/y (Cande and Leslie, 1986; DeMets et al., 1994; Angermann et al., 1999). This convergence develops the strongest compressional-transpressional regime along the Andean margin (Ramos, 2009) (Figure 1-1). The Nazca plate subducts under the western edge of South America, generating first-order tectonic and magmatic processes in the short- and long-term, such as earthquakes, volcanism, folding, faulting, and mountain building.

Convergent margins with "Chilean-type" subduction are characterized by highly compressive tectonic regimes (Uyeda, 1982) with frequent seismic activity. The main fault in a subduction zone corresponds to the interface between the subducted oceanic plate and the upper continental crust, and generates thrust earthquakes with large magnitudes. Several earthquakes with moment magnitudes (Mw) larger than 8.5 (e.g., Mw 9.5 Valdivia, 1960; Mw 8.8 Maule, 2010) have been recorded in Chile. Earthquake recurrence times in the Chilean Andes have been estimated at 80–120 years for earthquakes with Mw >7.5, and 250–500 years for earthquakes with Mw >8.5 (Comte et al., 1986; Barrientos and Ward, 1990; Lomnitz, 2004; Cisternas et al., 2005; Barrientos, 2007). Such "megathrust" subduction-type earthquakes are considered to be the main seismic hazard in Chile, with the potential to cause significant damage to its population and economy. The seismic zones along Chile proposed by Barrientos (1980) are used in the Chilean Seismic Design of Buildings Code (Chilean Standard NCh 433), which only accounts for the subduction earthquake hazard.

The subduction seismic cycle, as described by Nelson et al. (1996), starts with the accumulation of inter-seismic strain in the upper plate above the coupled zone at the boundary between the plates (forearc, Figure 1-2 a). The more gradual deformation in the inter-seismic part of the subduction cycle includes short-term pre- and post-seismic movements that are generally opposite to the direction of co-seismic deformation in the

same sites; subsidence is recorded closest to the subducting plate and uplift is recorded to the eastern part of the forearc Accumulated strain is released through sliding in the coupled zone during the co-seismic part of the cycle (Figure 1-2 b). During the largest earthquakes, the region closest to the plate interface (60–160 km in width and hundreds of kilometers in length) experiences uplift, while a margin-parallel domain located closer to the top of the uplift zone simultaneously experiences rapid subsidence.

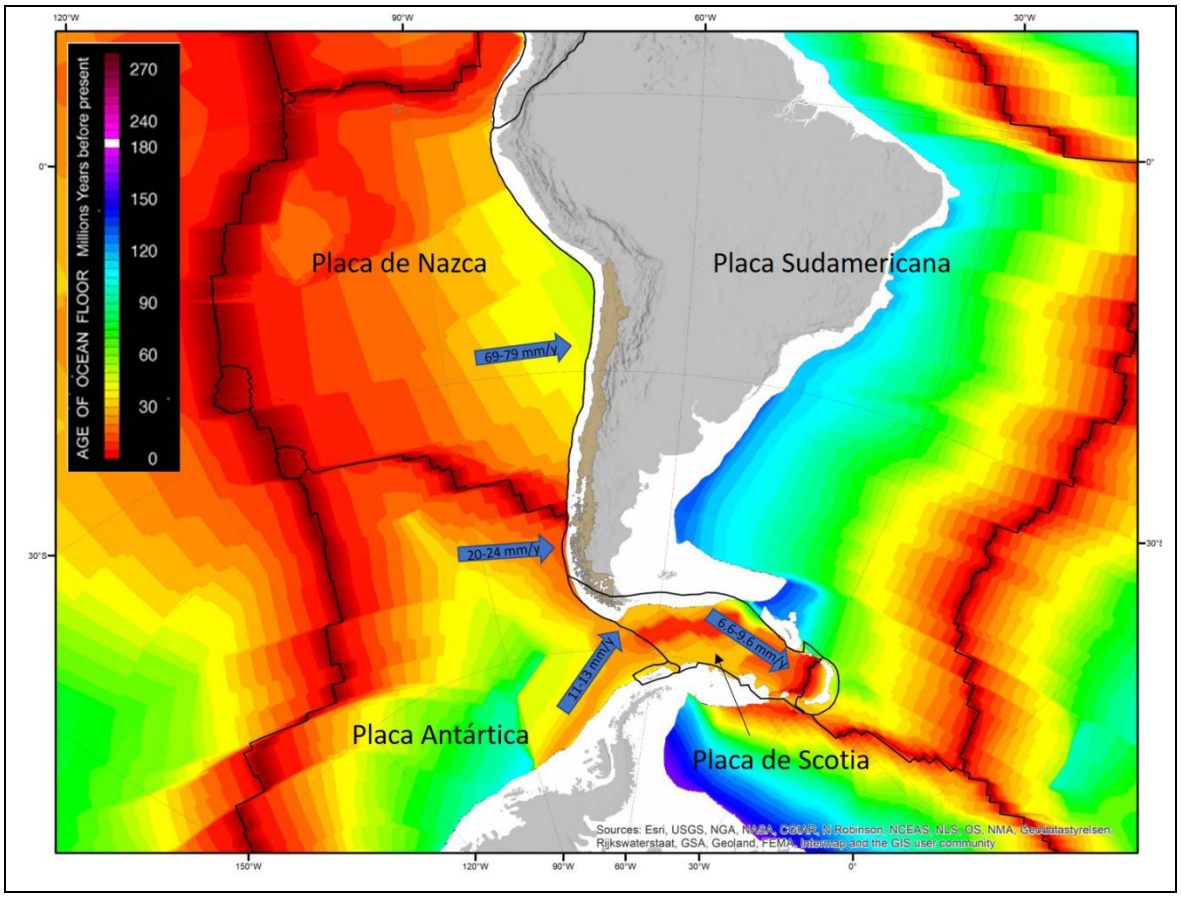

Figure 1-1: General context of the Nazca–South American subduction zone.

The subduction interface between the subducted oceanic plate and the overlying continental lithosphere is usually locked or coupled up to a depth of approximately 50 km (Bevis et al., 2001; Khazaradze and Klotz, 2003; Moreno et al., 2010, 2011 Suarez and Comte, 1993, Tichelaar and Ruff, 1991, 1993), which causes the accumulation of strain in the overriding plate. Part of the accumulated strain is transformed into permanent deformation of the continental crust.

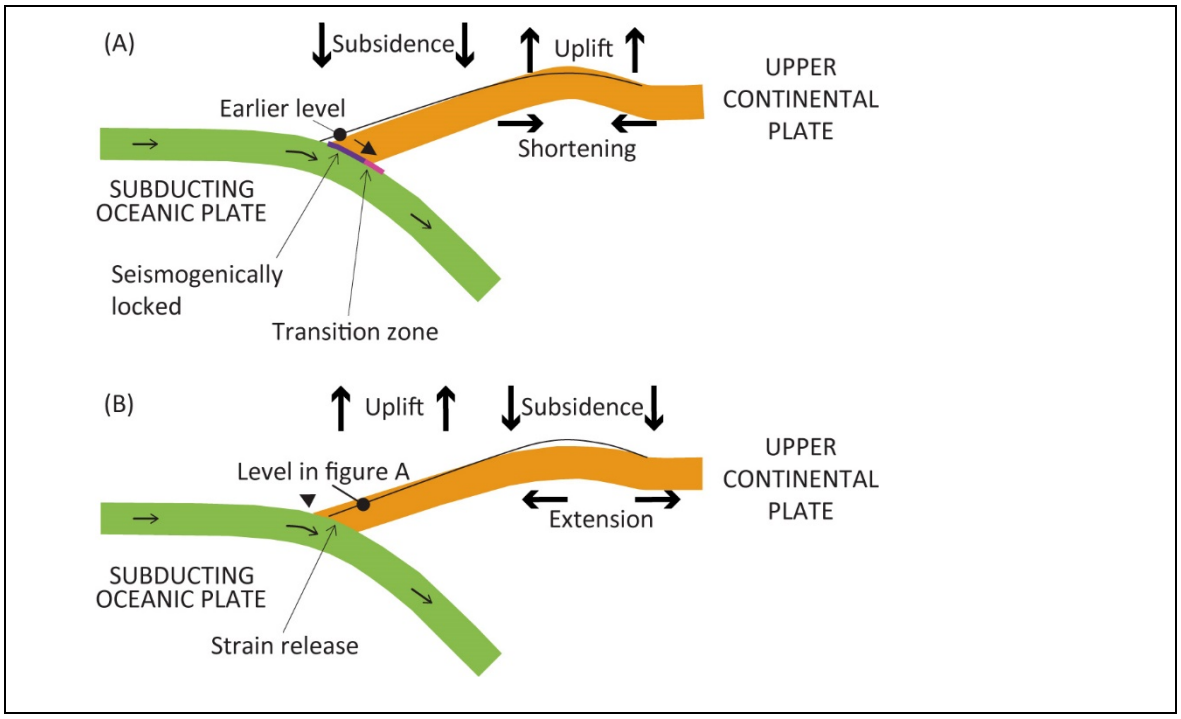

Figure 1-2: Schematic depiction of the subduction seismic cycle and forearc deformation. Deformation pattern during (a) inter-seismic and (b) co-seismic stages associated with a subduction earthquake is presented (modified from Hyndman and Wang, 1993; Nelson et al., 1996; and Hamilton and Shennan, 2005).

Studies of large historical subduction earthquakes have revealed the slip of discrete segments of the subduction interface, evidencing a convergent margin segmentation (e.g., Nelson et al., 1996). In the few locations where several seismic cycles have been recorded, the segmentation has been differentiated from one cycle to the next (e.g., Shimizaki and Nakata, 1980; Schwartz and Coppersmith, 1984; Thatcher, 1986; Stein et al., 1988; Ruiz and Madariaga, 2018). Several authors have suggested that the ends of segments of subduction-earthquake rupture coincide with prominent structures in the lower and/or upper plates (e.g., Scholz, 1998). Causes of segmentation of subducting plates, such as the Nazca plate, include changes in the geometry of the subducting plate, and displacements, jumps, or abrupt changes along-strike and downdip of the Wadati–Benioff zone, fracture zones, seamounts and oceanic plateaus, rifts, and plate boundaries (Aki, 1979; Burbach and Frolich, 1986; Guffanti and Weaver, 1988; Cloos, 1992; Bilek, 2007; Das and Watts,

2009; Sparkes et al., 2010; Contreras-Reyes and Carrizo, 2011; Müller and Landgrebe, 2012; Álvarez et al., 2014; Maksymowicz et al., 2015; Shrivastava et al., 2019). Other factors which have been related to segmentation along subduction zones include structures in the upper plate (both old inherited structures and more recent crustal faulting and cracking) and changes in the composition of the continental crust (e.g., Tassara and Yáñez, 2003; Loveless et al., 2010; Aron et al., 2013). Yáñez and Cembrano (2004) postulate that arc-foreland deformation is controlled by the absolute velocity of the continental plate and the degree of plate coupling between the oceanic and continental plates. Plate coupling is stronger where the subducting oceanic plate is older, whereas the absolute velocity of the upper plate is the key factor, which enhances bulk compression and mountain building.

In recent years, various authors have studied crustal faulting and the associated hazard by considering evidence of near-Holocene/Pleistocene (paleoseismic) earthquakes and instrumentally recorded earthquakes (e.g., Cortés et al., 2012; Aron et al., 2013; Vargas et al., 2013; Pérez et al., 2014; Vargas et al., 2014).

In contrast to large subduction earthquakes, crustal faults within the overriding South American plate cause earthquakes with shorter recurrence times of thousands of years (e.g., Barrientos et al., 2004; Silva, 2008; Leyton et al., 2010; Vargas et al., 2011; Vargas et al., 2014). Crustal faults produce earthquakes with moderate magnitudes (Mw <7.5) without evidence of surface rupture. However, the lack of detailed seismic and neotectonic studies may have biased our current understanding of crustal faults. Such faults are controlled by contemporary tectonics, or "neotectonics" (e.g., Mw 6.2, Aysén, 2007; Vargas et al., 2013), or are produced by the reactivation of mechanical anisotropies inherited from an earlier tectonic setting (paleotectonics) that was different from the present-day stress field (e.g., Mw 6.9 and Mw 7.0, Pichilemu, 2010; Aron et al., 2013).

The available structural, paleoseismological, and geodetic data, although limited, suggest that the current slip rates of Chilean crustal faults range from 0.2 mm/y in the forearc to up to 6.5 mm/y in the intra-arc (e.g., Wang et al., 2007; Armijo et al., 2010; Cortés et al., 2012; Stanton-Yonge et al., 2016). This implies recurrence times for Mw >6

crustal-fault earthquakes in the range of hundreds of years to tens of thousands of years (Sibson, 2002). The various modes of tectonic fault reactivation and the wide range of slip rates that these faults exhibit greatly complicate the assessment of the crustal seismic hazard in Chile. Many faults that are considered active under the traditional classification (i.e., those which have been active in the last 10,000 years; USGS, 2018) may not be capable of generating significant earthquakes over thousands of years (Machette, 2000; Costa, 2004; Costa et al., 2006a); meanwhile, faults of Quaternary age or older with no instrumentally recorded seismicity may have the potential to trigger earthquakes with Mw >7 (e.g., 2011 Mw 7.1 Darfield earthquake, New Zealand; Li et al., 2014).

Neotectonic studies along the Chilean subduction-margin show that, in general, the predominant deformation regime in the forearc, between Arica and the Arauco Peninsula, is one of EW extension (see Table 1-1). Examples of EW forearc extension during the co-seismic stage, as determined by the studies summarized in Table 1-1, include:

- The activation of normal ~NS-striking faults, which produces significant (Mw >6.5) earthquakes (Loveless, 2007; Cortés-Aranda et al., 2014)
- Convergence-parallel cracks (Loveless, 2007; Allmendinger and González, 2010)
- Shore uplift (Lavenu et al., 1999; Heinze, 2003; Marquardt et al., 2004)
- Geodetic data (Plafker and Savage, 1970; Heinze, 2003)
- Large changes in Coulomb stress, promoting normal deformation (Farías et al., 2011; Aron et al., 2013; Cortés-Aranda et al., 2014)
- An elliptical rupture area of subduction mega-earthquakes that is spatially related with the trends of the major upper-crustal structures (Aron et al., 2013).

Additionally, inter-seismic extension and uplift/subsidence occur due to margin flexure. Models of the accumulation of inter-seismic elastic strain for a convergent plate boundary show that the extension or shortening of a particular area depend on the distance from the trench and the degree of interplate coupling (Loveless, 2007).

The predominant long-term deformation signature in the Chilean forearc is extensional, coincidental with the effects of co-seismic stress changes, namely major long-

lived normal-slip crustal faults, their orientation with respect to subduction-earthquake slip patches, and coeval ~EW-striking reverse faults and folds. In general, the deformation of the forearc occurs at a very slow rate compared to subduction slip-rates and recurrence times. Permanent deformation velocities of 1.5 nstrain/year and slip rates of less than 0.5 mm/year have been estimated for the Chilean forearc (Allmendinger and González, 2010).

Table 1-1: Evidence of neotectonic deformation in the Chilean forearc.

Fault/Site	Reference	Methodology	Subduction earthquake cycle		Long-Term
			Inter-seismic	Co-seismic	
Northern Coastal Cordillera (19–25ºS)	Allmendinger and González (2010)	Coulomb Failure Stress Change models	EW extension (flexure of the continental margin)	EW extension (elastic rebound and subduction erosion of converging plates)	
		Surface cracks	NS shortening in the top of EW-striking faults/folds scarps	EW extension in NS cracks	
		Fault data	NS shortening in ~EW-striking reverse faults		
Northern Chile	Loveless (2007)	Model of inter-seismic elastic strain accumulation for a convergent plate boundary	EW extension due to elastic flexure of continental plate		
		Numerical models of Surface cracks		EW extension in NS-oriented cracks	
Salar Grande	González et al. (2003)	Fault data, Geomorphology			NW-striking strike-slip faults and NS- to NNE-striking normal faults
Mejillones Peninsula	McCaffrey (1996)	Oblique subduction			NS shortening on ~EW-striking reverse faults
Mejillones Peninsula	Lavenu et al. (1999)	Fault-slip data		Intraplate earthquakes indicate normal stress with EW-oriented σ3	Uplift; EW extension

Fault/Site	Reference	Methodology	Subduction earthquake cycle		Long-Term
			Inter-seismic	Co-seismic	
Mejillones Peninsula	Bevis et al. (2001)	Elastic modeling of curved margin			NS shortening on ~EW-striking reverse faults
Mejillones Peninsula	Armijo and Thiele (1990); Niemeyer et al. (1996); DeLouis et al. (1998); Marquardt (2005)	Normal faults data			EW extension
Mejillones Peninsula	Von Huene and Ranero (2003)	Subduction erosion			Normal faults
Mejillones Peninsula	Loveless (2007)	Elastic dislocation model and INSAR analyses of co-seismic displacements.		Tensional stress field on NS-striking faults	
Coast, 22.7–24°S	Cortés-Aranda et al. (2014)	Coulomb Stress Change models			Normal activation of upper-plate faults
Copiapó	Comte et al. (2002)	Historic, teleseismically and locally recorded seismicity		Interplate earthquakes show reverse stress with σ1 perpendicular to the trench	
Caldera	Lavenu et al. (1999)	Fault-slip data			Uplift; EW extension

Fault/Site	Reference	Methodology	Subduction earthquake cycle		Long-Term
			Inter-seismic	Co-seismic	
Caldera	Marquardt et al. (2004)				Vertical uplift and NW-SE extension
Puerto Aldea Fault	Heinze (2003)	Analysis of fault-slip data; neotectonic profiles; elastic dislocation modeling			ENE-WSW extension and NNW-SSE contraction
		GPS residual velocities	ENE-WSW extension and NNW-SSE shortening		
		Dislocation model of the plate interface		Uplift of Coastal Cordillera, E-W extensional and N-S contractional strains	
Santiago	Lavenu et al. (1999)	Fault-slip data			NS contraction
Pichilemu Fault	Aron et al. (2013)	Coulomb stress change	Coupling; EW shortening	Activation of crustal NW fault	Coincidental elliptical pattern of subduction mega-earthquake rupture and major upper-crustal structures trends
Pichilemu Fault	Farías et al. (2011)	Seismological data; Coulomb stress changes; geomorphology		Triggering of crustal NW fault	Compressional deformation on NS- to NNE-SSW-striking faults, extensional deformation on NW-SE- to NNW-SSE-striking faults

Fault/Site	Reference	Methodology	Subduction earthquake cycle		Long-Term
			Inter-seismic	Co-seismic	
Pichilemu–Navidad	Lavenu and Encinas (2005)	Fault-slip data			EW extension
Arauco	Lavenu et al. (1999)	Fault-slip data			Uplift; EW extension and NS contraction
Isla Mocha	Nelson and Manley (1992)	Geology/geomorphology		Raised shorelines	Uplift
Isla Santa María	Melnick et al. (2014)	Geology/geomorphology		Meter-scale uplift (1960)	Uplift and tilting caused by reverse faults rooted in the plate interface
Valdivia	Plafker and Savage (1970)	Geodetic triangulation data of co-seismic and postseismic deformations associated with the 1960 Valdivia earthquake		Sinistral strike-slip and E-W extension along N-S striking intraplate faults	

1.3 Seismogenic Potential of Crustal Faults

In order to assess the seismic hazard posed by a given fault, it is first necessary to identify whether that fault is capable of generating an earthquake. The seismogenic potential of a fault involves the slip rate of the fault and, just as significantly, the established general tectonic environment and the particular local stress field.

Old crustal faults which are optimally oriented with respect to inter- or co-seismic stress fields may be reactivated and produce shallow earthquakes with magnitudes of up to Mw 7 (e.g., Farías et al., 2011; Aron et al., 2013; González et al., 2015). This scenario is particularly relevant for optimally oriented basement (inherited) crustal faults undergoing sudden high strain rates, a condition which can potentially be achieved co-seismically with large megathrust subduction earthquakes (Mw >8; King et al., 1994; Stein et al., 1994; Stein, 1999; Kilb et al., 2000; Lin and Stein, 2004; Loveless et al., 2010; Seeber and Armbruster, 2010). In contrast, during the inter-seismic period, when the crustal deformation rate is relatively low, the reactivation of optimally oriented faults may be less likely (e.g., Aron et al., 2014).

The estimation of earthquake magnitudes from geological data is typically performed using empirical relationships and assumptions of earthquake parameters based on the premise that the rupture parameters of an earthquake are proportional to its magnitude (Slemmons, 1977; Hanks and Kanamori, 1979; Bonilla, 1984; Slemmons and de Polo, 1986; Wells and Coppersmith, 1994; Hanks and Bakun, 2008; Wesnousky, 2008; and many others summarized in Stirling et al., 2013). Accordingly, the rupture length and surface displacement, which are preserved in the paleoseismological record, can be used in empirical regression relationships to estimate earthquake magnitude. The uncertainties of these parameters must be considered for the estimation of earthquake magnitude, and the assumption that a fault will always rupture with a constant displacement and slip rate, thus creating a “characteristic earthquake”, must be used with caution (Kagan, 1993; Burbank and Anderson, 2001; McCalpin, 2009). Accordingly, the assessment of the key

earthquake parameters in the field, and the subsequent estimation of other parameters using empirical relationships, are subject to significant uncertainties (see McCalpin (2009) for a review).

Models of fault behavior acknowledge that faults may be segmented into discrete sections that act distinctly over their seismic cycle (e.g., Schwartz and Coppersmith, 1986; Slemmons, 1995). Such segmentation can control the onset and termination of fault rupture, and accordingly can also control the size of the rupture area and earthquake magnitude (Grant, 2002). Commonly, the length of a single fault segment (which can be identified through field observations and/or satellite imagery) indicates the maximum possible surface rupture length during an earthquake, since field features are formed by several ruptures over time. Furthermore, if an inappropriate work scale is chosen, several consecutive segments could be mistaken for a single one. Additionally, fault segments which have generated earthquakes independently of each other may be capable of combining to generate a single segment rupture and thereby generate an earthquake of higher magnitude (e.g., Estay et al., 2016). Consequently, the estimation of earthquake size via paleoseismological or terrain analysis techniques introduces uncertainties that may be difficult to constrain.

1.4 Research Problem

The geological and geophysical nature of crustal faults raise many relevant scientific questions in the context explained previously and taking into consideration the aforementioned earlier studies

The question of how a bulk compressional regime reconciles with the predominantly extensional tectonics of the Andean forearc in the outer forearc has been addressed by several authors (González et al., 2003; Marquardt et al., 2004; González et al., 2006; Allmendinger and González, 2010; Cortés, 2012; Heinze, 2013), especially for Northern Chile. However, the nature and kinematics of crustal faulting at a larger scale, including

the whole forearc and the other margin-parallel tectonic domains, is still a matter of debate. In particular, the following questions are subject to ongoing debate:

- Are there common characteristics and behaviors of crustal faults along and/or across the Chilean Andes? For instance, do most forearc faults behave as normal faults in the long term?
- How do the different along- and across-strike tectonic settings (forearc and arc) relate to the crustal fault hazard?
- What are the geometry, kinematics, and slip rate of outer forearc faults?
- What seismotectonic hazard is posed by crustal faults in different tectonic domains along- and across-strike of the Chilean Andes?

1.5 Hypothesis

The hypotheses arising from the above main scientific questions are:

- Crustal faults exhibit similar geometry, kinematics, and slip rates according to their location along first-order margin-parallel domains—that is, the outer forearc, inner forearc, and arc.
- The overall regional-scale seismic hazard posed by crustal faults can thus be established according to their specific continental margin setting.

1.6 Objectives

The main objective of this work is to add to the knowledge gained by previous studies regarding the regional-scale nature of crustal faults in the Chilean Andes and to estimate the seismogenic potential of these faults.

Crustal faults have been studied from local to regional scales. The purpose of this thesis is to search for common characteristics and behaviors of crustal faults and their tectonic setting in order to simplify the broad knowledge and focus subsequent studies on the most dangerous areas of the Chilean Andes.

The specific objectives of this thesis are:

- Establish the general geometry and kinematics of crustal faults in the Chilean Andes.
- Better constrain the slip rates of these faults as well as the recurrence times of their largest possible earthquakes.
- Estimate the hazard associated with the displacement of these faults in terms of earthquake magnitude and location.

1.7 Methodology

Since the study of crustal faults in Chile has traditionally been focused on continental-scale faults such as the Atacama or Liquiñe–Ofqui fault systems, this thesis takes into account and integrates other relevant crustal faults in order to provide an internally consistent seismotectonic picture. To accomplish the above objectives, the following methodology was designed:

1. Compilation, elaboration, and critical analyses of existing crustal fault studies, considering key crustal fault parameters related to geometry and kinematics and general conditions related to the tectonic and geomorphological settings of the studied faults.

2. Mapping analysis of regional and local structural geology, integrating previously published data and new field work in selected areas. These areas include segments of the Atacama Fault System (AFS) between the Mejillones and Salar del Carmen faults.

3. Regional and local geophysical analysis obtained from previously published studies and new fieldwork.

2 CRUSTAL FAULTS IN THE CHILEAN ANDES: GEOLOGICAL CONSTRAINTS AND SEISMIC POTENTIAL

2.1 Introduction

Chile is located in an outstanding physical laboratory to investigate the nature of earthquakes and related seismic hazard. The Chilean Andes is a distinctive tectonic and geomorphological orogenic region formed, in the north, by the ocean–continent convergence between the South American and Nazca plates, and in the south by the convergence between the Antarctic and Scotia plates. Its primary features include the Coastal Cordillera, the Central Depression, and the Main and Patagonian Cordilleras (e.g., Pankhurst and Hervé, 2007; Ramos, 2009b).

Continental Chile is affected by three main types of earthquake: (1) Subduction, or thrust-type, events, caused by the interplate friction between the Nazca and South American plates. These events typically have a hypocentral depth of up to 60 km (e.g., Tichelaar and Ruff, 1993; Suarez and Comte, 1993; Allmendinger and González, 2010; Scholz and Campos, 2012); (2) intraplate earthquakes, which occur within the subducting Nazca plate and typically have hypocentral depths of 60–200 km (e.g., Barrientos, 1980; Campos and Kausel, 1990); and (3) crustal intraplate earthquakes, which occur within the overriding South American plate and generally have hypocentral depths of less than 30 km (e.g., Barrientos et al., 2004; Leyton et al., 2010).

The Nazca–South American Chilean subduction zone is capable of producing large earthquakes with Mw greater than 8.5 (e.g., Mw 9.5 Valdivia, 1960; Mw 8.8 Maule, 2010). Earthquake recurrence times in the Nazca-Southamerica subducting margin have been estimated at 80–120 years for earthquakes with Mw >7.5, and 250–500 years for earthquakes with Mw >8.5 (Comte et al., 1986; Barrientos and Ward, 1990; Lomnitz, 2004; Cisternas et al., 2005; Barrientos, 2007). Such ”megathrust” subduction-type

earthquakes are considered to be the principal seismic hazard in Chile, with the potential to cause significant damage to its population and economy.

By contrast, crustal faults within the overriding South American plate (intraplate crustal faults/earthquakes, hereafter simply named "crustal" faults/earthquakes) commonly have recurrence times of thousands of years (e.g., Barrientos et al., 2004; Silva, 2008; Leyton et al., 2010), and based on seismic records are known to produce earthquakes of only moderate magnitudes Mw <7.5 without inducing primary surface deformation. However, the lack of more detailed seismic and neotectonic studies may have biased our current understanding of crustal faults. Such faults are controlled by contemporary tectonics, or "neotectonics" (e.g., Mw 6.2, Aysén, 2007; Vargas et al., 2013), or are produced by the reactivation of mechanical anisotropies inherited from a previous tectonic setting (paleotectonics) that was different to the present-day stress field (e.g., Mw 6.9 and Mw 7.0, Pichilemu, 2010; Aron et al., 2013). Here, the term neotectonics, which has been used variably by previous authors (Mercier, 1976.; Fairbridge, 1981; Hancock and Williams, 1986; Vita-Finzi, 1987; Hancock, 1988; Pavlides, 1989; Mörner, 1994; Costa et al., 2006a), is used to refer to the study of the processes and structures acting since the contemporary stress field of a given region was established (Stewart and Hancock, 1994). In Chile, neotectonics refers to the tectonic system, which has been active since at least the start of the Pliocene (González et al., 2003; Cembrano et al., 2007; Ramos 2009a).

The available structural, paleoseismological, and geodetic data, though limited, suggest that current slip rates of Chilean crustal faults range from 0.2 mm/y in the forearc to up to 6.5 mm/y in the intra-arc (e.g., Wang et al., 2007; Armijo et al., 2010; Cortés et al., 2012; Stanton-Yonge et al., 2016). This implies recurrence times of crustal fault earthquakes in the range of hundreds of years to tens of thousands of years (Sibson, 2002). The various modes of tectonic fault reactivation, and the wide range of slip rates that these faults exhibit, greatly complicate the assessment of crustal seismic hazard in Chile. Many faults which are considered active under the traditional classification (i.e., those which have been active in the last 10,000 years; USGS, 2018b) may not be capable of generating significant earthquakes in thousands of years (Machette, 2000; Costa, 2004; Costa et al.,

2006a), while faults of Quaternary age or older with no instrumentally recorded seismicity may have the potential to trigger socially consequential earthquakes with Mw >7 (e.g., 2011 Mw 7.1 Darfield earthquake, New Zealand; Li et al., 2014).

In this work, we attempt to characterize and estimate key crustal-fault parameters, and general conditions related to the tectonic and geomorphological setting of crustal faults, in order to provide a first approximation for the crustal-fault seismic hazard assessment (SHA) in Chile. Despite the large epistemic uncertainties involved in most fault data, basic fault-condition parameters were populated in order to better understand the input of geological structures in SHA and to provide guidance for further investigations on this subject.

2.2 Geological Framework of Crustal Faults of the Chilean Andes

The oceanic Nazca plate subducts beneath the continental South American plate along almost all of the latter's western margin, in a compressional setting defined by Uyeda and Kanamori (1979) as "Chilean type". In Chile, the contact between these two plates runs offshore in a roughly north-south orientation for the majority of the country's length of more than 4000 km, from the Arica elbow in the north to the Chile ridge subduction site at the Nazca–South America–Antarctica Triple Junction (latitude 46°S, Figure 2-1). The subducted plate dips ~25–30°E beneath South America, except in the central "flat slab" segment between 28° and 32°S, where it dips ~5°E with a convergence oblique to the margin (N78°E) at a rate of 66–79 mm/y (Cande and Leslie, 1986; DeMets et al., 1994; Angermann et al., 1999) in the strongest compressional–transpressional regime along the Andean margin (Ramos, 2009a).

South of 46°S until ~52°S, the oceanic plate which subducts beneath South America is the Antarctic plate, which has a convergence rate of ~20 mm/y and a trench-perpendicular convergence direction since the early Eocene (Cande and Leslie, 1986).

The southernmost tectonic margin of Chile curves to the east and is characterized by a transform boundary between the South American and Scotia plates, whose continental segment is known as the Magallanes–Fagnano fault. This portion of the plate boundary has a left-lateral strike-slip motion estimated at between 6.6 ± 1.3 mm/y and 9.6 ± 1.4 mm/y (Smalley et al., 2003; DeMets et al., 2010). To the west and southwest of this margin, the Antarctic plate subducts beneath the South American plate at a rate of 20–24 mm/y (Cande and Leslie, 1986; DeMets et al., 1990) and beneath the Scotia plate at a rate of 11–13 mm/y (Pelayo and Wiens 1989; Thomas et al., 2003).

The convergence between the Nazca and South American plates has caused crustal shortening and thickening of the overriding (South American) plate, resulting in the formation of the modern Andes mountain range over the past 25 Ma (Mpodozis and Ramos, 1989; Tassara and Yáñez, 1996; Yáñez and Cembrano, 2004; Mpodozis and Ramos, 2008; Ramos, 2009a). The study of the present and past tectonics of the Andes has detected marked changes along both north-south and east-west transects. First-order tectonic segments have been identified in both the Nazca and South American plates, ranging from continental scale (e.g., Isacks and Barazangi, 1977; Jordan et al., 1983a; Jordan et al., 1983b; Jarrard, 1986; Yáñez and Cembrano, 2004; Hoffmann-Rothe et al., 2006; Ramos, 2009a) to local scale (e.g., Rosenau, 2004; Rosenau et al., 2006; Rehak et al., 2008) and trending both along- and across-strike. Several factors control this tectonic segmentation, most significantly the absolute motion of the overriding plate and slab retreat, the length of the Benioff zone, the relative plate convergence rate, the direction of mantle flow, climate, the crustal thickness of the South American plate, the age and subduction angle of the Nazca plate, and the subduction of passive and/or active ridges, among others.

The causes of this first-order segmentation are still a subject of debate. Tassara and Yáñez (2003) proposed a first-order segmentation caused by a change in the composition of the continental crust from north to south (more felsic in the central Andes (15–33.5°S) and more mafic in the southern Andes (33.5–47°S)), and a second-order segmentation associated with variations in the thermo-mechanical regime of the plate convergence

process. Yáñez and Cembrano (2004) postulated that the arc-foreland deformation is controlled by the absolute velocity of the continental plate and the degree of plate coupling between the oceanic and continental plates, with coupling being subordinate to the age of the subducting plate and the convergence rate. Ramos (2009a) indicates that the absolute motion of the upper plate relative to the hotspot frame and the consequent trench rollback velocity are the first-order parameters that control the arc-foreland deformation.

Along with fundamental tectonic causes, marked long-term latitudinal climatic variations have been invoked as controlling factors for the geological evolution and segmentation of the continental plate (e.g., Jordan et al., 1983a, 1983b, 2001, 2014; Jarrard, 1986; Mpodozis and Ramos, 1989; Kley et al., 1999; Gutscher et al., 2000; Yáñez et al., 2001; Lamb and Davis 2003; Tassara and Yáñez, 2003; Yáñez and Cembrano 2004; Sobolev and Babeyko 2005; Armijo et al., 2015). Climatic characteristics vary both along and across the Chilean Andes. Precipitation decreases from a hyperarid north to a cold and rainy south, exerting a critical control on the sediment contribution to the trench (Dunai et al., 2005; Hoke, 2006; Kober et al., 2007; Matmon et al., 2009), which is almost empty of sediment fill between 10 and 33.5°S. Hyperaridity has likely persisted since at least ca. 12 ± 1 Ma (Jordan et al., 2014), and has been recognized as a key factor in the formation of the Andes (Lamb and Davis, 2003; Jordan et al., 2014). Additionally, the Peru–Chile oceanic current and the associated upwelling transports colder oceanic waters and thus limits precipitation in the vicinity of the current (Lamb and Davis, 2003).

A latitudinal segmentation (across-strike relative to the continental margin/Chilean trench) of the Chilean continental lithosphere into at least five different tectonic domains has been recognized by various authors: Arica–Copiapó, Copiapó–Santiago, Santiago–Arauco, Arauco–Chile Triple Junction, and Southern Chile Triple Junction (e.g., Jordan et al., 1983a, 1983b, Tassara and Yáñez, 2003; Yáñez and Cembrano, 2004; Ramos, 2009b; Gerbault et al., 2009). The main tectonic characteristics of these domains are shown in Table 2-1 and Figure 2-1.

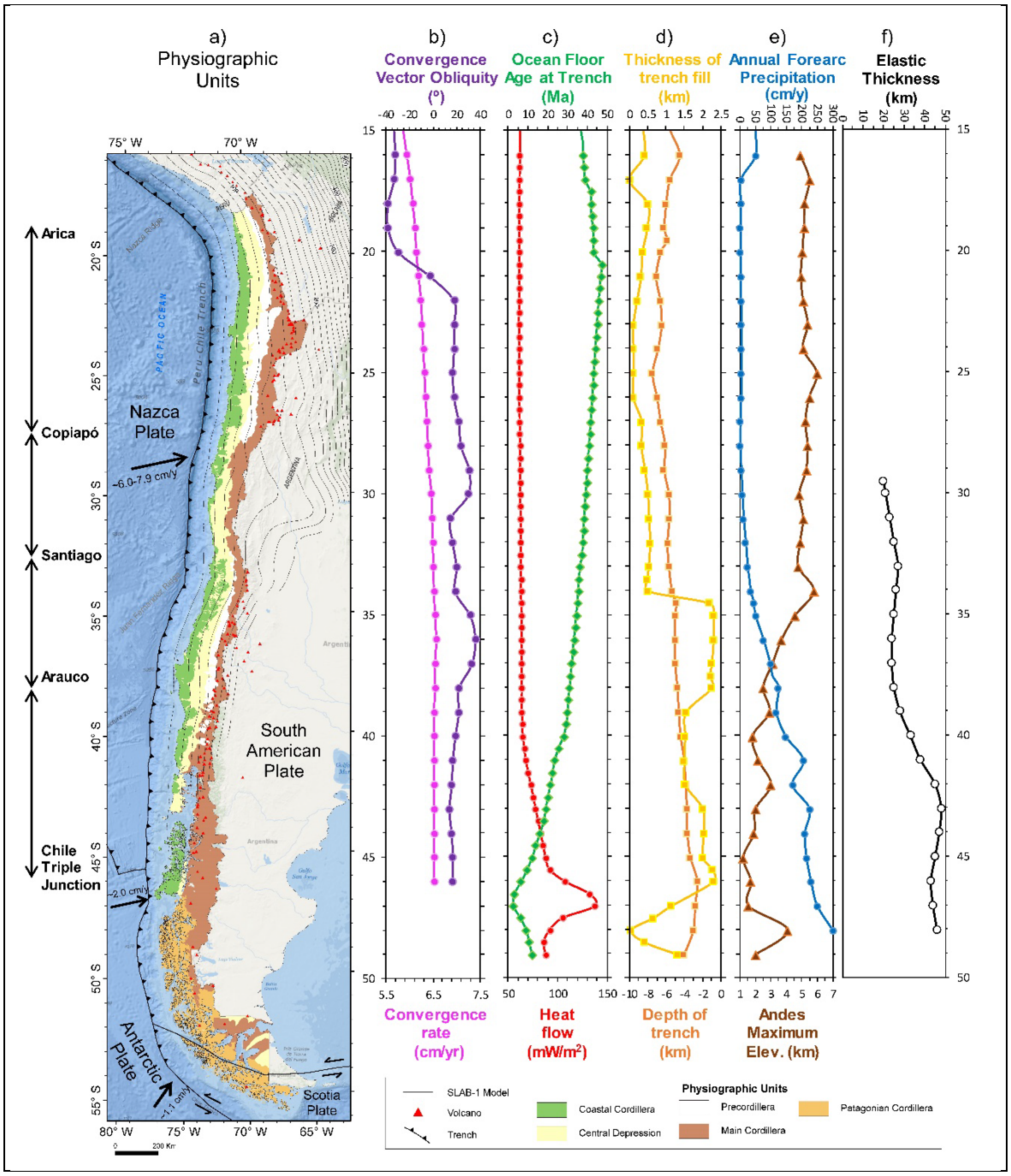

Figure 2-1: Morphotectonic context and segmentation of the Chilean Andes.
(a) The main physiographic units of the Chilean Andes: Coastal Cordillera, Central Depression, Precordillera, Main Cordillera, and Patagonian Cordillera (compiled and modified from Mpodozis and Ramos, 1989; Cembrano et al., 2007; Riquelme et al., 2007; Mpodozis and Cornejo, 2012; Armijo et al., 2015). Red triangles symbolize the present-day volcanic arc. Gray lines show the depth in km of the SLAB-1 model (Hayes et al., 2012), which represents the interface of the converging plates relative to the trench (bold black line). The graphs show: (b) Convergence vector obliquity

and convergence rate (Angermann et al., 1999); (c) the age of the subducting plate from north to south (Müller et al., 1997) and heat flow from Stein (2003); (d) maximum trench depth (shown in orange; Lindquist et al., 2004), which diminishes from N to S, and sediment filling depth (yellow; Bangs and Cande, 1997; Hampel et al., 2004), which increases from 33°S to the south; (e) average annual precipitation along the Chilean forearc (New et al., 2002) and topographic elevations of the Andes (Lindquist et al., 2004); and (f) variation of the crustal elastic thickness (Tassara and Yáñez, 2003).

Additionally, the Chilean continental lithosphere is also longitudinally segmented into three main tectonic domains aligned parallel to the Chilean coastal margin: namely, the Outer Forearc (OF), Inner Forearc (IF), and Volcanic Arc (VA). These domains are associated with the main physiographic units of the Chilean Andes: the Coastal Cordillera, the Central Depression, and the Main and Patagonian Cordilleras, respectively (Pankhurst and Hervé, 2007). These units broadly correspond to the seismic regionalization proposed along Chile by Barrientos (1980), which is used by the Chilean Seismic Design of Buildings Code (Chilean Standard NCh 433), which only accounts for the subduction earthquake hazard.

The aforementioned tectonic segmentation results in diverse deformation styles and subduction convergence rates along the length of Chile, as exemplified by the different fault systems (compressional, transpressional, normal, and strike-slip) and the strain partitioning across the Chilean Andes, which have been active within the same converging regime since the Late Cretaceous and none of which have covered the entire 3500 km length of the mountain range (Hoffmann-Rothe et al., 2006). Inherited structural anisotropy and current geodynamical conditions further complicate the understanding of the seismogenic potential of crustal faults in Chile.

The complicated interaction between the Nazca and South American plates has also complicated the understanding of plate interaction in other Andean countries, such as Peru and Ecuador, where the relationship between subduction and crustal seismicity is only just beginning to be understood (e.g., Machare and Ortlieb, 1992; Paris et al., 2000; Machare et al., 2003; Allmendinger and González, 2010; Costa et al., 2010; Alvarado et al., 2014; Yepes et al., 2016; Alvarado et al., 2016).

Table 2-1: Latitudinal tectonic segmentation of the Chilean Andes.

Segment	Continental margin trend	Subduction Angle (º)	Crustal Thickness	Elastic Thickness	Coupling level	Volcanic arc (actual)	Cenozoic Andean shortening	Trench depth (km)	Trench sediment fill (km)
Arica–Copiapó	N-S	Normal ~25–30°E	Up to 70 km	Low (<10 km) in arc	High	Active	200–300 km	>7.0	0
Copiapó–Santiago	N-S	Flat ~5°E	Up to 60 km	Very low (0–5 km) in arc	-	Non-active	100–200 km	6.0–6.5	<0.5
Santiago–Arauco	NNE	Normal ~25–30°E	<60 km (high-to-normal)	<10 km (medium to high)	Medium	Active	50–100 km	5.0–6.0	0.5–1.0
Arauco–Chile Triple Junction	N-S	Normal ~25–30°E	<40 km (normal to low)	>35 km (high)	Medium to low	Active	<50 km	<5.0	>1.0

Data compiled from: Jordan et al. (1983a, 1983b), Tassara and Yáñez (2003), Yáñez and Cembrano (2004), Asch et al. (2006), Tassara et al. (2007), Ramos (2009b), Gerbault et al. (2009).

2.3 Use of Geological and Paleoseismological Data in the Analysis of Seismic Hazard: Issues and Challenges

The amount, repeatability, and age of last movement on a fault are often included under the concept of fault "activity" and its related hazard. However, despite being widely used, the concept of fault activity has proved to be highly controversial and misleading, since it has no agreed definition (Costa et al., 2006a). For example, an "active fault" can refer to one which has undergone slip in either historic, Holocene, or Quaternary times, depending on the author (e.g., Wallace, 1986; Yeats et al., 1997; Aki and Lee, 2003; McCalpin, 2009; USGS, 2018b). Still other authors define active faults as ones "that may have movement within a future period of concern to humans" (Wallace, 1981), or else fail to define the term at all.

In order to assess the seismic hazard posed by a given fault, it is first necessary to identify whether that fault is capable of generating an earthquake. The seismogenic potential of a fault—that is, the size and recurrence rate of the earthquakes it produces—may be clearer and more tectonically significant when that fault is viewed in the geodynamic context of the subduction earthquake cycle. For example, inactive crustal faults which are optimally oriented with respect to inter- or co-seismic stress fields may be reactivated and produce shallow earthquakes with magnitudes of up to Mw 7 (e.g., Farías et al., 2011; Aron et al., 2013; González et al., 2015). This scenario is particularly relevant for optimally oriented basement (inherited) crustal faults undergoing sudden high strain rates, a condition which can potentially be achieved co-seismically with large megathrust subduction earthquakes (Mw >8; King et al., 1994; Stein et al., 1994; Stein, 1999; Kilb et al., 2000; Lin and Stein, 2004; Loveless et al., 2010; Seeber and Armbruster, 2000). In contrast, during the inter-seismic period, when the crustal deformation rate is relatively low, the reactivation of optimally oriented faults may be less likely (e.g., Aron et al., 2014).

The estimation of earthquake magnitudes from geological data is typically performed using empirical relationships and assumed earthquake parameters based on the

premise that the rupture parameters of an earthquake are proportional to its magnitude (Slemmons, 1977; Hanks and Kanamori, 1979; Bonilla et al., 1984; Slemmons and de Polo, 1986; Wells and Coppersmith, 1994; Hanks and Bakun, 2008; Wesnousky, 2008; and many others summarized in Stirling et al., 2013). Accordingly, the rupture length and surface displacement, which are preserved in the paleoseismological record, can be used in empirical regression relationships to estimate earthquake magnitude. The uncertainties of these parameters must be considered, and the assumption that a fault will always rupture with a constant displacement and slip rate, thus creating a "characteristic earthquake", must be used with caution (Kagan, 1993; Burbank and Anderson, 2001; McCalpin, 2009). Accordingly, the assessment of the key parameters in the field, and the subsequent estimation of other parameters using empirical relationships, are subject to significant uncertainties (see McCalpin (2009) for a review).

Models of fault behavior acknowledge that faults may be segmented into discrete sections that act distinctly over their seismic cycle (e.g., Schwartz and Coppersmith, 1986; Slemmons, 1995). Such segmentation can control the onset and termination of fault rupture, and accordingly can also control the size of the rupture area and earthquake magnitude (Grant, 2002). Commonly, the length of a single fault segment (which may be identified through field observations and/or satellite imagery) indicates the maximum possible surface rupture length during an earthquake, since field features are formed by several ruptures over time. Furthermore, if an inappropriate work scale is chosen, several consecutive segments could be mistaken for a single one. Additionally, fault segments which have generated earthquakes independently of each other may be capable of combining to generate a single segment rupture and thereby generate an earthquake of higher magnitude (e.g., Estay et al., 2016).

The co-seismic displacement of faults is another difficult parameter to assess. The reason for this is that slip is often measured from a colluvial wedge, which forms co-seismically in dip-slip faults (Nelson, 1992; McCalpin, 2009); this estimation requires the assumption that the colluvial wedge has not experienced erosion, represents a single event, and is representative of the entire rupture zone slip. If all of these assumptions are met, the height of the colluvial wedge is considered to be half of the total slip displacement

(McCalpin, 2009). Accordingly, paleoseismological studies should be conducted along the entire length of a fault in order to better represent its behavior. Even when all of this is taken into account, the estimation of earthquake size via paleoseismological or terrain analysis techniques introduces uncertainties which may be difficult to constrain.

2.4 Historical and Instrumentally Recorded Crustal Earthquakes

Seismic data is an essential tool to constrain and characterize plate tectonics. Major seismic catalogs, such as those maintained by the International Seismological Centre (ISC), the National Earthquake Information Centre (NEIC), the ANSS Comprehensive Earthquake Catalog from the USGS (2018a), the Integrated Plate Boundary Observatory Chile (IPOC), and Harvard Centroid Moment Tensor (CMT), include data from crustal earthquakes all over the Chilean Andes. Nevertheless, in several cases, the hypocentral locations of these events are not sufficiently well constrained to distinguish shallow intra-crustal earthquakes from subduction earthquakes. This is particularly important for events recorded in the forearc, where seismicity in the overriding plate detected from teleseismic observations is often masked by the stronger interplate seismicity. Nevertheless, catalog data show a clear concentration of seismicity in the Chilean forearc region, in contrast with scarce intraplate crustal seismicity in the Main Cordillera of the Andes (e.g., Pardo et al., 2002; Asch et al., 2006). Along the length of the Central and Southern Andes, intraplate seismicity tends to be localized within the weak lithosphere, where the brittle–ductile transition is located at less than 15 km depth (Tassara et al., 2007).

There are relatively few published studies which document crustal earthquakes in Chile (e.g., Pardo et al., 2002; Barrientos et al., 2004). In recent years, the Pichilemu Mw 7.0 earthquake (which struck 12 days after the 2010 Maule interplate mega-earthquake) and the Pisagua Mw 6.7 earthquake (16 days before the 2014 Iquique interplate earthquake) have attracted the attention of geologists and seismologists. These events motivated several studies regarding the nature of these events and their tectonic significance in the subduction cycle, due to their spatial proximity to the trench and the

fact that they were temporally associated with Mw 8.8 and Mw 8.1 interplate earthquakes (e.g., Farias et al., 2011; Aron et al., 2014; González et al., 2015).

In order to assess the modern crustal seismicity in the Chilean Andes, we used the Harvard CMT catalog (http://www.globalcmt.org/), which is one of the most accurate global seismic event catalogs (Kagan, 2002). When hypocentral depth is undetermined (which is the case for more than 30% of historical earthquakes in the different earthquake catalogs), a hypocentral depth is assigned based on tectonic setting or nearby seismicity (Bondar et al., 2015). The CMT catalog assigns events a "fixed-depth solution" with an assumed hypocenter located at a depth of 10, 15, or 33 km.

The CMT catalog was searched for earthquakes located in the Chilean Andes having hypocentral depths shallower than 50 km and magnitudes above Mw 4.9 and occurring in a 39 year period between January 1976 and April 2015. This search yielded 6601 events. The information for each event included the date, latitude, longitude, depth, half-duration, moment tensor, magnitude metrics (Mw, Ms, mb, etc.), and fault-plane solution. From this population we selected 372 earthquakes that were considered to be of crustal origin by eliminating events that were determined to be subduction-related via analysis of their focal mechanisms while also eliminating events with poorly determined hypocentral locations (Figure 2-2). These 372 events are spatially distributed in two bands, one in the coastal outer forearc and one located inland in the volcanic arc.

Several earthquakes from this population of 372 events have been of scientific and/or public interest due to their large magnitude (Mw >6.0) and shallow hypocentral depth (<16 km). The epicentral locations of these events are distributed across several different latitudinal and longitudinal domains and are good models of crustal earthquake types, as explained later in this section (see Table 2-2). Moreover, the hypocenters and focal mechanisms of some of these earthquakes correspond strongly with the identified traces and slip characteristics of crustal faults in the region.

In this section, we detail some prominent crustal earthquakes (Mw >6.0) among the 372 crustal earthquakes that were selected from the CMT catalog (see Figure 2-2).

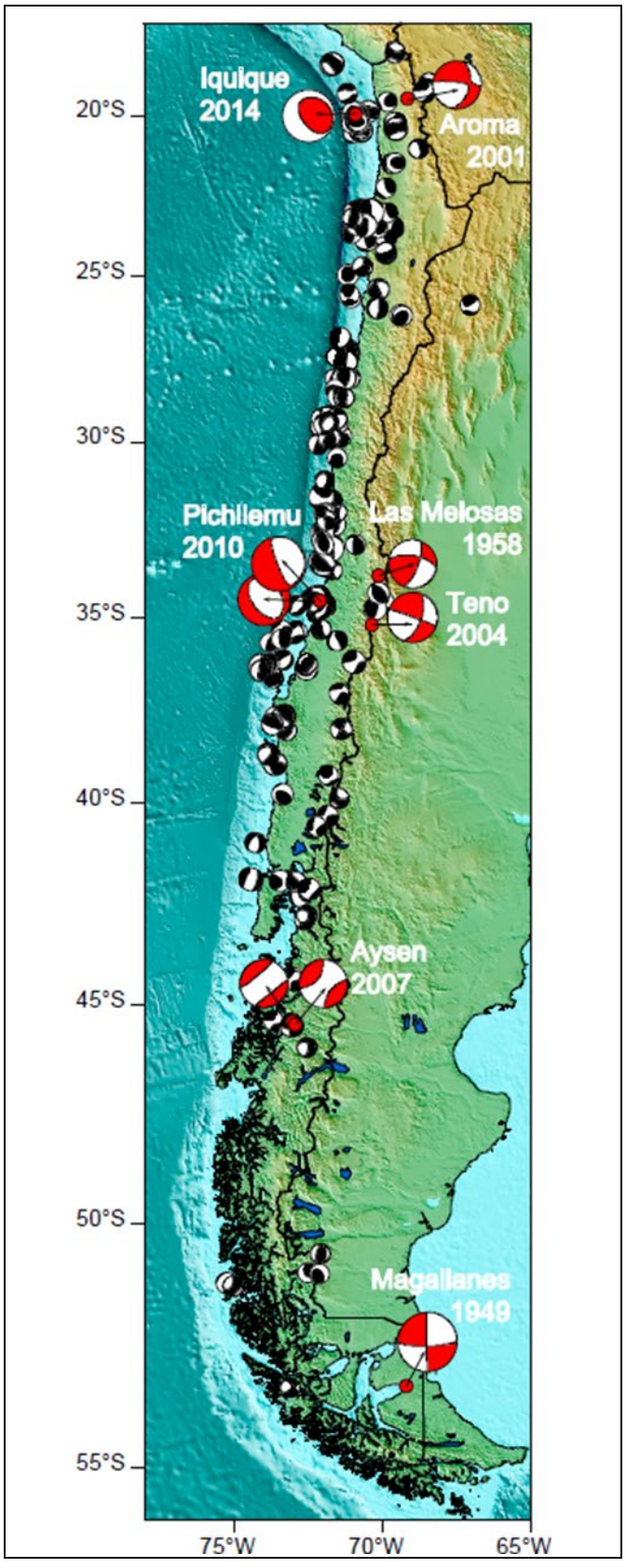

Figure 2-2: Map showing the locations of 372 crustal earthquakes recorded along the Chilean Andes between January 1976 and April 2015.
Data are taken from the Harvard Centroid Moment Tensor (CMT) catalog (http://www.globalcmt.org/). Circle sizes correspond to magnitude. Focal mechanisms of crustal earthquakes with Mw ≥6 are displayed. Larger historical crustal events are highlighted with red focal mechanisms: Aroma 2001, Iquique 2015, Las Melosas 1958, Pichilemu 2010, Teno 2004, Aysén 2007, and Magallanes 1949.

Table 2-2: Selected instrumentally recorded crustal earthquakes in Chile.

Location	Year	Magnitude (Mw)	Epicentral Location			Reference	Longitudinal Tectonic Domain
			Latitude (°S)	Longitude (°W)	Depth (km)		
Aroma	2001	6.3	19.5	69.2	~5.0	Legrand et al. (2007)	Inner forearc
Las Melosas	1958	6.3	33.9	70.2	5.0–9.0	Alvarado et al. (2009)	Arc
		6.9-6.7-6.8				Sepúlveda et al. (2008)	
Pichilemu	2010	6.9	34.5	72.1	~12.9	Farías et al. (2011)	Outer forearc
		7.0			16.3	Aron et al. (2013)	
Teno	2004	6.5	34.9	70.6	4.7	González (2008)	Arc
Aysén	2007 (21 Apr)	6.2	45.4	73.0	<8.0	Mora et al. (2010)	Arc
					4.0	Legrand et al. (2011)	
Aysén	2007 (02 Apr)	6.1	45.4	73.1	5.3	Legrand et al. (2011)	Arc

2.4.1 2001 Aroma Earthquake, Inner Forearc Domain

A Mw 6.3 earthquake occurred on 24 July 2001 in the Aroma region of Northern Chile (Table 2-2, Figure 2-2). This event is one of the few shallow earthquakes to have occurred in Northern Chile in recent years (Comte et al., 2001). Legrand et al. (2007) used seismic data to locate the event and its aftershocks. Additionally, the same authors constrained the focal depth of the event using the SP phase and its focal mechanism. Their analysis returned a fault plane solution of the main event with a strike of 14 ± 10°, a dip of 53 ± 15°, and a rake of 163 ± 15°, indicating dextral movement on an oblique fault. This is consistent with the distribution of aftershocks, which indicated a fault direction of N14°E and a dip of 50°E. Additionally, Legrand et al. (2007) determined the earthquake's hypocentral depth to be 5 ± 1 km, although neither surface deformation nor related morphotectonic features were reported.

2.4.2 1958 Las Melosas Earthquake, Volcanic Arc Domain

On 04 September 1958, a seismic event with a hypocentral depth of 15 km was recorded in the Cordillera Principal region, near the intersection of the Maipo and Volcán rivers (Table 2-2, Figure 2-2). No field evidence of surface rupture associated with this event was observed (Sepúlveda et al., 2008). The earthquake involved a sequence of three separate events with surface wave magnitudes of between Ms 6.7 and 6.9 (Sepúlveda et al., 2008) and moment magnitudes of Mw 6.3 (Alvarado et al., 2009). The focal mechanism of the main event is consistent with either sinistral slip on a NS-oriented fault plane or dextral slip on a nearly EW-striking fault plane (Lomnitz, 1960; Sepúlveda et al., 2008; Alvarado et al., 2009; Alfaro, 2011). Sepúlveda et al. (2008) analyzed the hazard associated with the Las Melosas earthquake, estimating intensities and Peak Ground Acceleration (PGA) values from the reinterpretation of historical documents and the study of landslides caused by similar earthquakes. The maximum felt intensity (MSK scale) was 9 in the epicentral area and 6 at a distance of 40 km from the hypocenter. Furthermore, according to analysis of two landslides, which were triggered by this event using the Newmark method, a PGA of 0.58−1.30 g was estimated for the event. These findings

highlight the large seismic hazard that exists near this blind fault, which occurs close to the El Fierro Fault System (Farías et al., 2010).

2.4.3 2004 Teno Earthquake, Volcanic Arc Domain

A magnitude Mw 6.7 earthquake occurred on 28 August 2004 in the Cordillera Principal of the Maule region, near the headwaters of the Teno River, north of Peteroa volcano (Comte et al., 2008; González, 2008; Alfaro, 2011). According to the National Seismological Service of Chile, the hypocenter was located at 35.2°S, 70.5°W, and 5 km depth, with a local magnitude of ML 6.2. The focal mechanism for this event given in the Harvard CMT catalog indicates either dextral movement on a fault plane 21/61 and a rake of −178 or sinistral movement on a fault plane 290/88 and a rake of −29. González (2008) relocated the hypocenter at 34.9°S, 70.5°W, and 4.7 km depth. By analyzing aftershocks which occurred near to this structure, she was able to delimit a structure trending N20E and dipping to the west with a length of 18 km and a depth of 11 km. The same author also suggests a northward spreading of the rupture, from the area of Termas del Flaco to the Maipo River valley, where a Mw 5.6 magnitude earthquake with a reverse focal mechanism occurred on 12 September 2004. If we consider the focal mechanism reflecting a NNE-oriented structure and associated dextral fault movement, this earthquake would relate coherently with east-vergent fault systems that reflect the tectonic control proposed by various authors in the south-central Principal Cordillera area (e.g., the El Diablo Fault in Fock, 2005 and the El Fierro fault in Farías, 2007).

The intensities recorded by the Chilean National Seismological Service for the Teno earthquake reveal that only moderate-to-weak damage was caused in the Teno area, with a maximum intensity of VI on the Modified Mercalli Intensity Scale, while in the Talca and Curicó areas, intensities of V to VI were recorded.

2.4.4 2007 Aysén Earthquakes, Volcanic Arc Domain

In 2007, a swarm of 7200 events occurred within a small area in the Aysén Fjord region of Southern Chile. The largest two earthquakes in this swarm were the Mw 6.1 and

Mw 6.2 earthquakes of April 2007. These events triggered a landslide which induced a tsunami that killed 10 people (Mora et al., 2010; Legrand et al., 2011). The hypocentral depths of the two events have been variously estimated at less than 12 km (Legrand et al., 2011) and at 8 km (Mora et al., 2010). Fault plane solutions indicate an almost NS strike and a high dip, similar to the other events in the swarm, which is consistent with the long- and short-term tectonics of the Liquiñe–Ofqui Fault System (LOFS). The earthquakes of this swarm have also attracted research interest due to their combined tectonic and volcanic origin (Legrand et al., 2011).

The locations of these earthquakes coincide with the Punta Cola Fault (PCF) and with the location of the submarine rupture observed in sub-bottom profiles (Vargas et al., 2013; Villalobos-Claramunt et al., 2015). The PCF, a main branch of the LOFS, is a 15–20 km long NS-striking structure that crosses the Aysén Fjord about 5 km to the east of the main Liquiñe–Ofqui Fault (Legrand et al., 2011),

2.4.5 2010 Pichilemu Earthquakes, Outer Forearc Domain

A series of crustal earthquakes were felt in the area of Pichilemu, Central Chile, for more than a year following the Mw 8.8 Maule subduction earthquake that struck Central Chile on 27 February 2010 (Arriagada et al., 2011; Alfaro, 2011; Farías et al., 2011).

The magnitudes of the two main events in this series, which occurred on 11 March 2010, were Mw 6.9 and 7.0 (Farías et al., 2011). Additionally, significant aftershocks with magnitudes of Mw 6.4, 6.1, 6.0, and 5.9 were also recorded. Both, the aftershocks and the largest earthquake, had normal fault plane solutions (Harvard CMT catalog).

The epicenters of the Mw 6.9 and 7.0 earthquakes were located at ~34.3°S, 71.9°W, and the events had hypocentral depths of 12 and 20 km, respectively, and had normal-type focal mechanism solutions with fault planes trending 144/55/90 and 155/74/90 (Ruiz et al., 2014). The Mercalli intensities of these two earthquakes recorded by the ONEMI were VII in Rancagua and VI in Talca, while the USGS recorded intensities of IX near Pichilemu town (Alfaro, 2011).

The earthquake series and its aftershocks correlate spatially with a NW-oriented normal fault dipping to the SW from the surface to the interplate boundary. Equally oriented extensional fault structures in the region are shown in the 1:1,000,000 scale geological map (Sernageomin, 2003).

The 2010–2011 earthquake series has been proposed to have been caused by the large change in Coulomb stress caused by the Maule earthquake (Farías et al., 2011; Aron et al., 2013). These authors link the Pichilemu earthquake with other neotectonic activity, in agreement with the short-term deformation, and suggest that this event may have been closely related to the long-term subduction seismic cycle: namely, extensional faulting during co-seismic subduction earthquakes and thrusting events in the inter-seismic period.

2.5 Neotectonic Crustal Faults

Chile hosts several prominent crustal faults which have undergone neotectonic activity and which are predominantly spatially and/or temporally associated with strike-slip fault systems formed by the strain partitioning since at least the Middle Jurassic (Hoffmann-Rothe et al., 2006). In this work, we reassess and compile over 1600 faults from existing publications (Figure 2-3). The basis of our work included the compilations of Lavenu et al. (2000), Lavenu (2005), PMA (2009), and SARA (2016).

The main neotectonic crustal faults and fault systems in Chile are spatially distributed across the three main longitudinal tectonic domains that are oriented parallel to the country's coastline: namely, the Outer Forearc (OF), the Inner Forearc (IF), and the Volcanic Arc (VA). These domains are crossed by a series of long-lived transverse faults (T). Previous research has primarily focused on geomorphological and tectonic analysis, with relatively very few paleoseismological studies being carried out. More than 1000 fault structures which are regarded as having neotectonic activity but for which a rigorous assessment of basic fault parameters has not been performed are currently under study. This lack of basic fault parameter data is largely due to the fact that neotectonic faults are spatially associated with older tectonic structures, which makes it difficult to separate

ancient activity from recent activity. In the current work, we characterize 141 faults using various fundamental parameters for the assessment of seismic hazard by compiling information from well-studied faults (Figure 2-3).

Figure 2-3: Compilation of crustal faults in the Chilean Andes which show evidence of neotectonic activity.

Normal faults are shown in blue, reverse faults in red, strike-slip dextral faults in green, strike-slip sinistral in magenta, and undetermined faults are shown in black. Many of the faults belong to fault systems such as the Atacama Fault System (AFS), the East-West Transverse Fault System (EWFS), the West-Vergent Thrust Fault System (WVFS), the Domeyko Fault System (DFS), the Liquiñe–Ofqui Fault System (LOFS), and Andean Transverse Faults (ATF).

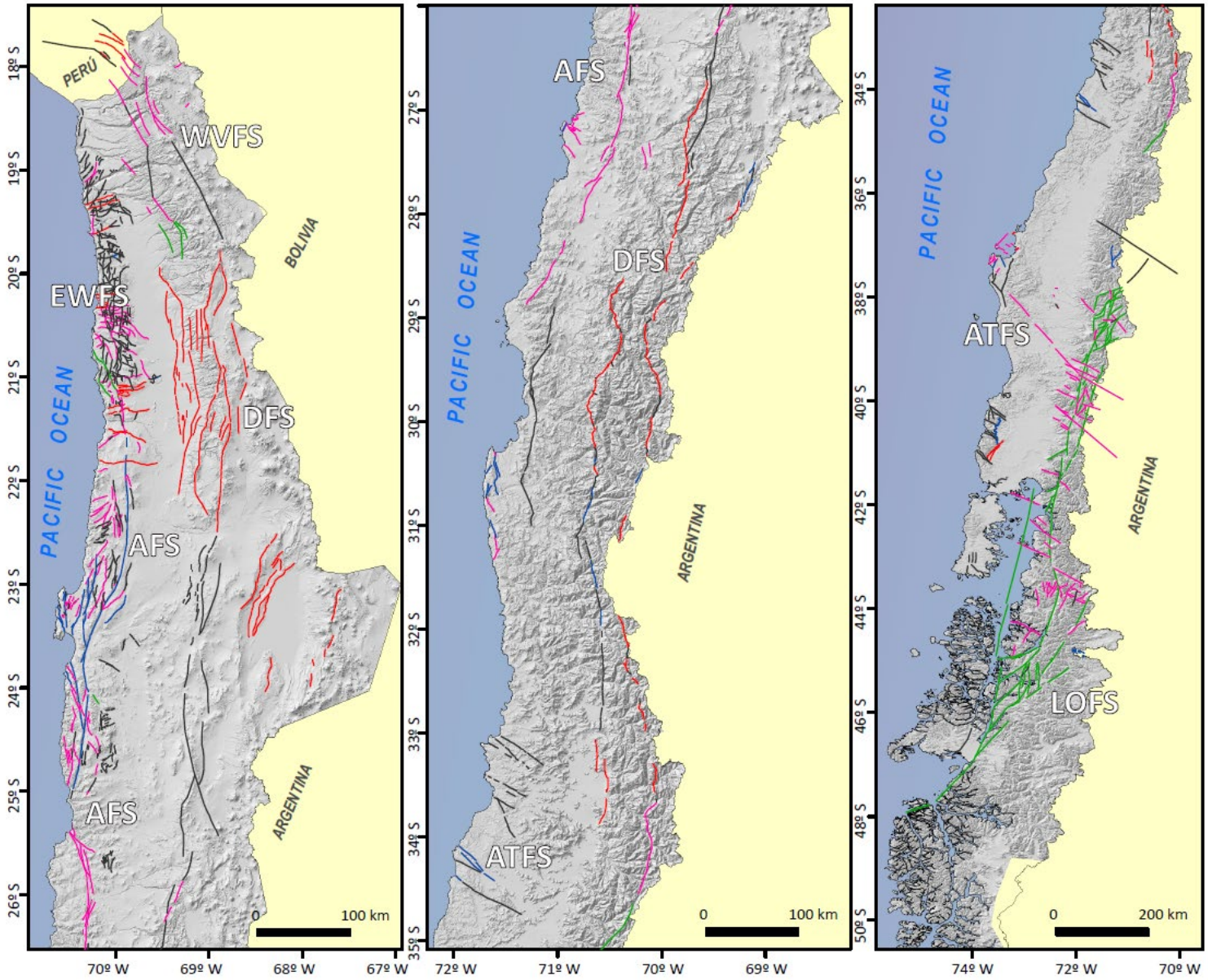
PERÚ
BOLIVIA
ARGENTINA
PACIFIC OCEAN
WVFS
EWFS
DFS
AFS
AFS
ATFS
LOFS
0
100 km
200 km
18º S
19º S
20º S
21º S
22º S
23º S
24º S
25º S
26º S
27º S
28º S
29º S
30º S
31º S
32º S
33º S
34º S
35º S
36º S
38º S
40º S
42º S
44º S
46º S
48º S
50º S
70º W
69º W
68º W
67º W
72º W
71º W
70º W
69º W
74º W
72º W
70º W

2.5.1 Outer Forearc Domain

The master faults of the outer forearc strike predominantly NS and exhibit concave morphologies (e.g., the three segments of the AFS; Arabasz, 1971). Regional-scale fault segments are steeply dipping and have lengths of up to several hundreds of km. These structures commonly display evidence of early strike-slip to late dip-slip displacement. NW-striking subvertical secondary faults splay off the master faults and show similar kinematics to the master faults. The most relevant faults of the outer forearc domain are the following:

2.5.1.1 Atacama Fault System

The AFS is a ca. 1000 km long fault zone running along the Coastal Cordillera of Northern Chile from Iquique (20°S) to La Serena (30°S). The AFS has been the focus of several studies since the late 1960s due to its prominent geomorphological characteristics, which reflect a displacement history dating to the Jurassic. Three main segments of the AFS have been identified, all of which are curved and concave to the west: namely, the Salar del Carmen, Paposo, and El Salado segments (Okada, 1971; Arabasz, 1971; Naranjo, 1987; Hervé, 1987).

The earliest AFS activity is evidenced by mylonitic and cataclastic rocks formed under sinistral displacements in the volcanic arc as result of oblique convergence in the Jurassic–Early Cretaceous (Scheuber and Andriessen, 1990; Brown et al., 1993).

Progressive cooling of the magmatic arc in the mid-Cretaceous may have coincided with a change in the deformation style of the AFS from ductile sinistral strike-slip to brittle sinistral strike-slip (Brown et al., 1993). The structures generated in this brittle phase of the AFS are duplex-type, limited by NS- and NW-trending strike-slip faults, and segmented into numerous sections, each of which exceeds 60 km in length (e.g., Cembrano et al., 2005).

Several authors have documented regional-scale sinistral and locally dextral strike-slip displacements along various segments of the AFS. However, the main Neogene-to-recent displacements are normal-style, which is consistent with the extensional regime of the present-day forearc (Arabasz, 1971; Okada, 1971; Hervé, 1987; Naranjo, 1987; DeLouis et al., 1998; Scheuber and González, 1999; González et al., 2003; Riquelme et al., 2003; Cembrano et al., 2005; González et al., 2008; Vargas et al., 2011; Allmendinger and González, 2010; Cortés et al., 2012). Quaternary deformation of the AFS is preserved in the horst-and-graben and hemi-graben coastal topography, developing fault scarps with heights from a few meters to over 100 meters.

Seismic activity had not been definitively associated with any segments of the AFS until the study of Metcalf and Kapp (2015). These authors compiled crustal seismicity data from existing catalogs, and found extensional focal mechanisms in the forearc region, consistent with the distribution of mapped active fault scarps. However, this interpretation should be viewed with caution considering that the seismic data which were used were not obtained from local networks.

One of the best-known segments of the AFS fault is the Salar del Carmen fault (SCF), which develops near Antofagasta (23°S) as a N15°E-striking, 75°SE-dipping normal fault. Several displaced ~400 ka old alluvial-fan sediments, which form east-dipping scarps with heights between 3 and 5 m, reflect the most recent deformation along the AFS (González et al., 2006; Cortés, 2012). These authors constrain the age of the youngest displacement on the SCF to the Late Pleistocene. More recent work including paleoseismological trenching and Optically Stimulated Luminescence (OSL) dating of colluvial sediments indicates that the SCF has generated at least two earthquakes in the last ca. 5 ka, with ~2.2 m of fault slip for each event. Additionally, by using relationships from Wells and Coppersmith (1994), it has been estimated that each earthquake had a Mw of ~7 (Cortés, 2012).

2.5.1.2 Mejillones Fault

The Mejillones Fault (MF) is a 40 km long (30 km onshore, 10 km offshore to the north), N10°E-striking, 75°SE-dipping normal fault located in the northern Mejillones Peninsula, 60 km NW of Antofagasta city. Activity on this fault has been established since at least 3.3 My, and has formed a conspicuous scarp with a height of ~500 m at its northern termination and progressively lowering southward to ~65 m in height (Marquardt, 2005). The most recent activity on the MF is expressed in the deformation of the piedmont area, which formed an escarpment in Late Pleistocene alluvial gravels (Marquardt et al., 2004; Cortés et al., 2012). This escarpment has an approximate length of 12 km and reaches a height of 3–10 m.

The surface rupture pattern of the MF indicates that the fault consists of at least two segments which are connected at depth (Cortés et al., 2012). By combining morphological observations, maps of displaced alluvial surfaces, ^{10}Be dating, OSL dating of colluvial deposits at the foot of the escarpment, and paleoseismological trench mapping, it has been determined that this fault has generated two earthquakes of Mw ~7 between ca. 35 ka and ca. 14 ka, as well as possibly an earthquake of Mw ~6.6 more recently (ca. 3 ka). These results indicate a slip rate of 0.61 ± 0.26 mm/y during the first three intervals of the fault evolution and a slip rate of 0.22 ± 0.06 mm/y during the fourth interval. The displacement involved in each of these events has been estimated to range from 0.7–2.2 m, distributed along rupture surfaces ~40 km in length and 23 km in width. Recurrence times for earthquakes of Mw ~7 on the MF has been estimated at 5.0 ± 3.5 ka (Cortés et al., 2012).

2.5.1.3 Caleta Herradura Fault

The Caleta Herradura (CHF) fault is located in the southwestern half of the Mejillones Peninsula (Arabasz, 1971; Okada, 1971). Its morphological expression, an escarpment in Quaternary alluvial gravels, suggests that this is a normal fault with conspicuous tectonic activity. The CHF has a length of ~40 km, and five distinct fault sections can be identified. These have accumulated hectometric displacement (Espinoza,

2013; Marquardt, 2005). The state of preservation of the Quaternary scarps is similar to that of the MF, and therefore a late activity of similar age, from Pleistocene to Holocene times, is inferred (Cortés-Aranda et al., 2014). Ongoing research on neotectonic activity on the CHF suggests a transfer of deformation between the MF and the CHF, likely through a connection between the two at a depth of around 15 km.

2.5.1.4 E-W Fault System

One of the most distinctive features of the Coastal Cordillera of Northern Chile is a series of EW-oriented topographic highs located between 19º and 22ºS latitude which are spatially associated with eroded fault- and fold-scarps which form the E-W Fault System (EWFS). These scarps are between 20 and 300 m in height, contain open fractures in zones with widths of 20–1600 m, and extend from the coast to the eastern side of the Coastal Cordillera, ending in fault-propagation folds affecting the Tertiary infill of the Central Depression (Allmendinger et al., 2005; González et al., 2008). The scarps are associated with reverse faults oriented sub-perpendicular to the (NS-oriented) coastline, with dip-slip displacement being accommodated parallel to the trench shortening (Allmendinger et al., 2005; González et al., 2008; Allmendinger and González, 2010). Some of the scarps are related to emergent reverse faults while others result from surface folding by blind reverse faults.

Morphotectonic and geochronological studies conducted at a local scale, as well as regional-scale mapping, indicate that the EW-oriented scarps formed in the Late Miocene to Early Pliocene, and that activity persisted into the Quaternary (Allmendinger et al., 2005). The scarps blocked the ancient drainage system, leading to the formation of evaporite deposits. The authors suggest that climatic conditions in the Coastal Cordillera were probably wetter during the Late Miocene–Pliocene than during the present day. Their results further indicate that the Coastal Cordillera uplift is younger than Middle Miocene and/or that the Coastal Escarpment has retreated substantively to the east (Allmendinger et al., 2005), and suggest that the origin of the EWFS is linked to the curved continental

margin of the Bolivian Orocline, due to its limited latitudinal extent. Moreover, the EWFS may be associated with north-trending shortening resulting from the oblique convergence between the Nazca and South American plates (e.g., Allmendinger et al., 2005; Carrizo et al., 2008).

The Bajo Molle Fault (BMF), located to the south of the city of Iquique, is one of the ~EW-striking transverse faults exposed in the coastal cliff area with an orientation of N80°E/30°NW. The most recent activity on this fault is evidenced by a gently sloping fold scarp produced by fault propagation, placing Jurassic volcanic rocks above Late Pleistocene marine deposits (Allmendinger and González, 2010). The OSL dating of deformed marine deposits suggests that at least one Mw 7.0 earthquake has occurred on the BMF in the last 10 ka (González et al., 2015, Supplemental Information). These authors estimated an uplift rate of 0.38 ± 0.02 mm/y, a horizontal shortening rate of 0.135 ± 0.015 mm/y, and a net slip rate of 0.4 ± 0.1 mm/y. Calculations suggest that the rupture displacement for the Mw 7.0 event was 0.3–2.0 m, and that this displacement was distributed between the main fault and its branches. Based on two methods, the depth of the earthquake source was ~14 km (González et al., 2015, Supplemental Information).

2.5.1.5 Chomache Fault

The Chomache Fault (ChF) is a strike-slip fault aligned N42°W/78°NE which is located at 21°10' S, in the vicinity of Salar Grande. The main evidence of recent activity on this fault is the dextral offset of channels which are developed in Quaternary alluvial surfaces. This deformation pattern occurs along the three main segments of the ChF for a total length of 20 km (González et al., 2003; Masana et al., 2005; Carrizo et al., 2008; Allmendinger and González, 2010). The OSL dating of alluvial/colluvial deposits and paleoseismological trench mapping suggest that at least two seismic events of Mw ~7 have occurred along this fault during the last ca. 4 ka. The fault displacement for these events has been estimated at 3–6 m over a rupture area with a length of around 20 km and a width

of ≥20 km. The time between two events was ~2.1 ka, which gives some indication of the recurrence time of Mw ~7 earthquakes on the ChF.

2.5.1.6 Pichilemu Fault

Two earthquakes, one with Mw 6.9 and one with Mw 7.0, occurred 12 days after the 2010 Mw 8.8 Maule megathrust earthquake. These nucleated on the Pichilemu Fault (PF), an upper-plate normal-fault (Aron et al., 2013). The focal mechanisms of these events showed that the rupture planes have an orientation of 145°/55º and 155º/74º, respectively, and extend down to the plate interface, which in this region lies at a depth of approximately 33 km (Farías et al., 2011; Ryder et al., 2012; Aron et al., 2013; Ruiz et al., 2014). Ryder et al. (2012) and Ruiz et al. (2014) suggest that both earthquakes were related to part of a typical normal-fault diverging splay where the secondary fault connects to the main fault at depth. Interferometric Synthetic-Aperture Radar (InSAR) and GPS measurements show that ~0.6 m of vertical offset occurred during the main Mw 7.0 event, while finite-slip inversions suggest maximum normal-fault displacements of ~3 m (2.4 m along the vertical component) at a depth of 10–11 km (Ryder et al., 2012).

The main fault plane of the Pichilemu earthquake has been spatially associated by Aron et al. (2014) with a 141°-striking SW-dipping normal-fault trace mapped in the 1:1,000,000 geologic map (Sernageomin, 2003). Several studies have concluded that there was no surface rupture associated with the 2010 Pichilemu earthquakes (Arriagada et al., 2011; Farías et al., 2011; Aron et al., 2014). Nevertheless, Aron et al. (2014) state that the geological relations found in the field, as a history of Pleistocene–Holocene uplift of paleo-beach sequences in the footwall, indicate that the Pichilemu fault has repeatedly broken the surface in the past and has moved as a normal fault.

2.5.2 Inner Forearc Domain

The fault systems of the inner forearc exhibit a general NS strike, a sinuous shape, and splay faults to both the west and east (e.g., the Domeyko Fault System; Reutter et al., 1991, 1996). The main fault segments reach tens of kilometers in length, have subvertical dips, and exhibit both dextral and sinistral strike-slip movements. There are also reverse faults, such as the West-Vergent Thrust System (WVTS) in Northern Chile (Muñoz and Charrier, 1996) and the San Ramon Fault in Central Chile (Vargas et al., 2014).

2.5.2.1 Domeyko Fault System

The Domeyko Fault System (DFS) is an anastomosed system of mostly NS-striking, steeply-dipping faults comprising a complex array of strike-slip, normal, and reverse faults, together with thin- and thick-skinned folds and thrusts. The DFS is traceable parallel to the Chilean Trench for more than 1000 km and has a width of 40–60 km (e.g., Reutter et al., 1991, 1996; Cornejo et al., 1997; Lindsay et al., 1995; Mpodozis and Cornejo, 2012). The DFS consists of several regional-scale segments, each of which has undergone distinct deformation events at various times.

The DFS has been active since the Upper Eocene–Lower Oligocene (Reutter et al., 1996), and has contributed to the emplacement and mineralization processes of some of the largest porphyry copper deposits on Earth. Many authors have documented an initial dextral strike-slip movement in the Incaic tectonic phase, followed by sinistral deformation associated with lower convergence rates (e.g., Reutter et al., 1996; Lindsay et al., 1995). The youngest deformation is evidenced by dextral strike-slip fault zones, the same kinematic regime that prevailed during the earliest Eocene–Oligocene phase. Tectonic inversion of this fault system is evidenced by the dissimilar displacement amounts that have been determined for dextral and sinistral displacement, respectively: namely, dextral displacement of 0.5–2.0 km and sinistral displacement of 35–37 km (Reutter et al., 1991; Tomlinson and Blanco, 1997a, b).

Seismic records from the Domeyko Cordillera at 21ºS show that the present-day activity of the DFS includes, at least in part, both dextral- and reverse-faulting kinematics (Salazar, 2011; Bloch et al., 2014). Field observations in the Chuquicamata mine pit document active *en echelon* tension cracks, further supporting ongoing dextral displacement along traces of the DFS (Daniel Faulkner, Thomas Mitchell, Erik Jensen, pers. comm., 2011).

2.5.2.2 San Ramón Fault

Studies carried out along the San Ramón fault (SRF) associate this fault with the structural system which controls the morphotectonic boundary between the Central Depression and the Main Range in Central Chile, at a latitude of approximately 33ºS, near the eastern fringe of the Santiago de Chile metropolitan region (Farías, 2007; Armijo et al., 2010; Rauld, 2011). This west-vergent reverse structure is part of the larger West Andean Thrust system, where regional-scale deformation has migrated eastward (Farías, 2007). Surface observations show that volcanoclastic rocks of the folded and faulted Eocene–Miocene Abanico Formation thrust over Quaternary deposits (Rauld, 2002).

The surface morphology in the region of the SRF is a semi-continuous escarpment that extends north-south for at least 35 km, from the Mapocho River to the Maipo River (Armijo et al., 2010), decreasing its expression southward. Rauld (2011) applied a kinematic deformation model to the mountain front and piedmont, where a series of west-verging kilometric folds affect rocks of the Abanico and Farellones (both Miocene) formations. These structures were modeled by the propagation of a fold-thrust-belt to the west by four reverse faults with dips of 45–65º attached to a detachment plane with a dip of 4–5ºE at a depth of 10–12 km.

Rauld (2011) conducted a quantitative study of deformation associated with fault scarps in the Andean piedmont (Lower Pleistocene–Holocene deposits) and its morpho-stratigraphic relationship with deformed fluvial terraces of the Maipo and Mapocho Rivers. The results showed fault scarps with heights of 3–200 m along three segments.

The terraces of these two rivers (which were dated using OSL) are deformed by the SRF, suggesting Pleistocene incision rates of 0.5–1.0 mm/y.

A more recent study using fault trenching and cosmogenic isotope data documents two large earthquake ruptures (Mw 7.5) on the SRF within the past 8–19 ka, with fault displacements of ~5 m in each event (Vargas et al., 2014). Other research shows scattered present-day (recorded between 2000 and 2011) crustal seismic activity clustered at a depth of around 10 km around 20–25 km east of Santiago (Perez et al., 2014). According to Perez et al. (2014), these data provide the first evidence of seismic activity that is consistent with the crustal-scale structural model proposed for the SRF system in the area (Armijo et al., 2010). Additionally, Perez et al. (2014) modeled different rupture models for a Mw 6.9 earthquake on the San Ramon Fault, obtaining maximum PGA values on the order of 0.7–0.8 g.

Recently, Estay et al. (2016) defined four segments along the trace of the SRF, with a mean length of 10 km. They used time-integration methodologies to estimate the most likely scenarios of rupture and seismic event distribution along the fault, and also used Transient Electromagnetic (TEM) measurements to constrain the fault dip angle (65°) and the fault's capacity for surface rupture. Furthermore, by subsequently applying the empirical equation of Chiou and Youngs (2014) for crustal faults and considering the characteristic seismic event (high-angle thrust fault, 10 km length, Mw 6.2–6.7), the authors provided estimates for the PGA distribution in Santiago that would be caused by such an event, and thereby identified hazard zones which are capable of experiencing PGA in excess of 0.5 g.

2.5.2.3 West-Vergent Thrust System

The WVTS is the largest tectonic feature in the Precordillera of Northern Chile. The system, which is of Miocene–Pliocene age, flanks the western reach of the Altiplano (Muñoz and Charrier, 1996), and has emplaced Precambrian rocks over Neogene rocks. Faults can be observed at the surface at 18°S; further south, these faults turn blind, and

form surface flexures. The WVTS may be responsible for part of the uplift of the Altiplano (David, 2007, Farías et al., 2005).

Seismic activity on the WVTS has been documented by David et al. (2002) and Legrand et al. (2007). This activity includes the 2001 Mw 6.3 Aroma earthquake, which had a dextral focal mechanism, similar to WVTS earthquakes reported further to the south and east by Salazar (2011). Although the Aroma earthquake did not develop a surface rupture, its hypocentral position has been correlated with a high-angle reverse fault that underlies a regional-scale flexure at the western boundary of the Domeyko Cordillera (Farías et al., 2005).

2.5.3 Volcanic Arc Domain

The present-day volcanic-arc faults exhibit roughly north-south strikes with horsetail-type terminations, subvertical dips, and strike-slip kinematics (e.g., LOFS; Cembrano et al., 1996). These develop in the present-day volcanic arc region, where deformation partitioning has taken place from at least the Late Miocene.

2.5.3.1 Liquiñe–Ofqui Fault System

The LOFS is the most prominent seismogenic crustal fault in the Chilean Andes. It runs for more than 1200 km from Copahue Volcano in the north (37°S) to Golfo de Penas in the south (47°S), which lies approximately 150 km SE of the Chile Triple Junction. Early studies by Moreno and Parada (1976), Hervé (1976), and Hervé et al. (1979) recognized the LOFS only along its northern stretch. Later, Forsythe and Nelson (1985) identified and studied the southernmost segments of the LOFS, and postulated a causal link between the Chile Ridge subduction and Cenozoic activity of the fault system. Field, structural, and geochronological studies conducted in the 1990s by Pankhurst et al. (1992), Cembrano and Hervé (1993), Cembrano et al. (1996), and Lavenu and Cembrano (1999) provided regional-scale constraints on the geometry, nature, and timing of ductile-to-

brittle deformation along the fault system. The LOFS is currently regarded as a major dextral strike-slip duplex associated with both Miocene–Pliocene deformation and present-day volcanism. In the last decade, more detailed structural and geochronological studies have documented Pliocene ductile-to-brittle transpressional deformation within a regional-scale transpressional double-vergent system associated with high exhumation rates during the last 4 Ma (Adriasola et al., 2006; Cembrano et al., 2002, Thomson, 2002; Rosenau et al., 2006).

Brittle fault segments, tens of kilometers in length, commonly overprint pre-existing ductile deformation zones along the LOFS, forming typical strike-slip fault geometries such as duplexes, Riedel-type splay faults, pull-apart basins, and tension cracks that are spatially associated with Holocene volcanoes. The master fault has an orientation of N10°E, and subsidiary branches of this fault are mainly NE- to ENE-striking faults.

Teleseismic data and data from local seismic networks show that the LOFS is currently active as a dextral strike-slip fault (e.g., Cifuentes, 1989; Lange et al., 2008; Legrand et al., 2011; Mora et al., 2010; Agurto et al., 2012; Agurto et al., 2014). Recent seismic activity on the LOFS includes the April 2007 Mw 6.2 dextral strike-slip earthquake, which had a hypocentral depth of 4 km and was one in the swarm (from January to June 2007) of thousands of lower-magnitude earthquakes, including one normal dip-slip Mw 6.1 earthquake on a NE-striking splay fault with a hypocentral depth of 5.3 km (Legrand et al., 2011). Legrand et al. (2011) re-located 10 events, obtaining hypocentral depths between 1 and 8.5 km. Sielfeld et al. (2017) report maximum depths for tectonic seismic activity on the LOFS of 12 km.

However, the lack of paleoseismological studies, coupled with the scarcity of exposures of related Quaternary deformation, prevents a more detailed assessment of the Holocene displacement history—and thus the seismogenic potential—of the LOFS. Slip rates can only be roughly estimated from long-term geological data (Adriasola et al., 2006) and short-term regional-scale GPS surveys (Wang et al., 2007). Estimates of slip fall in the range of 1–9 mm/y, and decrease northward (e.g., Rosenau et al., 2006). The results

of a boundary element numerical model employed by Stanton-Yonge et al. (2016) suggests slip rates in the range of 2–7 mm/y for the LOFS master faults. Furthermore, the results of the finite element model of Iturrieta et al. (2017) show slip rates of 5–10 mm/yr for the eastern master fault and slip rates of 1–5 mm/yr for the western and subsidiary faults.

Recent work (De Pascale et al., 2016, 2018; Astudillo et al., 2018) using remote sensing, field mapping, and lidar data have revealed deformation represented by both horizontal and vertical displacements that range from tens of centimeters to hundreds of meters; this deformation is at least partially due to earthquakes. Preliminary results suggest Late Cenozoic to Quaternary LOFS slip rates of ~5–19 mm/yr (geologic) and 12–25 mm/yr (geomorphic).

2.5.4 Other Crustal Faults

2.5.4.1 Andean Transverse Faults

The Andean Transverse Faults (ATF) are deep-seated lithosphere-scale structural elements that cross all margin-parallel tectonic domains. These structures display variable alignments, the most conspicuous of which are the arc-oblique WNW-striking fault systems, as defined by Pérez-Flores et al. (2016) based on the previous work of several authors (e.g., Cembrano et al., 1996; Yáñez et al., 1998; Rosenau et al., 2006; Cembrano and Lara, 2009; Sánchez et al., 2013). The ATF are well developed from the Andes Main Cordillera to the Coastal Cordillera between 33° and 46°S. The ATF comprise a series of discrete faults with a predominantly NW strike which are spatially or genetically related to either of the following features and/or processes: (1) Regional basin boundaries (e.g., Radic, 2010); (2) the location of several ore deposits (e.g., Chernicoff et al., 2002); (3) rupture zones of subduction earthquakes (Melnick et al., 2009); (4) Quaternary volcanism in the Central and Southern Andes (Cembrano and Lara, 2009; Cembrano and Moreno, 1994; Lara et al., 2004, 2006; Sánchez et al., 2013; Tibaldi et al., 2005). The ATF exhibit

evidence of long-term fluid flow pathways, volcanic activity, and shallow seismic activity (Haberland et al., 2006; Lara et al., 2006, 2004; Sánchez et al., 2013; Tardani et al., 2016). Segments of the ATF are included in the longitudinal classification of this paper, as is the Pichilemu fault in the Outer Arc domain, since fault segments act as independent faults; there is no record of a single entire fault within the ATF system with neotectonic displacement. Consequently, although the ATF have long surface traces which cover various domains, the behavior of fault segments is generally consistent with the characteristics of the domain in which that segment is located.

Other prominent ATF include the Lanalhue Fault—which is associated with inter-seismic transpressional deformation in the forearc (38°S), including a ML 5.2 earthquake at a depth of 12 km with a left-lateral focal mechanism (Haberland et al., 2006)—and the Biobio–Alumine Fault System (Melnick et al., 2006; Muñoz and Stern, 1988).

The observations of Haberland et al. (2006) in the Arauco Peninsula using a temporal seismic network shows seismicity in the continental crust situated between 10 and 30 km depth. In most cases, these authors associated these earthquakes with mapped faults, revealing that these faults almost all extend through the entire forearc crust.

2.5.4.2 Magallanes–Fagnano Fault System

The 600 km long Magallanes–Fagnano Fault System (MFS) is a transform-type margin, and is one of the major segments of the boundary between the continental South American plate and the oceanic Scotia plate. The MFS runs from the western arm of the Magallanes Strait—where the triple junction between the South American, Scotia, and Antarctic plates is located—to the offshore Atlantic Ocean, and transects Isla Grande, Tierra del Fuego, into two continental blocks (Lodolo et al., 2002; Lodolo et al., 2003; Cisternas and Vera, 2008; Civile et al., 2012).

Lodolo et al. (2003) describe the MFS as consisting of distinct tectonic lineaments that are segments of the transform system and predominantly consist of near-vertical faults. In their study of asymmetric basin sediments, they suggest that there is a close

relationship between strike-slip motion and transform-normal extensions, a commonly encountered feature in other continental transtensional environments.

South of the Chile Triple Junction, the South American and Antarctic plates, converge at a rate of ca. 1.9 cm/y, in a direction, which varies from margin-perpendicular in the north to strongly oblique in the south. To the south, the convergence rate reduces to <1.2 cm/y since part of the convergence is accommodated by the MFS at a rate of <0.5–0.7 cm/y (Lodolo et al., 2003; Cisternas and Vera, 2008). This convergence is almost perpendicular at 52°S, however rapidly becomes oblique to the south, reaching 60° at 57°S.

In the Magallanes region, two important historical earthquakes of ML 7.5 and MS 7.8 occurred, in 1879 and 1949, respectively (Lomnitz, 1970; Cisternas and Vera, 2008; Costa et al., 2006b). Lower-magnitude seismicity (ML 4.3) recorded in 1997 and 1998 occurred within the continental crust. Furthermore, some very shallow concentrated earthquakes have occurred around the active Reclus and Burney volcanoes (Cisternas and Vera, 2008).

The main geomorphological expression associated with the MFS is an 11 m high scarp developed in Late Pleistocene–Holocene (?) deposits. This suggests that this feature was formed by various earthquakes, since the vertical slip of the 1949 event was less than 1 m. Paleoseismic stratigraphic analysis of the MFS indicates two, or possibly three, pre-1949 paleoearthquakes (Costa et al, 2006b).

More recent work (González-Bonorino et al., 2012), reported normal faults buried beneath gravelly strand plains on the Atlantic coast of Patagonia, with displacement ages between 0.9 and 6.4 ka and a recurrence rate of about 1 ka. Their most likely co-seismic source is the MFS, more than 300 km distant, which suggests high-magnitude earthquake activity on this fault system throughout the Holocene.

2.6 Discussion

One of the main aims of this work is to address how the seismogenic potential of neotectonic faults in Chile can be estimated. We have examined the main parameters involved in determining the magnitude of an earthquake, including the lengths, widths, and mean displacements of crustal faults. We compiled the characteristics of the most significant crustal faults regarding their morphotectonic imprint and characteristic rupture/displacement segments revealed by their surface trace. This study highlights the similarity of neotectonic fault parameters along and across different tectonic domains, with longitudinal segmentation being dominant.

Hence, we collected crustal fault parameters and recorded crustal earthquakes in the corresponding longitudinal domain in order to gather all of the necessary parameters to estimate earthquake moment magnitude and check the consistency of such estimations. The length of fault rupture and slip during an earthquake are the general parameters used for the estimation of earthquake magnitude (Bonilla et al., 1984; Wells and Coppersmith, 1994; McCalpin, 2009). Here, we applied one of the most commonly used formulae for estimating earthquake magnitude, developed after Hanks and Kanamori (1979):

$$Mw = 2/3 (\log Mo - 9.1), \text{ with } Mo = \mu A D$$

where μ = shear modulus (=30 GPa in crust)

A = Length * Width = area

D = average displacement during rupture

Where the rupture plane is in km^2 and ranges from km^2 to tens of km^2, and the average displacement ranges from centimeters to meters, with the latter parameter being the most sensitive to changes in the formulae.

This initial calculation of Mw constrains the order of magnitude of fault parameters very well, and indicates which parameters are key for the assessment of seismogenic hazard.

2.6.1 Fault Parameters for Longitudinal Domains

In the seismogenic zone, deformation processes are predominantly frictional and earthquakes can be nucleated and propagate as slip on pre-existing fault surfaces or intact rock failure (Lockner and Beeler, 2002). The progressive transition from predominantly frictional deformation to mainly quasi-plastic deformation is commonly referred to as the base of the seismogenic zone, or as the brittle–plastic transition (e.g., Scholz, 1988; Sibson, 2002), and the location of this transition bounds the maximum possible depth for an earthquake in the continental crust.

Crustal heterogeneities, coupled with variations in regional heat flow, account for much of the observed variation in the depth of the seismogenic zone (Sibson, 1984; Smith and Bruhn, 1984). The main parameters controlling crustal heterogeneity are plate rheology, thermal gradient, and elastic and crustal thickness. Fault zone rheology is strongly affected by the quartz/feldspar ratio: the temperature of the transitional zone can change from ~350 °C for quartz-rich material to ~450 °C when feldspar is the dominant load-bearing constituent of the rock mass. However, complexity at the base of the seismogenic zone may be further compounded by fluid-pressure cycling near the transition zone (Sibson, 1992, 1994).

Since the general recognition of subduction processes in the 1960s, numerous studies have been performed involving the evaluation and modeling of the structure and geometry of the subducting (Nazca) plate in the Andes region. Most models postulate a large, predominantly east-verging ramp detachment thrusting structure connecting the subduction zone with the cordillera throughout the Andes (e.g., Isacks, 1988; Farías et al., 2010; McQuarrie et al., 2005; Lamb, 2011; Armijo et al., 2015; Lamb, 2016). These

models depict a brittle and rigid forearc crust (high elastic thickness) and a weak ductile lower crust under the arc region (low elastic thickness), thus implying variable thicknesses of the brittle–ductile transition from the subduction trench to the Andes Cordillera.

By analyzing seismicity and surface geology in Central Chile, Farías et al. (2010) predicted that the brittle–ductile transition occurs at a depth of less than 10 km, and at a depth of ~25 km, under the Main Cordillera and the Central Depression, respectively, and also predicted that the ramp detachment structure connects with the subduction zone at a depth of ~60 km. Their results also suggest the presence of similar structures in Northern and south-central Chile. The lower limit of crustal seismicity correlates well with the 350 °C isotherm (Figure 2-4).

Based on analysis of the thermal and elastic behavior of three granodioritic rocks from the Coastal Cordillera of Northern Chile, Arndt et al. (1997) suggested that the brittle–ductile transition occurs at depths of less than 20 km in this region. Additionally, ongoing thermal lithospheric modeling suggests that almost all of the crustal seismicity between 1996 and 2006 at latitudes of 33–34°S is constrained in depth by the 350 °C isotherm (Valdenegro et al., 2019). It follows that, in the outer forearc domain, earthquakes can be generated at any depth above the Benioff zone; from the Outer Forearc domain to the arc, the 350 °C isotherm shallows progressively from 30 to 15 km, which allows a rough estimate to be made of the maximum depth of earthquake nucleation (Figure 2-4).

Accordingly, fault depth increases away from the high-heat-flow volcanic arc domain, reaching a maximum in the colder outer forearc region.

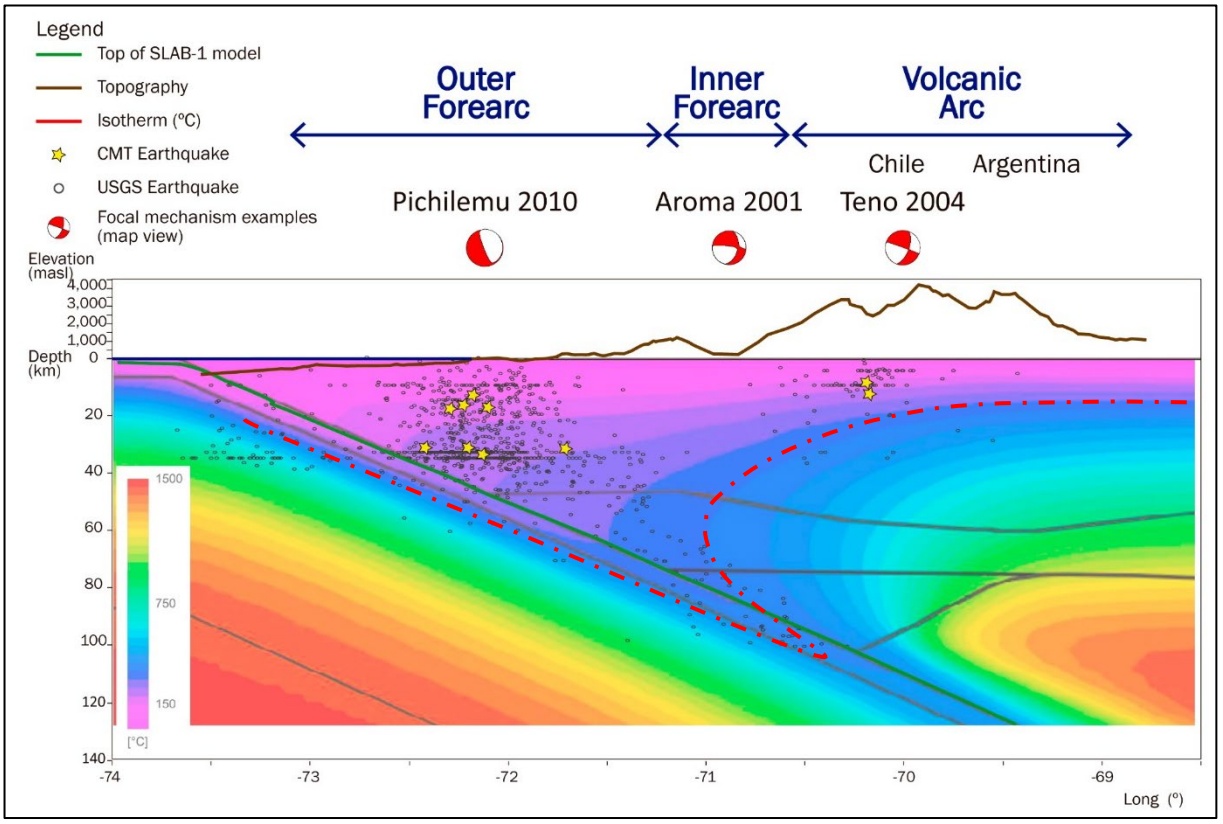

Figure 2-4: Schematic W-E cross-section of the subduction zone in Central Chile (~34ºS) with selected earthquakes (between 33.5º and 34.5ºS).

Circles represent earthquakes from the USGS (2018b), while yellow stars represent the earthquakes from the Harvard CMT catalog, which were analyzed in this study. Shown are the locations of the three tectonic domains and examples of a crustal earthquake (with focal mechanism) for each domain. The Nazca–South American subduction zone is represented by the SLAB-1 model (Hayes et al., 2012), and the variable thickness of the brittle–ductile transition in the South American plate from the subduction trench to the Andes Cordillera is correlated with the generalized ~350 ºC isotherm (red segmented line, thermal structure model from Valdenegro et al., 2019). Note the distribution of crustal earthquakes from west to east; i.e., greater depths for outer-forearc events compared to inner-forearc and arc events, augmenting the potential fault rupture area thus generating greater magnitude events.

Our compilation of fault and earthquake data reveals that the maximum recorded depths of crustal hypocenters are 25–30 km for the Outer Forearc domain, 15–20 km for the Inner Forearc domain, and 8–12 km for the Arc domain. Accordingly, the width of fault planes will depend on the fault-plane dip; subhorizontal faults could have larger rupture areas, for example, listric faults. Earthquakes on strike-slip faults, which have almost vertical fault planes, will also be limited to the same depth ranges as mentioned above.

The length of fault planes was estimated from the geomorphic features of the numerous crustal faults along the Andean region. Fault segments with lengths of up to 40 km are easily identifiable in satellite images and Digital Elevation Models (DEMs) for different fault systems and single fault traces. However, these fault traces may have been formed by several seismic events, whose effects have been superimposed over thousands of years of slip on the same segment and different segments of the fault.

Two of the most difficult parameters to estimate are the fault slip rate and the accumulated net displacement, both of which control Mw. Moreover, as fault slip is the most sensitive parameter in the earthquake magnitude equation, researchers should be cautious when assigning magnitudes to events with poorly estimated slip rates. The few paleoseismological works to have been conducted in the Chilean Andes indicate discrete measurable event slips, and the ages, slip rates, and recurrence times of these events were obtained (e.g., Cortés, 2012; Cortés et al., 2012; Vargas et al., 2014; González et al., 2015). These works suggest that the maximum average displacements during the studied earthquakes generally reach up to 2 m, only exceeding 2 m in extraordinary cases.

Based on our integration of studied faults, recorded earthquakes, and morphotectonic and rheological features, we present a conceptualization of the main characteristics of Chilean crustal faults in Table 2-3. The information shown in this table can be used to estimate where, how, and over what distance a crustal fault could slip during a seismic event.

We conclude that the along-strike tectonic domains (longitudinal domains) are the most relevant tectonic domains for the assessment of the seismogenic potential of crustal faults in Chile, since the depths of faults (and therefore of earthquakes) vary more significantly when transitioning between longitudinal domains than latitudinal domains.

2.6.2 Estimated Earthquakes

Based on the previous analysis (Section 2.6.1), it is possible to estimate the maximum earthquake magnitude for each longitudinal domain using scaling relationships (Stirling et al., 2013) and the seismogenic depth, length, and slip, and assuming a constant shear modulus of 32 GPa for the crust. The estimations of maximum earthquake magnitude made in this work are in complete agreement with the recorded seismic events for each domain (Table 2-3).

The earthquakes with the largest moment magnitudes (Mw 7.5 for normal and strike-slip faults and Mw 7.0 reverse faults) occur in the Outer Forearc domain, which experiences slip rates of 0.2–0.6 mm/y and recurrence times of a few thousand years. Events with magnitudes of 6.9–7.4 can occur in the Inner Forearc domain, which experiences slip rates of 0.1–0.4 mm/y and recurrence times of a few thousand years. Events smaller than Mw 6.7 may occur in the Arc domain, where the thickness of the upper brittle crust is lowest due to the presence of active magmatism. However, since the slip rates of some faults in the Arc domain are an order of magnitude higher than those of the Outer and Inner Forearc domains, recurrence times in this domain could be as short as a few hundred years.

2.6.3 Assessment of Parameter Uncertainties

The estimation, calculation, or assessment of fault parameters is susceptible to errors, with the largest source being field data collection. The identification of recurrent rupture planes in the field (tectonic morphologies and/or deposits) becomes very difficult

with the superposition of multiple seismic events. Consequently, the estimation of fault length for a characteristic earthquake or largest credible earthquake is challenging, and paleoseismological studies should be conducted along the entire length of a fault in order to be more fully representative and precise.

Fault displacement is also a difficult parameter to assess. For example, in order to estimate slip fault based on the thickness of the colluvial wedge which formed co-seismically in dip-slip faults, it is necessary to identify a colluvial wedge that was formed by a single seismic event and is representative of an entire rupture zone. If all these conditions are found and the colluvial wedge experienced "normal" erosion rates, as a "rule of thumb", the height of the wedge is considered to be half the total slip (McCalpin, 2009). However, this relation must be used with caution; there are many problems in measuring one event-only colluvial wedges, scarp-free faces, or displacement (e.g., Ostenaa, 1984; Nelson, 1992; McCalpin, 2009). However, even when all of this is considered, earthquake size is still commonly overestimated. The bigger range for average displacement with the common error percentage make this a key parameter.

Table 2-3: Seismogenic parameters of crustal faults in Chile.

Longitudinal Tectonic Domain		Maximum Depth (km)	Maximum Earthquake Magnitude (Mw)			Fault types	Examples	Slip rate (mm/yr)	Recurrence time (yr)	References
			Estimated	Recorded	Paleoseismological					
Outer Forearc	Coastal Cordillera	25–30	7.0–7.5		7.0	Normal-strike slip	Mejillones, Mititus	0.2–0.6	10^3	Cortés et al. (2012), Aron et al. (2013)
				7.0			Pichilemu			Arriagada et al. (2011), Farías et al. (2011), Ruiz et al. (2014)
			7.0	6.7	7.0	Reverse	Pisagua, Bajo Molle			Allmendinger and González (2010), Cortés-Aranda et al. (2014)
Inner Forearc	Central Depression, Main Cordillera	10–15	7.2	6.9	-	Strike slip	Aroma, Las Melosas, Domeyko, Teno	0.1–0.4	10^3–10^4	Comte et al. (2002), Legrand et al. (2007)
			6.9–7.4	-	7.5	Reverse	San Ramón			Armijo et al. (2010), Pérez et al. (2014)

Longitudinal Tectonic Domain		Maximum Depth (km)	Maximum Earthquake Magnitude (Mw)			Fault types	Examples	Slip rate (mm/yr)	Recurrence time (yr)	References
			Estimated	Recorded	Paleoseismological					
Volcanic Arc	Main Cordillera	8–12	6.2–6.7	6.2	-	Strike-slip	LOFS, Aysén	7.0	10^2–10^3	Mora et al. (2010), Legrand et al. (2011), Vargas et al. (2013)
Transform fault (plate boundary)	Magallanes –Fagnano Fault	30	7.8	7.5	-	Strike slip	Magallanes –Fagnano Fault	7.0	10^2–10^3	Lomnitz (1970), Cisternas and Vera (2008)

NOTE: The parameters shown in this table should be used with caution and are not necessarily suitable for specific local studies. Maximum earthquake magnitudes, slip rates, and recurrence times, as well as other fault and seismological parameters, need to be evaluated for each specific location.

2.6.4 Fault Activation Mechanisms and Hazard Assessment

Crustal faults are widely dispersed across the entire length and breadth of the Andes. After analyzing fault characteristics in their morphotectonic environment, we predicted some seismogenic parameters for crustal faults located in particular tectonic domains. A summary of these conditions is given in Table 2-3.

A strong correlation has been documented between crustal seismicity and large interplate earthquakes, resulting in earthquake segmentation (e.g., Ecuador and Colombia, Collot et al., 2004 and Alvarado et al., 2016; Peru, Audin et al., 2008), slip partitioning (Melnick et al., 2006), or acting as triggers for mega-earthquakes (González et al., 2015) or co-seismic/postseismic pseudo-aftershocks (Farías et al., 2011; Aron et al., 2013).

Recent outstanding examples of crustal fault activation in Chile include the Pichilemu and Iquique crustal earthquakes, which were related to the 2010 Maule and 2014 Iquique megathrust earthquakes, respectively. The Mw 7.0 and 6.9 Pichilemu earthquakes (see Section 4.5), which occurred two weeks after the 2010 Maule earthquake, were allegedly caused by the large change in Coulomb stress caused by that earthquake (e.g., Farías et al., 2011; Aron et al., 2013). The other activation case is a Mw 6.7 reverse crustal earthquake, which was apparently the trigger for the 2014 Iquique–Pisagua Mw 8.1 megathrust earthquake, also by creating a change in the stress conditions, as suggested by González et al. (2015). That work indicates that several other crustal earthquakes with reverse and normal slip took place before and after the intraplate Mw 8.1 earthquake.

Additionally, crustal earthquake clusters were temporally associated with the 1985 Valparaiso, 2005 Antofagasta, and 2007 Tocopilla thrust earthquakes, with the amount of crustal earthquakes generally increasing in the period following these large earthquakes.

Normal-faulting crustal earthquakes were also observed following the 2011 Tohoku (Mw 9.1) and 2004 Sumatra–Andaman (Mw 9.1) mainshocks (e.g., Dewey et al., 2007; Asano et al., 2011; Nettles et al., 2011; Hardebeck, 2012; Miyakawa and Otsubo, 2015).

The findings of Toda et al. (2011a, 2011b) suggest that the faults which caused the aforementioned two earthquakes were activated by changes in static stress complementing local normal-faulting regimes and stress heterogeneity. Hardebeck (2012) studied the rotations of the principal stress axes in these two events, and found that they exhibited similar co-seismic rotations, with a shallowly plunging pre-event σ1 (maximum compressive stress axis) changing abruptly to a σ1 and σ3 with plunges of 45º (maximum and minimum compressive stress axes) immediately after the event. In that context, crustal faults can be oriented for either reverse or normal faulting in the post-mainshock stress field, depending on their dip, which can explain the observed normal-faulting aftershocks. However, Hardebeck (2012) also states that the stress rotation following these three earthquakes does not occur in all subduction earthquakes; deeper earthquakes exhibit smaller co-seismic stress rotations, likely due to the increase in deviatoric stress with depth.

Farías et al. (2011) recommend that crustal faults, especially those in the outer forearc, should be considered for seismic hazard analysis despite the absence of historic seismic activity, since events such as those of the Pichilemu sequence following the Maule earthquake prove the seismogenic potential of such faults.

The seismogenic potential of crustal faults in Chile is fundamentally linked to the subduction earthquake cycle. For instance, optimally oriented faults, regarding the deformation field and stress changes, may be reactivated at virtually any time (King et al., 1994; Stein et al., 1994; Stein, 1999; Kilb et al., 2000; Lin and Stein, 2004; Loveless et al., 2010; Seeber and Armbruster, 2000). This is particularly true for optimally oriented ancient basement faults which are subjected to high strain rates—a condition which can be reached co-seismically with large subduction earthquakes—and onto which slip can be partitioned (e.g., Melnick et al., 2006; Aron et al., 2013). In contrast, during the inter-seismic period, strain rates are relatively low, which makes the reactivation of optimally oriented faults less likely. However, the precise nature of the link between crustal faults and the subduction zone earthquake cycle remains poorly understood.

We hypothesize that some crustal faults, especially those in the outer forearc, have the potential to reactivate co-seismically when optimally oriented with respect to the instantaneous extension direction arising from elastic rebound following mega-earthquakes (e.g., the Pichilemu Fault; Aron et al., 2013). Other faults may activate during the subduction inter-seismic period, including regional strike-slip faults and thrust faults in the Main Cordillera (e.g., LOFS; Legrand et al., 2011; Mora et al., 2010).

2.7 Conclusions

The continental margin of the Chilean territory is segmented longitudinally along its length into three tectonic domains—the Outer Forearc, Inner Forearc, and Volcanic Arc—which exhibit similar earthquake parameters for crustal faults, such as fault size, fault slip rate, and earthquake magnitude, thus allowing a first-order assessment of seismic potential.

Although sparse and limited, structural, paleoseismological, and geodetic data suggest that slip rates in Chilean crustal faults range from 0.2 mm/y in the forearc to up to 7.0 mm/y in the intra-arc. This implies recurrence times of 200–50,000 years for ca. Mw 7 earthquakes.

Faults in the Outer Forearc domain have the largest seismogenic potential among Chile's three tectonic domains, with earthquake magnitudes estimated at between Mw 7.0 and Mw 7.5; this is in agreement with recorded crustal earthquakes of ca. Mw 7.0 and similar magnitudes obtained from paleoseismological evidence. Slip rates range between 0.2 and 0.6 mm/y, and recurrence times for ca. Mw 7 earthquakes are on the order of several thousands of years.

By contrast, faults of the Volcanic Arc have the lowest estimated seismic potential among Chile's three tectonic domains, with earthquake magnitudes of Mw 6.2–6.7. However, these faults have slip rates which are an order of magnitude greater than those

of the Outer Forearc domain (7.0 mm/y) and have recurrence times of hundreds to thousands of years.

The various different tectonic modes for the reactivation of crustal faults in Chile—which are related to large interplate earthquakes and the stress field within the seismic cycle (Section 6.4)—have a wide range of slip rates, which greatly complicates the estimation of seismic hazard. Many structures that are considered to be active using traditional classification (see Machette (2000) for a review) might not generate significant earthquakes in thousands of years, whereas other less well known faults which have no instrumentally recorded seismicity could generate earthquakes with magnitudes up to Mw 7. Furthermore, fault segments that have generated earthquakes independently of each other may be capable of merging into a single rupture zone and thus generate an earthquake of greater magnitude.

Therefore, a rigorous assessment of seismic hazard must consider the different tectonic settings across the Chilean Andes, the timing within the interplate seismic cycle, and the slip rates of Andean crustal faults. Understanding the nature of these faults will help not only to better assess the associated seismic hazard, but also to better understand and constrain their connection with the subduction zone seismic cycle as earthquake triggers, slip partitioning, or the result of subduction earthquakes.

3 GEOPHYSICAL SIGNALS OF NEOTECTONIC ACTIVITY ON THE AEROPUERTO FAULT: A CASE STUDY IN THE ATACAMA REGION, NORTHERN CHILE

3.1 Introduction

Understanding the significance and nature of potentially seismogenic faults is a relevant task for the development of seismic hazard assessment and risk mitigation plans for populated and/or developed areas. In the Andean region, crustal faults within the continental (South American) plate are poorly studied due to their relatively low slip rates and recurrence times compared to megathrust subduction faults.

In convergent margins such as Chile, crustal deformation processes in the outer forearc are associated with the subduction earthquake cycle, given an optimal orientation regarding Coulomb stress changes in co-seismic and inter-seismic periods (e.g., Aron et al., 2013; Cortés-Aranda et al., 2014). Much morphological and instrumental evidence supports the occurrence of earthquakes on Chilean crustal faults, however the processes that induce slip on these faults is not fully understood.

Typical faulting-related landscape modification is the long-term outcome of earthquakes on crustal faults. However, the co-seismic outcomes are the most concerning in terms of human safety: since crustal faults occur relatively close to the surface, earthquakes on such faults can produce very high PGA in the surrounding area, and this PGA can be increased by site effects. Therefore, neotectonic activity on crustal faults is a key element of hazard studies.

Surface morphological expressions of a fault can easily be obliterated by climatic factors, particularly in areas with high precipitation rates. Consequently, the study of faults is optimal in regions with an arid or semi-arid climate, where cracks, escarpments, and deposits associated with fault displacement can be preserved for a long time (e.g., Marquardt et al., 2004; González et al., 2008; Loveless et al., 2009 and 2010).

Accordingly, one of the best places to study the nature of crustal faults is Northern Chile, due to this region's hyperaridity, which has prevailed since at least ca. 12 ± 1 Ma (Jordan et al., 2014) and which allows for the conservation of geomorphological evidence of fault activity.

In order to study crustal faults and their seismogenic potential, studies of fault geometry and kinematics should be conducted. Surface evidence is not sufficient to accurately determine the geometry or extent of a fault, and therefore several techniques are applied to perform this task.

As well as surface mapping, field geophysical techniques constitute a powerful tool to investigate underground fault structures. Such techniques are fast and non-invasive, and are additionally less expensive and cover larger areas than typical paleoseismological trenching. Moreover, geophysical analysis can help to decide where to construct costly trenches. Geophysical tools can also give information about basin shape, sediments, rock types, and the presence of groundwater.

Accordingly, this research attempts to generate a base methodology, using geophysical exploration techniques, in order to determine geometric and possibly kinematic aspects of a potentially seismogenic fault, thus providing evidence of its seismogenic potential.

In this work, a case study was selected to test an integrated field-based and geophysical-based methodology. The study region is an area of approximately 35 km^2 (~5 x 7 km) located between the Aeropuerto and Fortuna Faults in Northern Chile (). The area has good accessibility for the transport of geophysical equipment and lies a short distance from Antofagasta city. Special attention was paid to the relationship between sediments, rocks, and faults, which can be used to estimate the basin shape and the rate and age of normal-slip displacement.

3.2 Local Geology and Tectonics

The continental Northern Chile continental forearc (21–25ºS) is dominated by structures which show extension that is nearly parallel to the convergence direction of the oceanic Nazca plate, which subducts beneath the continental South American plate. Long-term neotectonic deformation is manifested by numerous normal faults, NS-aligned open cracks, and asymmetric tectonic basins limited by normal faults on the forearc's western margin (Arabasz, 1971; Niemeyer et al., 1996; DeLouis et al., 1998; González et al., 2003; Loveless et al., 2005; Loveless et al., 2010).

The majority of NS-striking faults exposed onshore and offshore in Northern Chile (21–25ºS) have noticeable eastward-facing scarps and recent normal displacement bounding on the west of a series of small basins elongated north-south (Arabasz, 1971; DeLouis et al., 1998; González et al., 2003; Loveless et al., 2005; González et al., 2008; Vargas et al., 2011; Allmendinger and González, 2010; Cortés et al., 2012). The preservation of these features is facilitated by the hyperarid conditions in the region, which have persisted since at least ca. 12 ± 1 Ma (Jordan et al., 2014). The Peru–Chile oceanic current and the associated upwelling induces colder oceanic waters and thus limits precipitation in its vicinity (Lamb and Davis, 2003).

The Mejillones and Salar del Carmen faults (Figure 3-1) are among these NS-striking faults. Paleoseismological and neotectonic studies of these faults have revealed the occurrence of earthquakes of Mw ~7 (Niemeyer et al., 1996; González et al., 2003, 2006; Marquardt, 2005; Cortés et al., 2012; Cortés-Aranda et al., 2014).

The Salar del Carmen Fault is one of the three main segments identified in the Atacama Fault System (AFS), together with Paposo and El Salado segments (Okada, 1971; Arabasz, 1971; Naranjo, 1987; Hervé, 1987). All of these segments are curved and concave to the west. The AFS is a ~1000 km long fault zone which runs along the Coastal Cordillera of Northern Chile from Iquique (20°S) to La Serena (30°S). This fault system has been the focus of several studies since the late 1960s due to the prominent

geomorphological characteristics that it displays, which reflect a displacement history since the Jurassic.

The earliest AFS activity is evidenced by mylonitic and cataclastic rocks formed under sinistral displacements in the volcanic arc as result of oblique convergence in the Jurassic–Early Cretaceous (Scheuber and Andriessen, 1990; Brown et al., 1993). Progressive cooling of the magmatic arc in the mid-Cretaceous may have coincided with a change in the AFS deformation from ductile to brittle sinistral strike-slip (Brown et al., 1993). The structures generated in this brittle phase of the AFS are duplex-type, limited by NS- and NW-trending strike-slip faults, and segmented into numerous sections, each in excess of 60 km in length (Cembrano et al., 2005).

Several authors have documented regional-scale sinistral and locally dextral strike-slip displacements along various segments of the AFS. However, the main Neogene-to-recent displacements are normal-style, consistent with the extensional regime of the present day forearc (Arabasz, 1971; Okada, 1971; Hervé, 1987; Naranjo, 1987; DeLouis et al., 1998; Scheuber and González, 1999; González et al., 2003; Riquelme et al., 2003; Cembrano et al., 2005; González et al., 2008; Vargas et al., 2011; Allmendinger and González, 2010; Cortés et al., 2012). Quaternary deformation of the AFS is preserved in horst-and-graben and hemi-graben coastal topography, developing fault scarps from a few meters to over 100 meters in height and displaced Quaternary alluvial surfaces (Marquardt, 2005; González et al., 2006; Cortés et al., 2012).

One of the faults associated with the AFS is the Aeropuerto Fault (Figure 3-2). This fault, which is located between the Mejillones and Salar del Carmen faults, is recognized as a geomorphological feature approximately 60 km in length that limits the west flank of the Costal Cordillera, strikes N-S to N35ºE, and dips steeply to the east (Órdenes, 2002). The Aeropuerto Fault may have originated in the Mesozoic (Cortés et al., 2007). A conspicuous escarpment, 0.5–2 m in height, is observed along its trace (Figure 3-4). The study area is bounded to the east by the Fortuna Fault, a N60ºE trending normal fault.

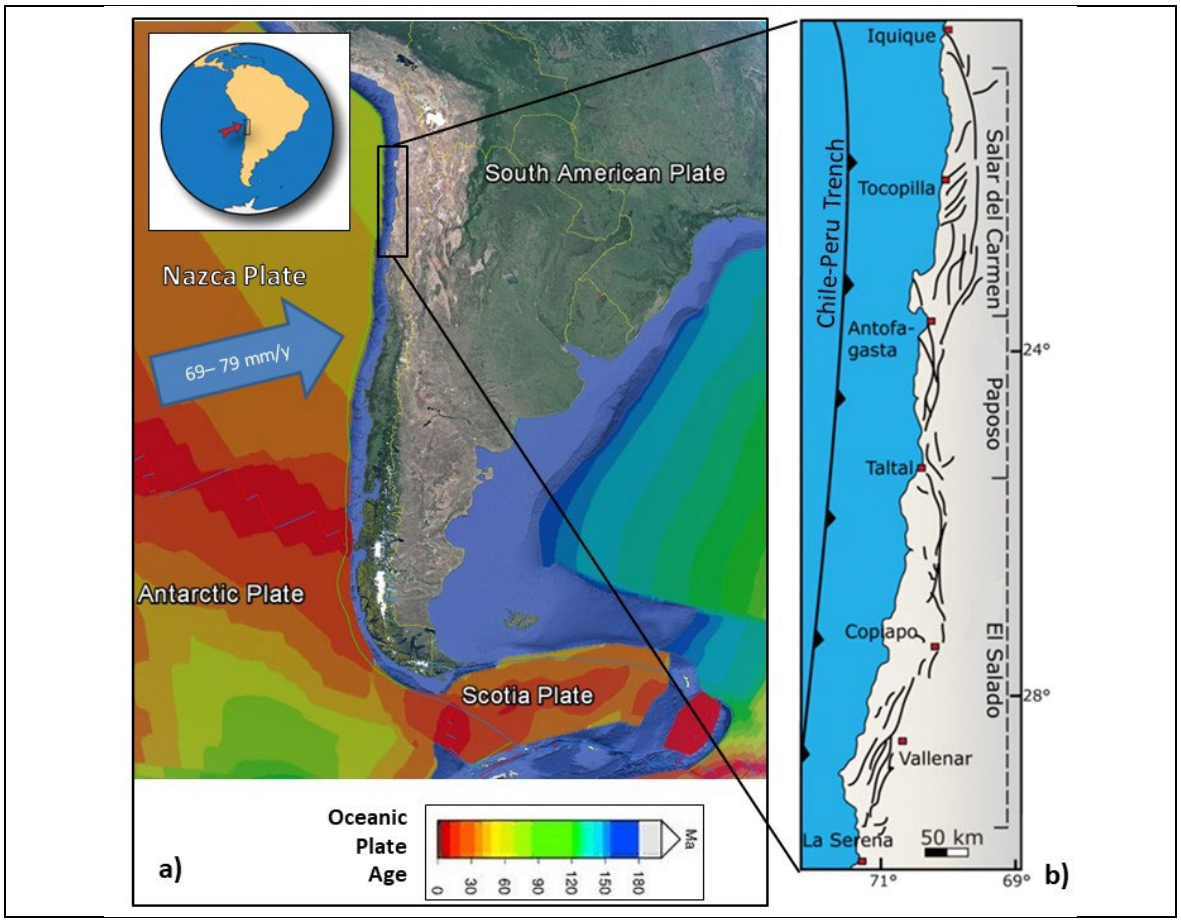

Figure 3-1: Tectonic setting of the forearc of Northern Chile.
(a) general context of the Nazca–South American subduction. (b) schematic view of the Atacama Fault System between Iquique and La Serena.

Cortés et al. (2007) and Marquardt et al. (2000) describe the Aeropuerto Fault with two generations of geomorphologic features. Although a previous normal activity has been indirectly inferred by confined topographic inversion, the first noticeable feature is an escarpment or flexure linked to reverse activity in the Pliocene. Later activity led to the superimposition of Pleistocene escarpments of steeply-dipping normal faults with limited sinistral slip (Armijo and Thiele, 1999; Niemeyer et al., 1996; DeLouis et al., 1998).

The Fortuna Fault (Figure 3-2 and Figure 3-3) is a relay fault between the Mititus Fault to the NE and the Aeropuerto Fault to the SW. This fault also shows evidence of extensional reactivation in the Neogene and Quaternary (DeLouis et al., 1998).

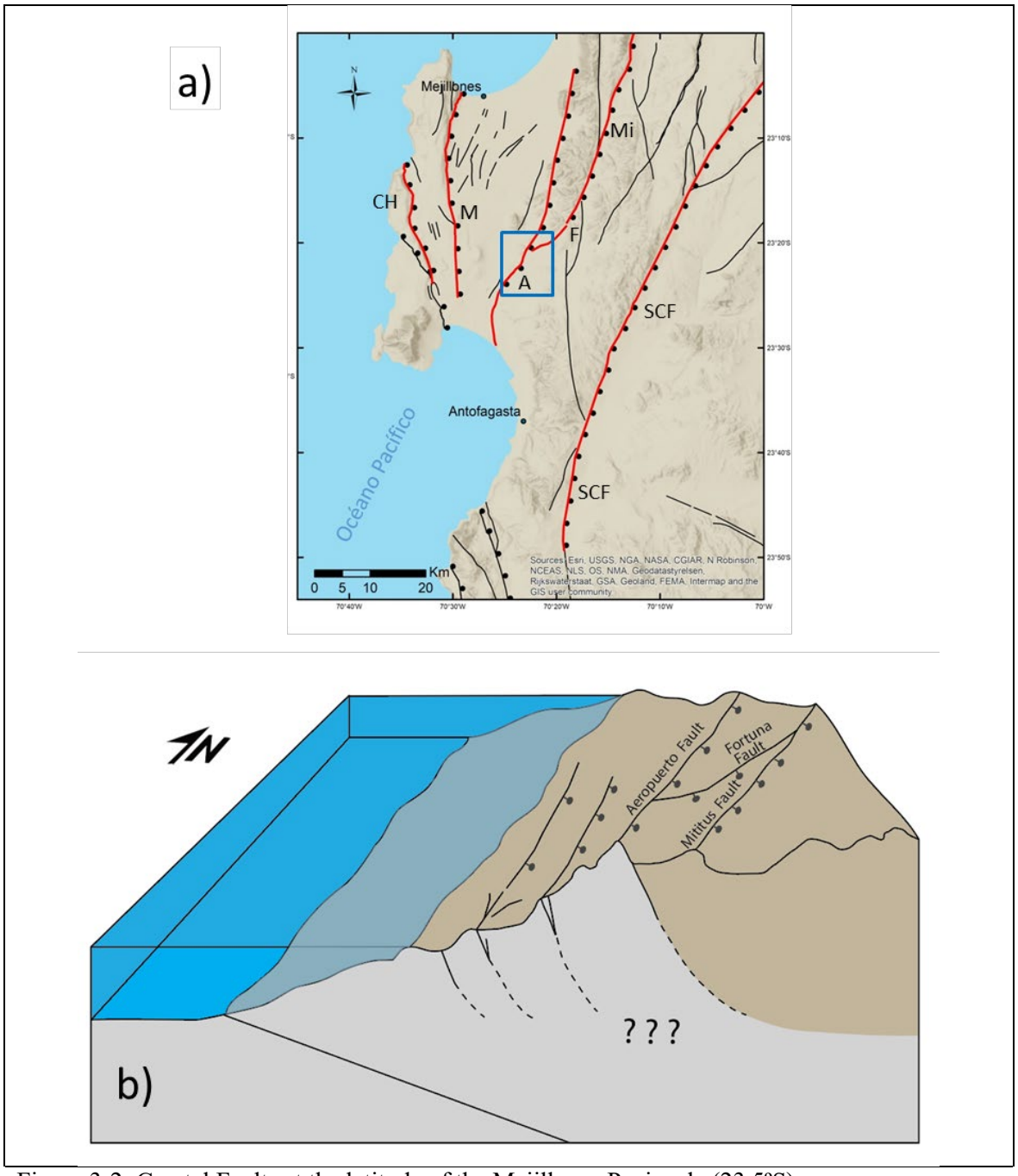

Figure 3-2: Crustal Faults at the latitude of the Mejillones Peninsula (23.5ºS).
(a) Main faults of the AFS and other normal faults. CH: Caleta Herradura; M: Mejillones; SC: Salar del Carmen; Mi: Mititus; A: Aeropuerto; F: Fortuna (from Cortés et al., 2007 and Basso, 2007). The blue rectangle shows the studied area. (b) Block diagram showing the domino normal-fault model of the AFS (modified from Cortés-Aranda et al., 2014 and González et al., 2003).

In the region, magmatic activity migrated to the east during the Lower Cretaceous. Simultaneously, a forearc sedimentary basin was formed on the Jurassic magmatic arc. Outcrops of the basin are not observed in the vicinity of the study area, however such outcrops could be covering subsurface Jurassic volcanic rocks through erosional unconformity at the basin bottom. Basin limits could be associated with present-day faults. Some isolated plutons and dike systems developed during the Early Cretaceous. In the local context, outcrops (Figure 3- 3) of a dark volcanic rock sequence from the La Negra formation are covered by alluvial-colluvial sediment sequences, which have been accumulating since the Miocene–Pliocene.

In the Coastal Cordillera, sequences of Miocene–Pliocene gravels, sands, and silt were deposited through erosion unconformity over the Mesozoic rocks, and formed alluvial fans in a typically arid to semi-arid climate. These fans record several episodes of relative uplift of continental areas and incision of these sedimentary units. The Quaternary continental deposits are associated with morphostratigraphic units such as alluvial fans and dunes.

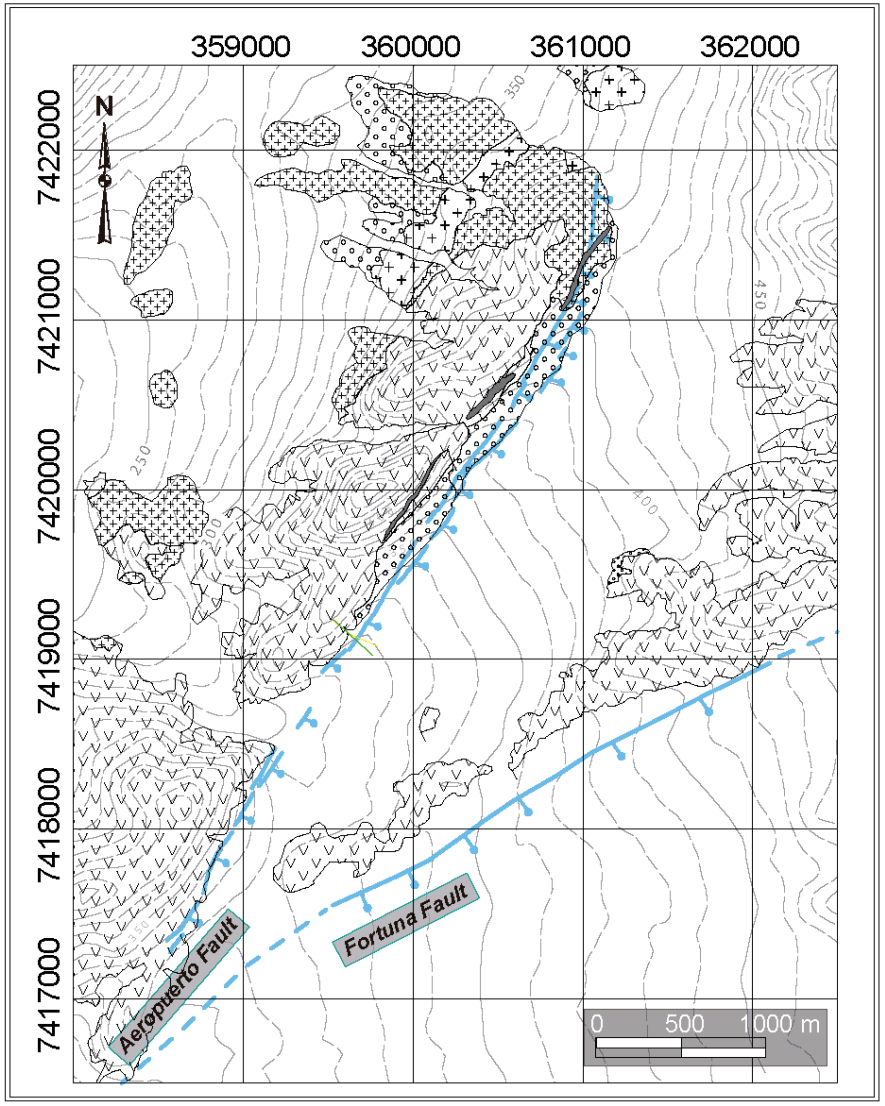

Figure 3-3: Local geological map of the study area.

Figure 3-4: Panoramic view of the Aeropuerto Fault.

3.3 Geophysical Methods and Data

Geophysical exploration methods are widely applied to detect covered geological features at different scales and for different purposes. In the research problem addressed in the present study, fault segments and the associated basin infill deposits are key elements to characterize fault behavior in terms of fault offset, net displacement, lateral extent, and, ultimately, the related seismic hazard. Shallow geophysical methods offer a non-invasive approach to estimate these parameters. Given the non-uniqueness of geophysical methods, we decided to apply a combined set of geophysical tools to reduce the inherent uncertainty.

For the case study, a combination of five geophysical methods—two active methods and two passive methods—was used. Profiles were made across-strike of the main fault in order to obtain consistent and integrated information. Fieldwork was carried out as shown in Figure 3-5. The equipment deployment is described in this section.

Gravimetric and magnetic measurement techniques are passive approaches which provide a quick and reliable 2D coverage of the study area. The gravimetric method allows the assessment of basin infill volume due to the density contrast between sediments and basement rocks. Consequently, we used gravimetric measurements to infer this density contrast to the east of the Aeropuerto Fault. On the other hand, the magnetic method allows the magnetization of basement rocks to be inferred. As such, we used this method to study the magnetization of basement rocks which outcrop in the NW of the study area and are covered by sediment towards the SE. Both the gravimetric and magnetic techniques allow the structure of the fault-basin in the study area to be inferred.

Additionally, in order to characterize the fault geometry and sedimentary infill stratigraphy, we used high-resolution electrical and seismic methods. This characterization is possible through the indirect measurement of seismic velocities (lithological contrast, soil composition, etc.) and electrical resistivity (as a function of lithology and humidity variations, permeability/porosity, and salinity).

3.3.1 Gravity Survey

A total of 12 across-fault gravity profiles were conducted (even lines L2 to L24, Figure 3-5). The profiles varied in length from 1 to 2 km. The sampling intervals along each line were 100 m in the basin and 40 m in the escarpment surroundings. Between 14-15 measurements were made for each profile, that is, a total of 175 measurements were made in the study area. The equipment used was a Scintrex CG-5 Autograv electronic gravimeter (0.1 mGal error; Scintrex, Concord, ON, Canada) and a differential GPS (Garmin Ltd., Olathe, Kansas, USA).

Data were considered valid if the height error was below 30 cm, which corresponds to a gravity error of <0.1 mGal.

The survey involved simultaneous gravity and GPS observations. Precise coordinates of the gravity measurement sites were determined by differential positioning using two geodetic GPS stations. In order to constrain the gravity modeling and interpretation, the density and magnetic susceptibility of rocks and sediments in the study area was measured in the field from 19 samples.

3.3.2 Magnetic Survey

A total of 24 magnetic profiles were carried out; 23 along the same profile lines used for the gravity analysis (Section 3.3.1) and in between them, with lengths of 1–3 km (lines L2 to L24 in Figure 3-5), and one 3 km profile along the Aeropuerto fault (line L1). The rover equipment was a Cesium Vapor Magnetometer. Additionally, a Proton Magnetometer was used as a base station, with measurements made every 60 s.

3.3.3 Seismic Survey

A total of six across-fault seismic surveys were conducted. Each profile was 300 m in length and followed the same lines as the electrical survey (ERT; see Section 3.3.4; L2, L6, L10, L14, L18 and L24, Figure 3-5). The equipment used was a Geometrics GEODE-24 24-channel seismograph (GeoMetrics, Inc., San Jose, CA, USA) with a fundamental

frequency of 4.5 Hz. A geophone spacing of 5 m was used, and a sledgehammer and plate were used as the seismic source.

3.3.4 Electrical Survey (ERT)

Apparent resistivity data were obtained from six profiles, using lines L2, L6, L10, L14, L18, and L24. Each profile was constructed with three overlapped settings of 32 ground electrodes with a separation of 5 m. The equipment used was a Tigre resistivity meter (range of measurements from 0.001 to 400,000 ohm, current injection 0.5–200 mA). Steel electrodes had a 20 m take-out.

Resistivity data were inverted using the commercial RES2DINV software (Loke and Barker, 1996) using a Gauss–Newton method and a finite element solver. The 2D assumption underlying the resistivity profiles is that the profiles were perpendicular to the geological structural heterogeneities. Highly erratic apparent-resistivity data (fluctuations of ~10^6 ohm-m) were dismissed.

3.3.5 Transient Electromagnetic (TEM) Survey

High-resolution 2D geoelectrical imaging was performed by carrying out two 450 m long sections following lines L10 and L18. The FastSnap TEM system was used in the field, with measurement sites separated by 50 m in a 50 x 50 m array.

The receiving coil records the voltage decay for 100 pulses at different sampling rates (frequencies). A stacking for each frequency is performed to reduce noise. Voltage decay vs. time curves are generated, modeled, and inverted. Inversion is performed via the iteration of different resistivity and depth models (assuming flat layers) until the result converges to a solution with an acceptable error (less than 5%). The inversion process and the modeling were done with the FastSnap computer software (TEMProcessing 1.1 Model 3.0). The 2D pseudo-depth section is obtained by gridding the 1D inversions of each TEM station. This TEM process provides a good constraint for the geological structure of the first 150–200 m of the vertical fault section.

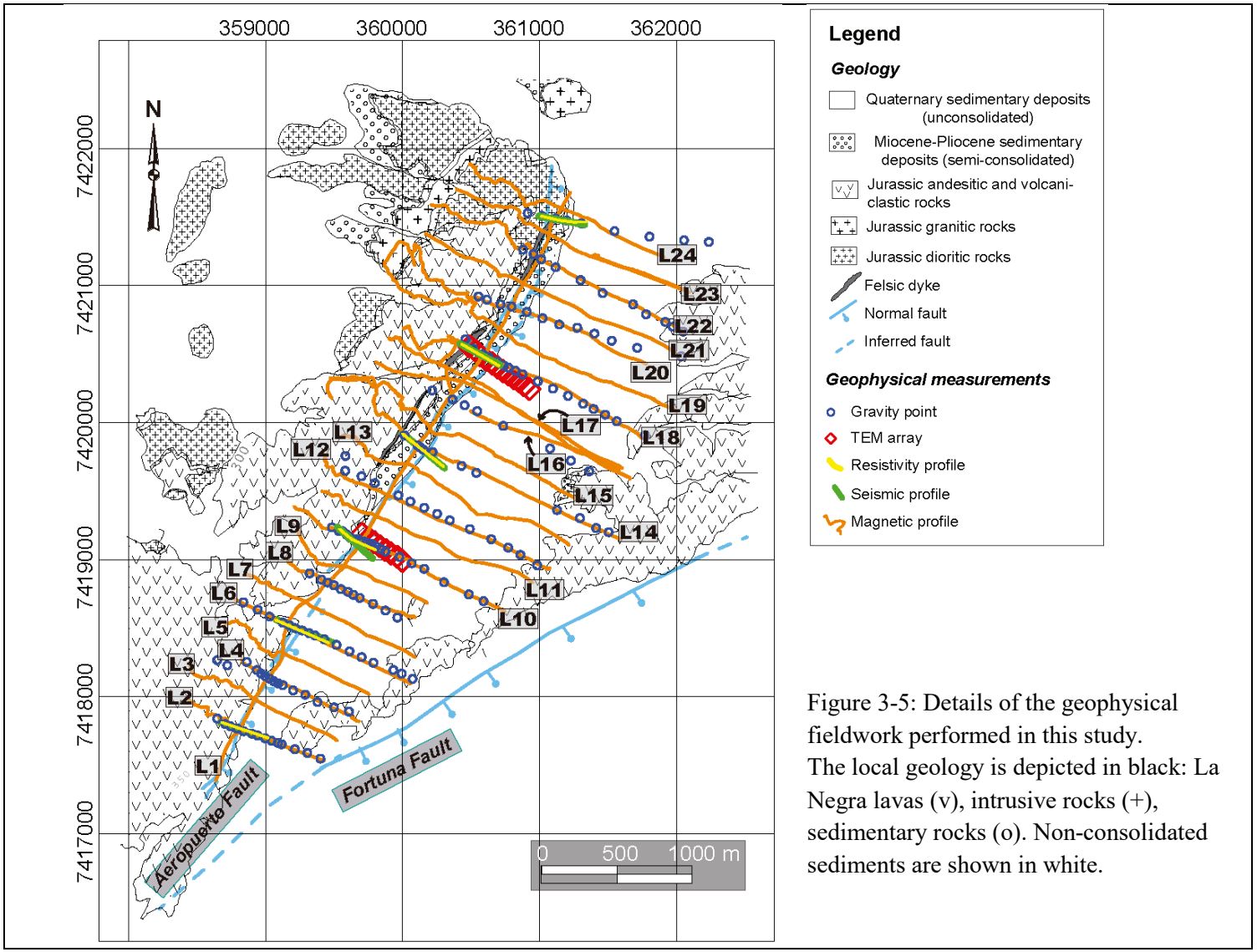

Figure 3-5: Details of the geophysical fieldwork performed in this study.
The local geology is depicted in black: La Negra lavas (v), intrusive rocks (+), sedimentary rocks (o). Non-consolidated sediments are shown in white.

3.4 Results and Discussion

The results of the petrophysical analysis of the different rocks and sediments in the study area are shown in Table 3- 1. The Bouguer anomaly results (Figure 3-6a) show a clear drift to lower gravity values to the east (a typical regional tendency in the western Andes). The residual gravity (Figure 3-6c), that is, the gravity anomaly after the subtraction of the first-order tendency, allows the definition of two different domains in the asymmetric basin morphology. To the southwest, a low residual anomaly suggests a basin depocenter (more fault activity?) while to the northeast the basin becomes shallower. These gravity signals are present in each profile, clearly showing that the basin morphology is related to the position of the Aeropuerto Fault.

The results of the gravity survey indicate a N35–40E elongated basin with a very steeply sloping western border (dip 75–80ºE); the eastern border is more diffuse and has a smaller dip, causing basin asymmetry. The gravimetric low in the west of the basin and close to the main lineament is almost certain to represent the location of the basin depocenter, which has an estimated depth of 150 m. Another lineament, which strikes N60E, is visible in profile L10 and in various other profiles to the north of this profile.

The magnetic field in the study area was found to be around 23,000 nT (33°S latitude). The residual magnetic field was calculated with IGRF correction and high-frequency filters (Figure 3-6 b and d). The results of the magnetic survey show three types of anomaly: (1) conspicuous dipole anomalies in the western border of the basin; (2) an elongated anomaly in the middle of the basin, with the positive pole near outcrops of the La Negra Formation; and (3) incomplete dipoles, the clearest being the negative pole in the northeastern part of the study area. These results can be used to infer the locations of igneous rocks, both outcrops and subsurface rocks. The Aeropuerto Fault is not evident on any of the magnetic profiles, probably since the mapped magnetic signal is only related to the basement rock, which is the same on both sides of the fault. Hence, the lack of strong magnetic signals is qualitatively consistent with the basin model derived from the results of the gravity survey.

For the electrical resistivity analysis, a 100 ohm-m limit was used for the identification of sediment and rock. The 2D inversion profiles obtained from the resistivity survey show a highly resistive shallow layer overlying two or more geological units. Two differentiated zones stand out as main features: (1) a conductive area to the SE of the sections, which coincides with the location of the non-consolidated Pleistocene–Holocene alluvial-colluvial sediments; and (2) a resistive sector NW of the sections, which corresponds to the La Negra Formation (andesitic or intrusive lavas further to the north). In addition to these main features, resistive sectors are observable within the conductive zones, which may correspond to secondary faults of the Aeropuerto system (Figure 3-7).

Table 3-1: Magnetic susceptibility and density of the analyzed rocks and sediments.

Sediment/Rock Type	**Zone**	**Density [g/cm^3]**	**Samples**	**Magnetic susceptibility [CGS]**
Andesite (La Negra Fm.)	1	2.806	12	0.001204
	2	2.779		0.000745
	3	2.791		0.001987
	4	2.682		0.001843
	mean	2.762		0.001614
Intrusive (La Fortuna diorite)		2.703	4	0.00198
Orthoconglomerate with sand matrix		1.786	3	0.0002077
Paraconglomerate with gypsum-rich matrix		1.379		0.0000563
Crystalline gypsum		1.362		0.0000357

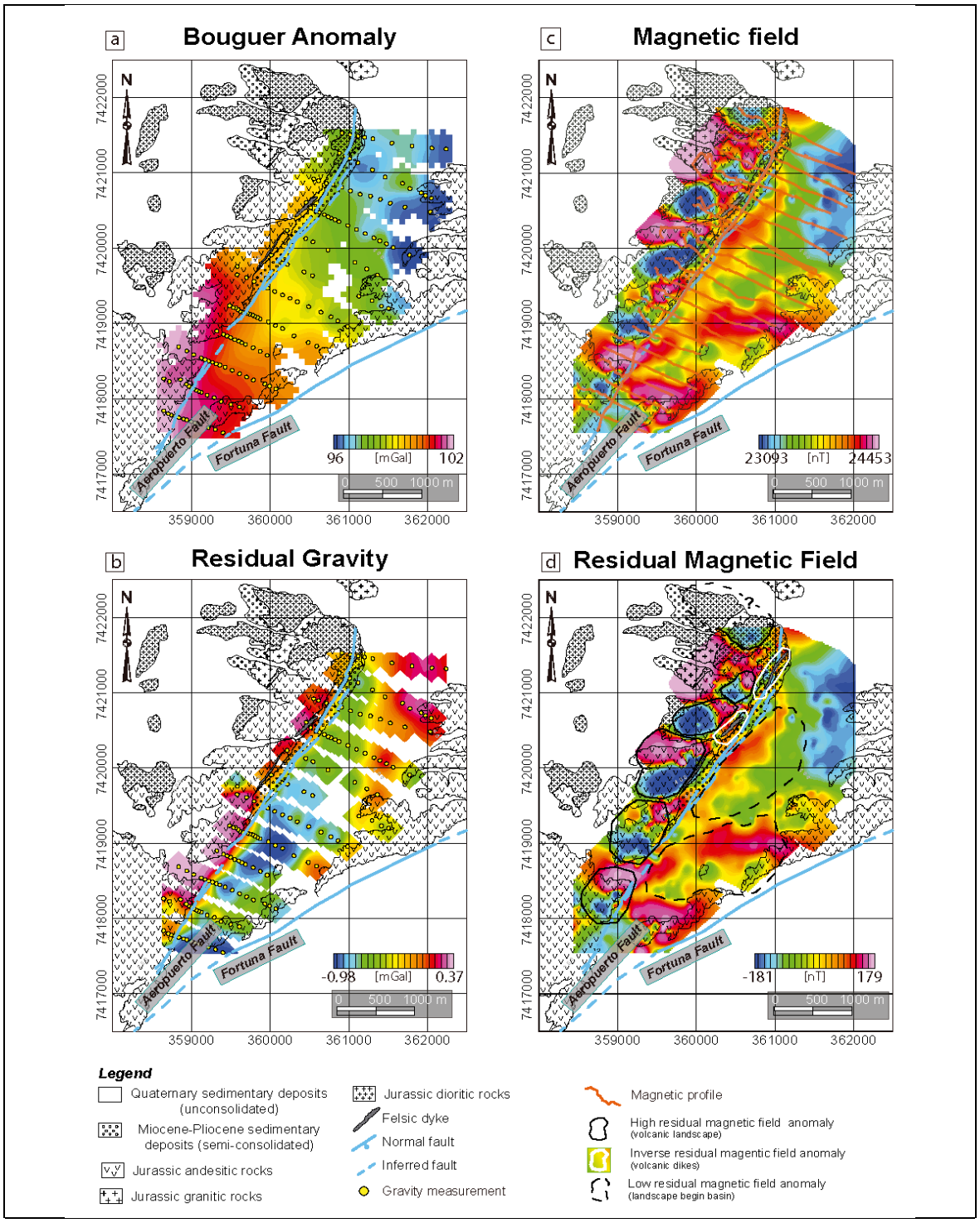

Figure 3-6: Results of the passive geophysical surveys.
Gravity survey: (a) Bouguer anomaly, (c) residual gravity. Magnetic survey: (b) magnetic field, (d) residual magnetic field.

The results of the seismic survey shows layers of different thicknesses as a function of their compression wave velocity (Vp). A limit of 2.2 km/s was used to determine the upper limit of the basement (Gardner et al., 1974). The profiles show a significant reduction of Vp below a depth of 100 m. The results of the seismic profiles can be used to infer the location of the fault escarpment and the escarpment's approximate dip angle. The lower part of the escarpment cannot be clearly determined since the depth resolution reached approximately 50 m (Figure 3-7).

The results of the TEM survey are presented in Figure 3-8. Resistivity values are generally relatively low; sediments show values of less than 80 ohm-m, while rock formations and fault zones have values of up to 240 ohm-m.

Analyzing the profiles of all of the geophysical methods together allows for a more complete evaluation of the basin structure. The two profiles for which all of the five geophysical methods were used, namely L10 and L18, are presented in Figure 3-9 and Figure 3-10, respectively.

From the comparison of the results of the various geophysical methods, is it clear that the seismic method used, does not allow a detailed view of the fault to be obtained. The main reason for this is probably the weak seismic source that was used in this study, rather than the resolution of the methodology. Future works should consider using a larger seismic source.

In contrast, the results of the electrical survey suggest a strong change in lithology at the location where the fault meets the surface. This lithological change is associated with the shape of the basin delimited by the fault to the west, suggesting a high-angle dip at depths below ~50 m. The results of the TEM survey show the same lithological units, namely the sedimentary basin and the volcanic basement, which have resistivities of ~10 ohm-m and ~200 ohm-m, respectively. The fault zone is visible as a moderately conductive region (50–80 ohm-m) and the damage zone as a more resistive region (100–150 ohm-m). Additionally, two regions with resistivities of <45 ohm-m are visible in the basement, which are probably associated with zones of fracturing and fluid percolation.

The results of the electrical surveys allow the geometry of the fault to be defined with different resolutions (TEM ~50 m, ERT ~5 m). Additionally, the results of the gravity and TEM surveys allow the identification of structures that do not appear on the surface, to the southeast of the main exposed fault.

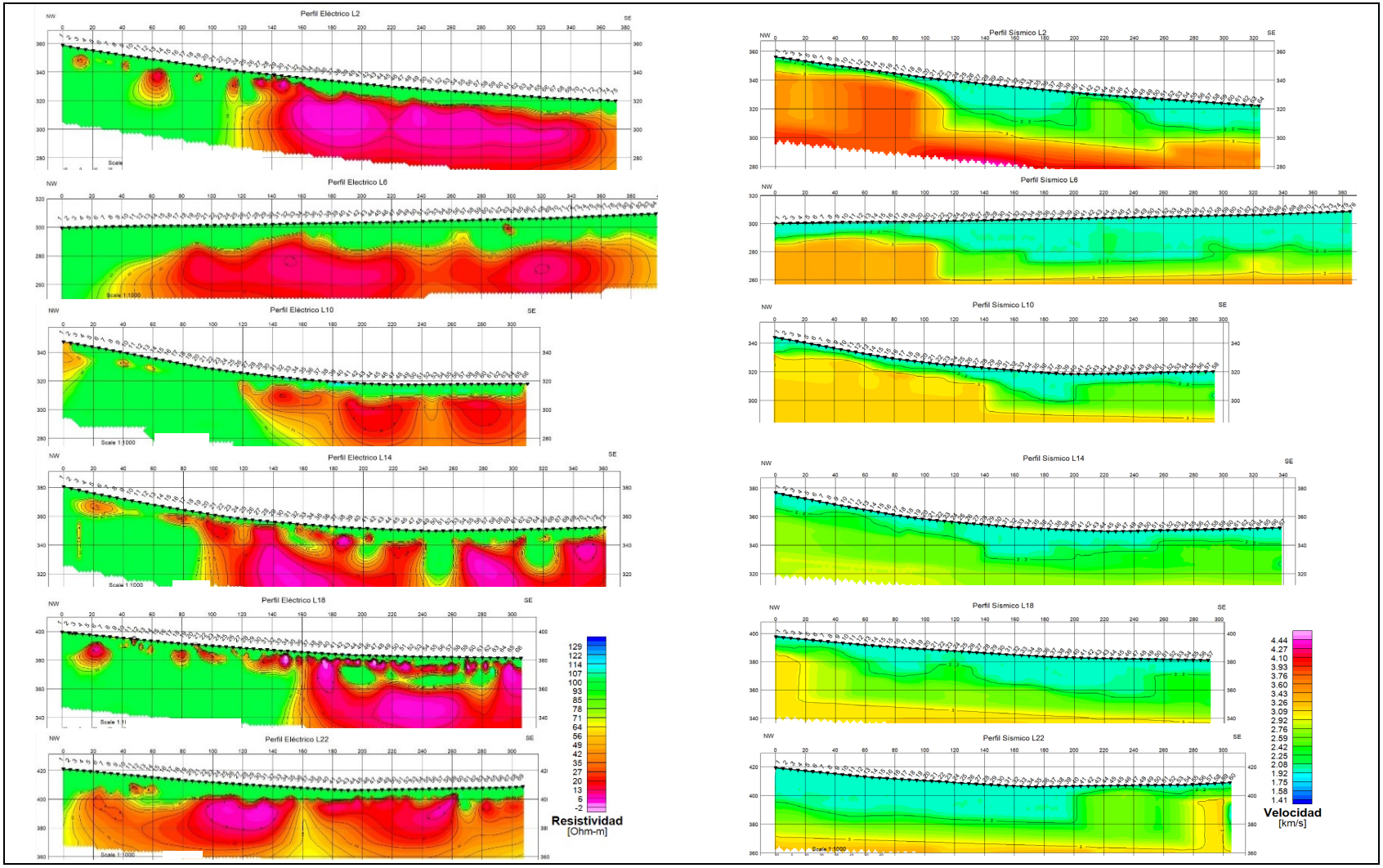

Figure 3-7: Results of the active geophysical surveys

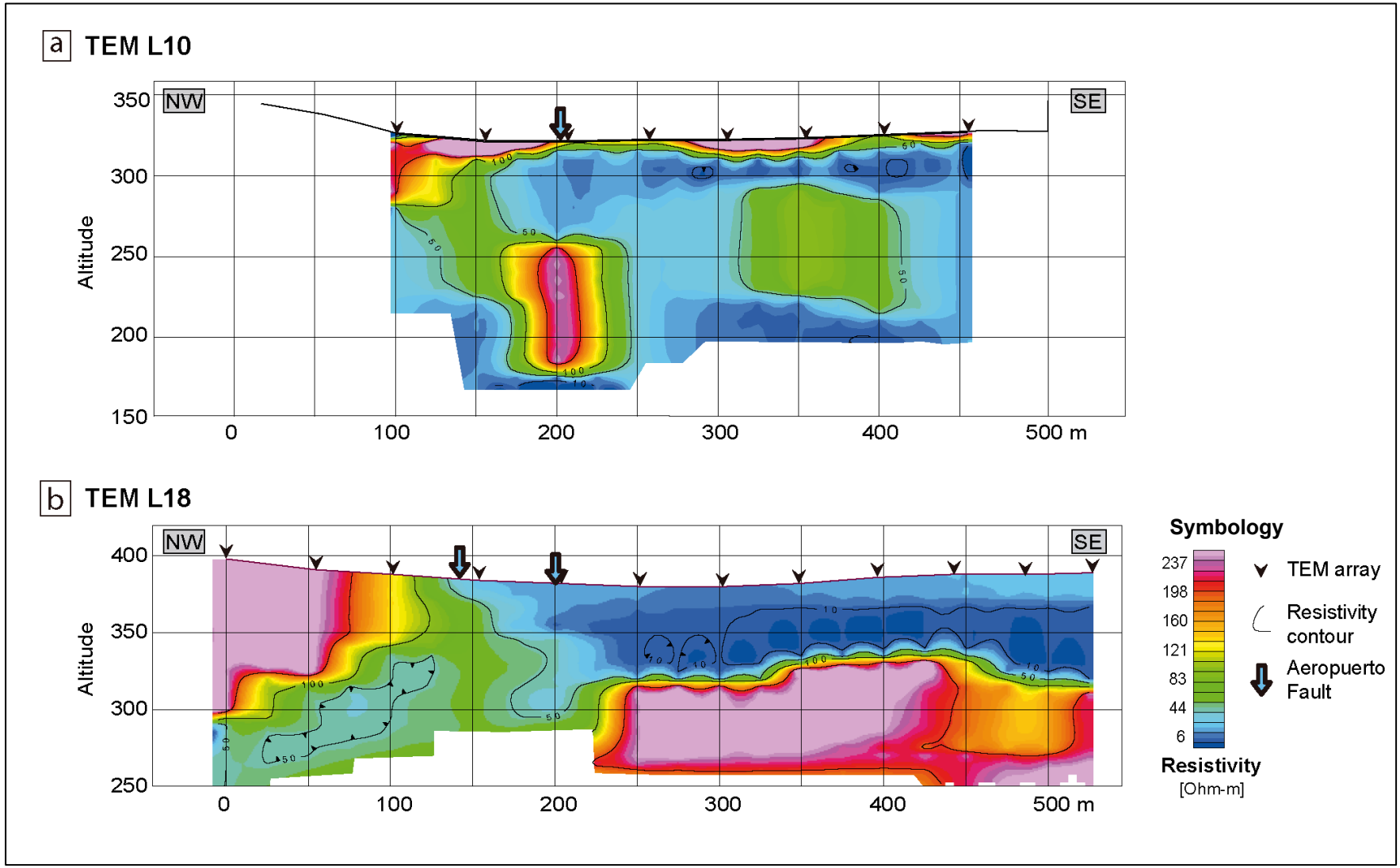

Figure 3-8: Results of the TEM survey for (a) profile L10. (b) profile L18

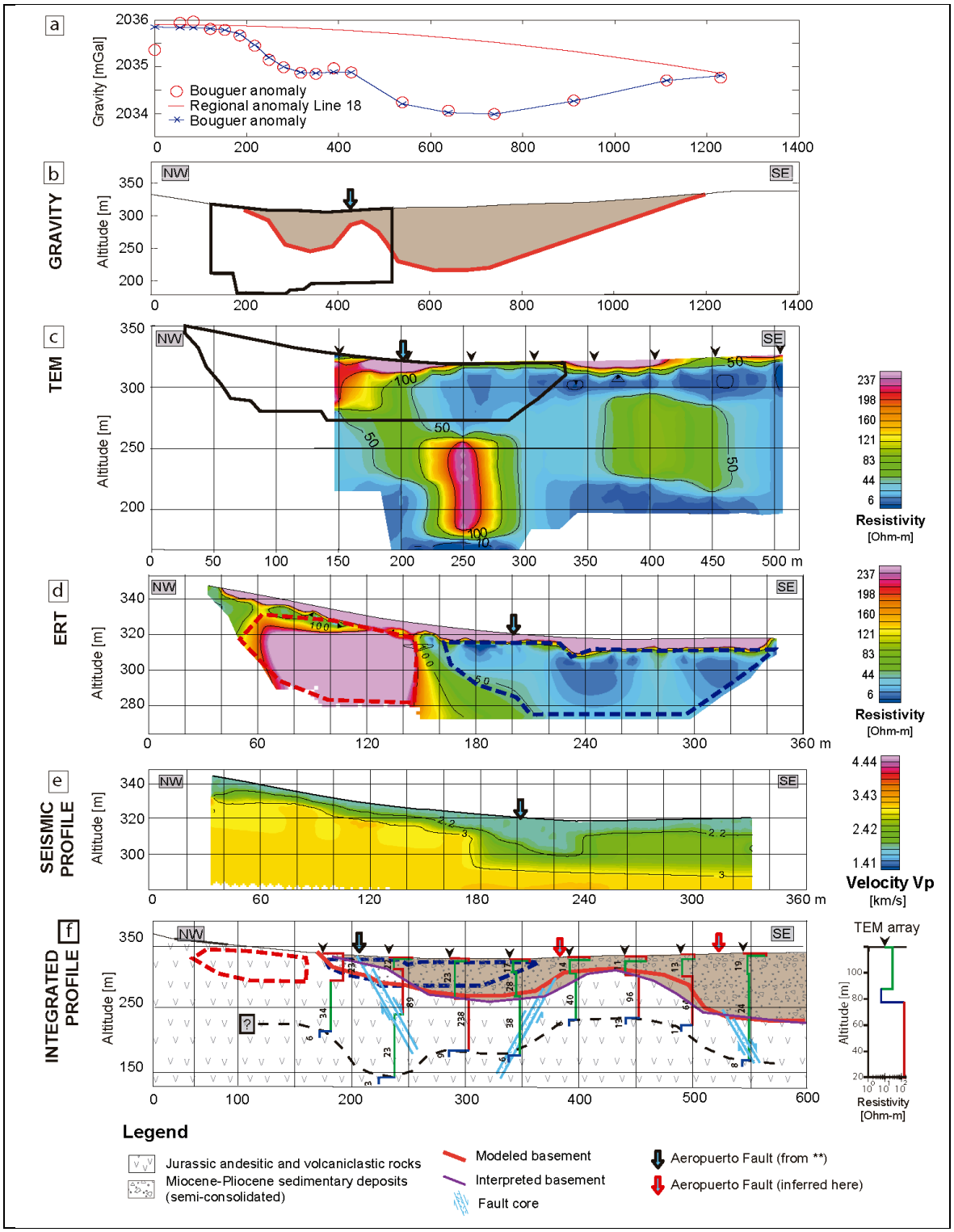

Figure 3-9: Results and integration for profile L10.
(a) seismic refraction profile. (b) electric tomography. (c) TEM. (d) Bouguer anomaly. (e) gravity anomaly. (f) integrated interpretation.

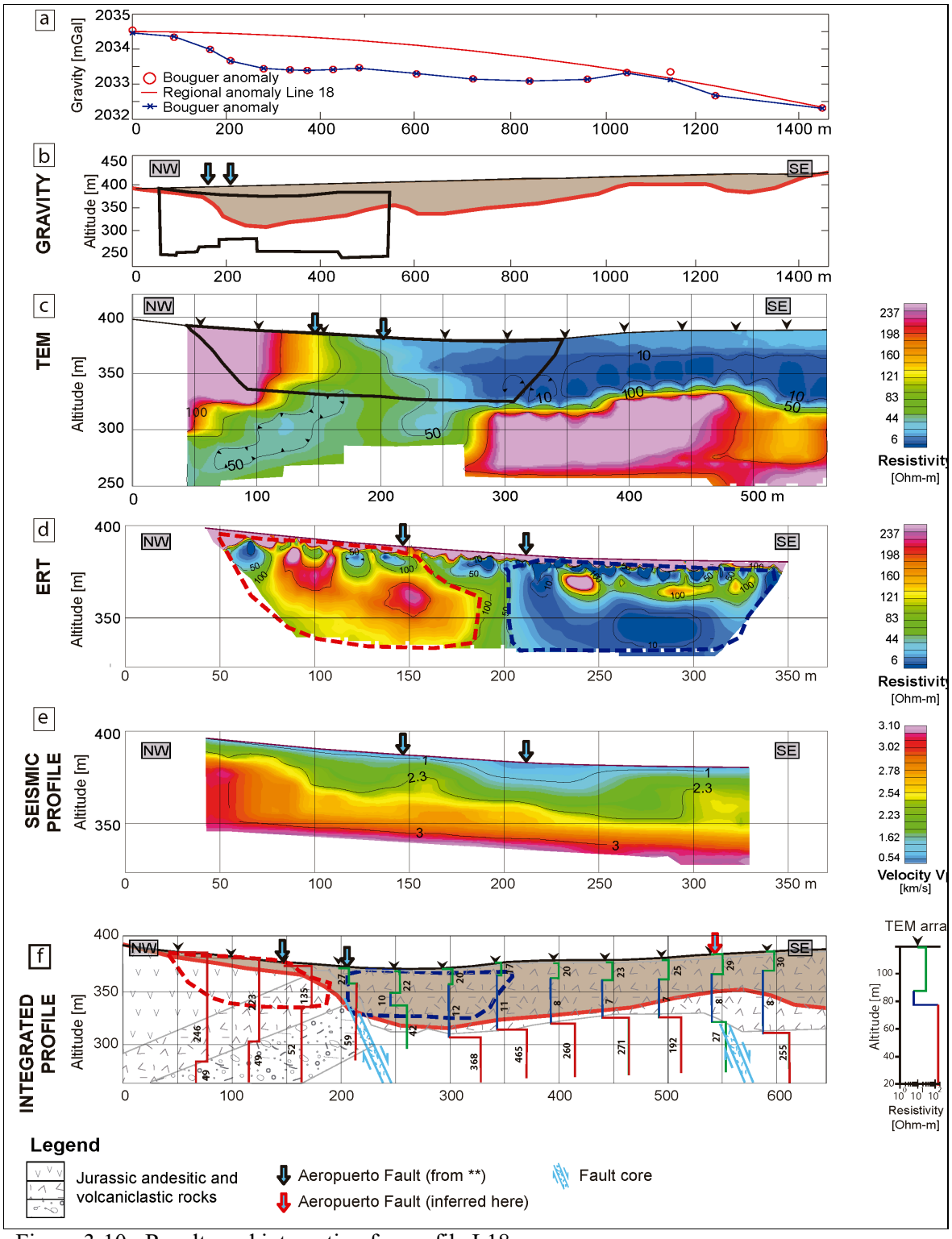

Figure 3-10: Results and integration for profile L18.
(a) seismic refraction profile. (b) electric tomography. (c) TEM. (d) Bouguer anomaly. (e) gravity anomaly. (f) integrated interpretation.

3.5 Conclusions

The main results of this work suggest the presence of a well-defined kilometer-scale fault whose attitude is N35ºE/60ºE. This corresponds to the Aeropuerto Fault, which limits an elongated and asymmetric Tertiary basin with a depocenter displaced towards the west, defining a hemi-graben. This conclusion is mainly supported by local combined electrical (TEM and ERT) and gravity surveys.

There also are several N30ºE-striking parallel faults, located tens of meters apart, and one subvertical blind N60ºE-striking fault cutting the volcanic basement: the latter is interpreted as a splay fault of the Aeropuerto Fault.

The results of the geophysical surveys show a high coherence between the different methods. The seismic refraction method accurately defines the fault-plane attitude. At a regional scale, the potential methods define the continuity of sub-surface structures fairly well and are capable of showing buried structures and basement heterogeneities.

The results of the gravity survey allow mass differences caused by the fault to be established, allowing the identification of underground structures that are not visible at the surface. To improve the resolution near the fault escarpment, it is advisable to make closer measurements, one every 10 m. The magnetic method only distinguishes between different geological units.

Regarding the active methods, TEM highlights the fault up to a depth of 150 m, although with low resolution (~50 m). The main limitation of the TEM method is the fact that it uses 1D modeling, which means that it is unable to properly discriminate sub-vertical structures. This can be improved by changing the geometry of the TEM array. The ERT method has a lower penetration depth than the TEM method, however allows higher-resolution imaging of the fault damage zone in the upper 40 m. Both methods reinforce the idea that the measurement of electrical resistivity is an excellent way to “observe” faults underground. In the future, further ERT and GPR surveys will be performed to better map 2D aspects of the fault and improve the understanding of the basement geology.

3.6 Acknowledgements

This research was supported by the +Andes Fondef Project D10I1027, CIGIDEN - Fondap Project 15110017, CEGA - Fondap Project 15090013, and the Conicyt doctorate scholarship.

We wish to thank A. Becerra, C. Benitez, A. Bosch, N. Clavería, G. De la Maza, A. Muñoz, and J. Requena, who were part of the "Geophysics methods" ICE 3800 course of spring 2013 and participated in the field work and data processing.

4 CONCLUSIONS

Crustal faults in Chile have been overlooked for decades due to the fact that the country's very large and frequent subduction zone earthquakes have concentrated the attention of most researchers in seismotectonics. In this thesis, I expound, using a combination of published and new data, the theory that crustal faults are capable of producing shallow Mw>6 earthquakes every few hundreds to thousands of years.

Crustal faults occur in the overriding South American plate throughout the Andes. In Chile, crustal faults can be organized into three margin-parallel domains according to their spatial distribution: (1) Outer Forearc; (2) Inner Forearc; and (3) Volcanic Arc. These three domains are crosscut by Andean transverse faults (ATF), which run oblique to the margin from the coast to the Main Cordillera.

In this thesis, the seismogenic potential of crustal faults from these three different domains was estimated based on their typical segment length (in tens of kilometers), slip rate, and associated thickness of the seismogenic layer, which is largest in the outer forearc (~30 km) and lowest in the intra-arc (<12 km).

Faults lying on each of the margin-parallel domains share some first-order geometric and kinematic potential seismogenic properties. The faults in the outer forearc are either margin-parallel (such as the Atacama Fault System) or margin-oblique (such as the Pichilemu fault), exhibit normal dip-slip displacements at rates of 0.2–0.6 mm/year. These faults have exceptionally well-exposed traces in Northern Chile and only limited exposure in Central and Southern Chile. Geological and geophysical surveys show the 3D geometry and kinematics of some key segments of the Atacama Fault System, such as the Aeropuerto Fault, located close to the Mejillones Peninsula.

Faults of the inner forearc include the margin-parallel Domeyko Fault System in Northern Chile and the San Ramón Fault in Central Chile. These include both low-angle and high-angle west-verging reverse faults and subvertical strike-slip faults. They commonly define the boundary between the Main Cordillera and the Central Depression,

and show slip rates of 0.1–0.4 mm/year, similar to the faults of the outer forearc. Some crustal faults of the inner forearc show present-day low-magnitude crustal seismicity.

Crustal fault systems of the intra-arc region of the Main Cordillera are represented by low-angle thrusts in Central Chile east of Santiago and by dextral strike-slip faults south of 35°S, from the Teno River valley to the triple junction at 47°S (the LOFS). Slip rates determined by previously acquired GPS data and numerical modeling range from 1 to 10 mm/year. Furthermore, preliminary geomorphological studies which were previously carried out in the northern part of the LOFS determined faster slip rates of ~5–19 mm/yr and 12–25 mm/yr.

Faults in the outer forearc region have the potential to generate Mw 7 earthquakes every few thousand years. One key characteristic of these faults is that they can be reactivated as the result of Mw ~8.5+ subduction earthquakes, as occurred on the Pichilemu Fault in 2010, which generated two earthquakes only a few days after the Mw 8.8 Maule earthquake. However, earthquakes with a Mw >7 can also occur since the cold, thick crust of the outer forearc region allows the nucleation of earthquakes with depths of up to 30 km.

Typical faults from the inner forearc, such as the San Ramón Fault, have been shown to generate Mw ~7–7.5 earthquakes with similar or slightly longer recurrence times than typical faults of the outer forearc.

Lastly, intra-arc faults, such as 40-km long segments of the Liquiñe–Ofqui Fault System in Southern Chile, are capable of producing Mw 6–7 earthquakes every few hundred years; however, their maximum size is limited by the relatively thin seismogenic crust (8–12 km), which prevents the propagation of earthquakes deeper down.

Block diagrams summarizing fault behavior in different margin-parallel domains are shown in Figures 4-1 to 4-4.

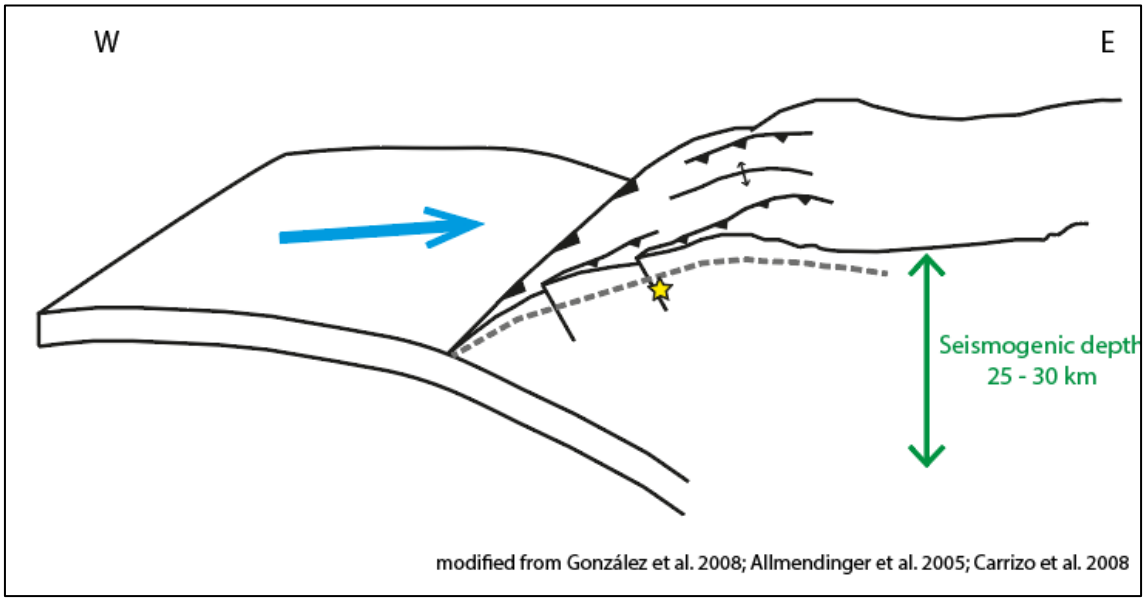

Figure 4-1: E-W reverse faults in the Outer Forearc domain (e.g., Bajo Molle Fault).

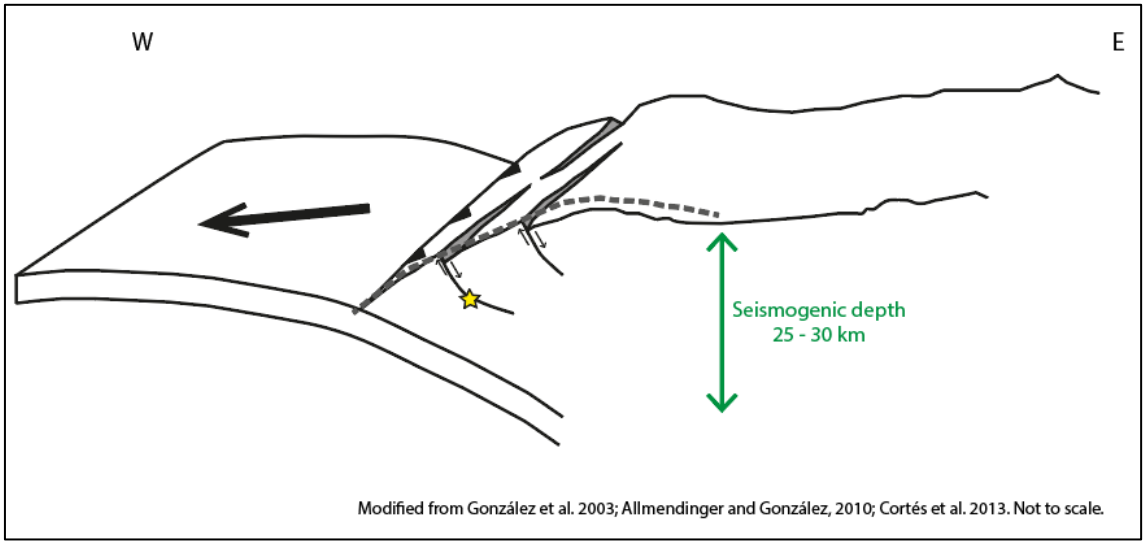

Figure 4-2: N-S normal faults in the Outer Forearc domain (e.g., the Atacama Fault System).

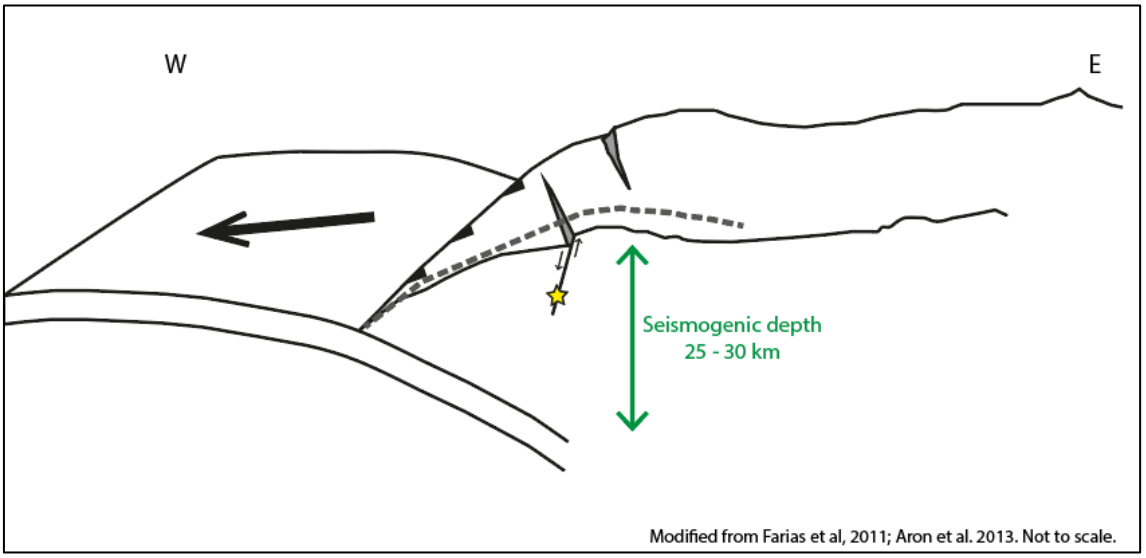

Figure 4-3: A trench-oblique normal fault in the Outer Forearc domain (e.g., Pichilemu Fault).

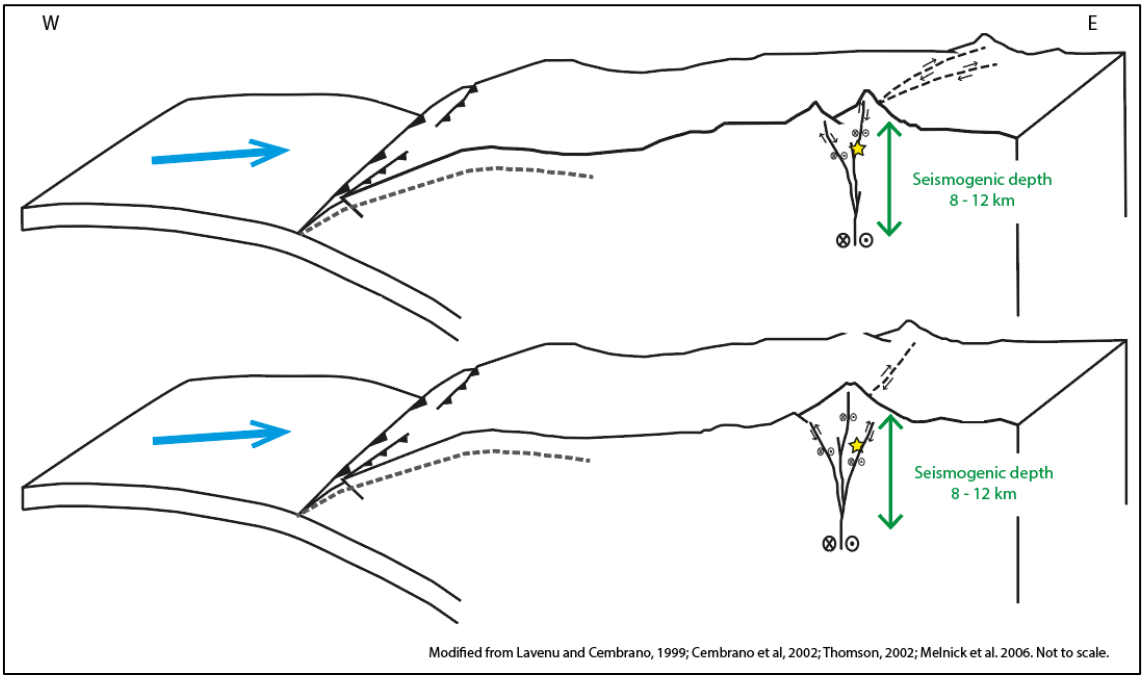

Figure 4-4: A trench-parallel strike-slip fault in the Volcanic Arc domain (e.g., Liquiñe–Ofqui Fault System).

By combining structural geological and geophysical fieldwork, a subsurface approach to fault geometry was achieved in this thesis. A case study of the Aeropuerto Fault study revealed a steeply-dipping fault up to a depth of 150 m. A hemi-graben basin shape was confirmed, supporting the domino-normal-fault model previously proposed for the Atacama Fault System (e.g., Allmendinger and González, 2010). Additionally, a system of N30ºE parallel faults which are not visible at the surface were identified by gravity and TEM surveys. All of these faults cut through basement rock, which is very significant for estimations of recurrence time and slip.

Finally, the correlation and significance of several geophysical methodologies used for the analysis of crustal faults could be of great benefit in future research.

5 REFERENCES

Adriasola, A.C., Thomson, S.N., Brix, M.R., Hervé, F., Stockhert, B. (2006). Postmagmatic cooling and late Cenozoic denudation of the North Patagonian Batholith in the Los Lagos region of Chile, 41°–42°15′S. International Journal of Earth Sciences 95 (3): 504–528.

Agurto, H., Rietbrock, A., Barrientos, S., Bataille, K., Legrand, D. (2012). Seismotectonic structure of the Aysén Region, Southern Chile, inferred from the 2007 Mw = 6.2 Aysén earthquake sequence. Geophysical Journal International 190: 116-130.

Agurto, H., Rietbrock, A., Bataille, K., Miller, M., Iwamori, H., Priestley, K. (2014). Seismicity distribution in the vicinity of the Chile Triple Junction, Aysén Region, southern Chile. Journal of South American Earth Sciences 51: 1-11.

Aki, K. (1979). Characterization of barriers on an earthquake fault. J. Geophys. Res. 84, 6140–6148.

Aki, K., Lee, W.H.K. (2003). Glossary of Interest to Earthquake and Engineering Seismologists. In International Handbook of Earthquake and Engineering Seismology, (Lee, W.H.K., Kanamori, H., Jennings, P., Kisslinger, C. Eds.). Academic Press: Vol. 81B, Appendix 1, 1793-1856. London.

Alfaro, A. (2011). Peligro Sísmico en el Segmento Norte de la Región del Maule, Chile. Memoria de Título (Inédito), Universidad de Chile, Departamento de Geología: 136.

Allmendinger, R. W., González, G. (2010). Invited review paper: Neogene to Quaternary tectonics of the coastal Cordillera, northern Chile. Tectonophysics 495 (1-2): 93–110.

Allmendinger, R., González, G., Yu, J., Hoke, G., Isacks, B. (2005). Trench-parallel shortening in the northern Chilean forearc: tectonic and climatic implications. Geological Society of America Bulletin 117: 89–104.

Alvarado, A., Audin, L., Nocquet, J. M., Jaillard, E., Mothes, P., Jarrín, P., Segovia, M., Rolandone, F., Cisneros, D. (2016). Partitioning of oblique convergence in the Northern Andes subduction zone: Migration history and the present-day boundary of the North Andean Sliver in Ecuador. Tectonics 35 (5): 1048-1065.

Alvarado, A., Audin, L., Nocquet, J. M., Lagreulet, S., Segovia, M., Font, Y., Lamarque, G., Yepes, H. Mothes, P., Rolandone, F., Jarrín, P., Quidelleur, X. (2014). Active tectonics in Quito, Ecuador, assessed by geomorphological studies, GPS data, and crustal seismicity. Tectonics 33: 67–83.

Alvarado, P., Barrientos, S., Saez, M., Astroza, M., Beck, S. (2009). Source study and tectonic implications of the historic 1958 Las Melosas crustal earthquake, Chile, compared to earthquake damage. Physics of the Earth and Planetary Interiors 175: 26–36.

Álvarez, O., Nacif, S., Gimenez, M., Folguera, A., Braitenberg, C. (2014). GOCE derived vertical gravity gradient delineates great earthquake rupture zones along the Chilean margin. Tectonophysics (ISSN0040-1951).

Angermann, D., Klotz, J., Reigber, C. (1999). Space-geodetic estimation of the Nazca–South America Euler vector. Earth Planet. Sci. Lett. (171: 329–334.

Arabasz, W. J. (1971). Geological and geophysical studies of the Atacama Fault Zone in northern Chile. Ph. D. Thesis (Unpublished), California Institute of Technology: 264.

Armijo, R., Lacassin, R., Coudurier-Curveur, A., Carrizo, D. (2015). Coupled tectonic evolution of Andean orogeny and global climate. Earth Sci. Rev. (143: 1–35.

Armijo, R., Rauld, R., Thiele, R., Vargas, G., Campos, J., Lacassin, R., Kausel, E. (2010). The West Andean Thrust, the San Ramón Fault, and the seismic hazard for Santiago, Chile. Tectonics 29: 1-34.

Arndt, J., Bartel, T., Scheuber, E., Schilling, F. (1997). Thermal and rheological properties of granodioritic rocks from the Central Andes, North Chile. Tectonophysics 271: 75-88.

Aron, F., Allmendinger, R., Cembrano, J., González, G., Yáñez, G. (2013). Permanent fore-arc extension and seismic segmentation: Insights from the 2010 Maule earthquake, Chile. J. Geophys. Res. Solid Earth 118: 1-16.

Aron, F., Cembrano, J., Astudillo, F., Allmendinger, R., Arancibia, G. (2014). Constructing forearc architecture over megathrust seismic cycles: Geological snapshots from the Maule earthquake region, Chile. Geological Society of America Bulletin 127 (3–4): 464–479.

Arriagada, C., Arancibia, G., Cembrano, J., Martínez, F., Carrizo, D., Van Sint Jan, M., Sáez, E., González, G., Rebolledo, S., Sepúlveda, S.A., Contreras-Reyes, E. Jensen, E., Yáñez, G. (2011). Nature and tectonic significance of co-seismic structures associated with the Mw 8.8 Maule earthquake, central-southern Chile forearc. J. Struct. Geol. 33 (5) 891–897.

Asano, Y., Saito, T., Ito, Y., Shiomi, K., Hirose, H., Matsumoto, T., Aoi, S., Hori, S., Sekiguchi, S. (2011). Spatial distribution and focal mechanisms of aftershocks of the 2011 off the Pacific coast of Tohoku earthquake. Earth Planets Space, 63(7), 669–673.

Asch, G., Schurr, B., Bohm, M., Yuan, X., Haberland, C., Heit, B., Kind, R., Woelbern, I., Bataille, K., Comte, D., Pardo, M., Viramonte, J., Rietbrock, A., Giese, P. (2006). Seismological Studies of the Central and Southern Andes. In: The Andes – Active Subduction Orogeny. Frontiers in Earth Science Series Part II (Oncken, O., Chong, G., Franz, G., Giese, P., Götze, H-J., Ramos, V.A., Strecker, M.R., Wigger, P. Eds.). Springer-Verlag: (21), 443–457. Berlin.

Astudillo, L.A., Cortés-Aranda, J., Melnick, D., Tassara, A. (2018, Holocene deformation along the Liquiñe – Ofqui Fault Zone, southern Chile: Field observations and

geomorphic analysis. 9th International INQUA Meeting on Paleoseismology, Active Tectonics and Archeoseismology (PATA), 25 – 27 June, 2018, Possidi, Greece.

Audin, L., Lacan, P., Tavera, H., Bondoux, F. (2008). Upper plate deformation and seismic barrier in front of Nazca subduction zone: The Chololo Fault System and active tectonics along the Coastal Cordillera, southern Peru. Tectonophysics, 459, Issues 1-4, 1, 174-185.

Bangs N.L., Cande, S.C. (1997). Episodic development of a convergent margin inferred from structures and processes along the southern Chile margin. Tectonics 16:489–503.

Barrientos, S. (1980). Regionalización sísmica de Chile. Tesis de Magíster en Ciencias (Inédito). Universidad de Chile, Departamento de Geofísica: 72.

Barrientos, S. (2007). Earthquakes in Chile. In The Geology of Chile (Moreno, T., Gibbons, W. Eds.). Geological Society: 263-287. London.

Barrientos, S., Vera, E., Alvarado, P., Monfret, T. (2004). Crustal seismicity in central Chile. Journal of South American Earth Sciences 16: 759-768.

Barrientos, S.E., Ward, S.N. (1990). The 1960 Chile earthquake: inversion for slip distribution from surface deformation. Geophysical Journal International, 103 (3): 589-598.

Bilek, S.L. (2007). Influence of subducting topography on earthquake rupture. In: The Seismogenic Zone of Subduction Thrust Faults, T. Dixon and C. Moore (Eds.), Columbia University Press, New York, 123–146.

Bloch, W., Kummerow, J., Salazar, P., Wigger, P., Shapiro, S. A. (2014). High-resolution image of the North Chilean subduction zone: seismicity, reflectivity and fluids. Geophys. J. Int. (197: 1744–1749.

Bondar, I., Engdahl, E.R., Villaseñor, A., Harris, J., Storchak, D. (2015). ISC-GEM: Global Instrumental Earthquake Catalogue (1900-2009), II. Location and seismicity patterns. Physics of the Earth and Planetary Interiors, 239: 2-13.

Bonilla, M.C., Mark, R.X., Lienkaemper, J.J. (1984). Statistical relations among earthquake magnitude, surface rupture length, and surface fault displacement. Bull. Seismol. Soc. Am. 74: 2379–2422.

Brown, M., Díaz, F., Grocott, J. (1993). Displacement history of the Atacama fault system 25°00'-27°00'S, northern Chile. Geological Society of America Bulletin 105: 1165-1174.

Burbank, D., Anderson, R. (2001). Tectonic Geomorphology. Blackwell Science Ltd.: 274 p. Oxford.

Campos, J., Kausel, E. (1990). The large 1939 intraplate earthquake of southern Chile. Seismological Research Letters, 61, 43.

Cande, S.C., Leslie, R.B. (1986). Late Cenozoic tectonics of the southern Chile Trench. J. Geophys. Res. 91: 471–496.

Carrizo, D., González, G., Dunai, T. (2008). Constricción neógena en la Cordillera de la Costa, norte de Chile: Neotectónica y datación de superficies con 21Ne cosmogénico. Rev. Geol. Chile 35 (1): 1-38.

Cembrano, J., Moreno, H. (1994). Geometría y naturaleza contrastante del volcanismo cuaternario entre los 38°y 46°S: Dominios compresionales y tensionales en un régimen transcurrente? In Actas VII Congreso Geológico Chileno: 240-244. Concepción, Chile.

Cembrano, J., González, G., Arancibia, G., Ahumada, I., Olivares, V., Herrera, V. (2005). Fault zone development and strain partitioning in an extensional strike-slip duplex: A case study from the Mesozoic Atacama fault system, northern Chile. Tectonophysics 400 (1–4): 105–125.

Cembrano, J., Hervé, F. (1993). The Liquiñe Ofqui Fault Zone: a major Cenozoic strike slip duplex in the Southern Andes. In 2nd International Symposium on Andean Geodynamics ISAG: 175-178. Oxford, UK.

Cembrano, J., Hervé, F., Lavenu, A. (1996). The Liquiñe-Ofqui fault zone: a long-lived intra-arc fault Zone in southern Chile. Tectonophysics, 259: 55–66.

Cembrano, J., Lara, L. 2009). The link between volcanism and tectonics in the Southern Volcanic Zone of the Chilean Andes: A review. Tectonophysics, 471 (1–2): 96–113.

Cembrano, J., Lavenu, A., Reynolds, P., Arancibia, G., Lopez, G., Sanhueza, A. (2002). Late Cenozoic transpressional ductile deformation north of the Nazca–South America–Antarctica triple junction. Tectonophysics 354: 289– 314.

Cembrano, J., Lavenu, A., Yáñez, G., Riquelme, R., García, M., González, G., Hérail, G. (2007). Neotectonics. In The Geology of Chile (Moreno, T., Gibbons, W. Eds.). Geological Society: 263-287. London.

Chernicoff, C.J., Richards, J.P., Zappettini, E.O. (2002). Crustal lineament control on magmatism and mineralization in northwestern Argentina: geological, geophysical, and remote sensing evidence. Ore Geol. Rev. (21: 127–155.

Chiou, B.S.J., Youngs, R.R. (2014). Update of the Chiou and Youngs NGA Ground Motion Model for Average Horizontal Component of Peak Ground Motion and Response Spectra. Earthquake Spectra 30: 1117–1153.

Cifuentes, I.L. (1989). The 1960 Chilean earthquakes. Journal of Geophysical Research 94 (B1): 665–680.

Cisternas, A., Vera, E. 2008). Sismos históricos y recientes en Magallanes. Magallania 36 (1): 43-51.

Cisternas, M., Atwater, B.F., Torrejón, F., Sawai, Y., Machuca, G., Lagos, M., Eipert, A., Youlton, C., Salgado, I., Kamataki, T., Shishikura, M., Rajendran, C. P., Malik, J.K.,

Rizal, Y., Husni, M. (2005). Predecessors of the giant 1960 Chile earthquake. Nature 437: 404–407.

Civile, D., Lodolo, E., Vuan, A., Loreto, M.F. (2012). Tectonics of the Scotia–Antarctica plate boundary constrained from seismic and seismological data. Tectonophysics 550–553: 17–34.

Cloos, M. (1992). Thrust-type subduction-zone earthquakes and seamount asperities: a physical model for seismic rupture. Geology 20, 601–604.

Collot, J.Y., Marcaillou, B., Sage, F., Michaud, F., Agudelo, W., Charvis, P., Graindorge, D., Gutscher, M-A., Spence, G. (2004). Are rupture zone limits of great subduction earthquakes controlled by upper plate structures? Evidence from multichannel seismic reflection data acquired across the northern Ecuador-southwest Colombia margin. J. Geophys. Res., 109, B11103.

Comte, D., Bordier, M., Boroschek, R., David, C., Martinod, J., Glass, B., Correa, E., Balmaceda, I., Dorbath, L., Haessler, H., Herail, G., Meneses, C., Frogneux, M., Cruz, A. (2001). Analysis of the 24 July 2001 shallow earthquake Mw = 6.3 recorded in the Northern Chile Altiplano. In Eos Trans. AGU Fall Meeting 82 (47) Abstract S52A-0616.

Comte, D., Dorbath, L., Pardo, M., Monfret, T.,, Haessler, H., Rivera, L., Frogneux, M., Glass, B., Meneses, C. (2002). Análisis del terremoto superficial del Altiplano, norte de Chile, ocurrido el 24 de julio de 2001, Mw=6.3. VIII Jornadas Chilenas de Sismología e Ingeniería Antisísmica. Valparaíso, Chile.

Comte, D., Eisenberg, A., Lorca, E., Pardo, M., Ponce, L., Saragoni, R., Singh, S. K. Y Suarez, G. (1986). The 1985 Central Chile Earthquake: A Repeat of Previous Great Earthquakes in the Region? Science 233 (4762): 449-453.

Comte, D., Farías, M., Charrier, R., González, A. (2008). Active Tectonics in the Central Andes: 3D tomography based on the aftershock sequence of the 28 August 2004 shallow crustal earthquake. In 7th International Symposium on Andean Geodynamics ISAG: 160-163. Nice.

Contreras-Reyes, E., Carrizo, D. (2011). Control of high oceanic features and subduction channel on earthquake ruptures along the Chile–Peru subduction zone. Phys. Earth Planet. Inter.186, 49–58.

Cornejo, P., Tosdal, R.M., Mpodozis, C., Tomlinson, A., Rivera, O., Fanning, M.C. 1997). El Salvador, Chile, porphyry copper deposit revisited: Geologic and geochronologic framework. International Geology Review 39: 22–54.

Cortés, J. A., González, G., Binnie, S. A., Ruth, R., Freeman, S. P. H. T., Vargas, G. (2012). Paleoseismology of the Mejillones Fault, northern Chile: Insights from cosmogenic 10Be and Optically Stimulated Luminescence determinations. Tectonics 31 (2).

Cortés, J. Marquardt, C., González, G., Wilke, N., Marinovic, N. (2007). Carta Mejillones y Península de Mejillones, Región de Antofagasta. Servicio Nacional de Geología y Minería, Carta Geológica de Chile, Serie Geología Básica, 1 mapa 1:100.000.

Cortés, J.A. (2012). Actividad de fallas de la placa superior en el antearco costero del norte de Chile (~23°30's): Paleosismología, implicancias neotectónicas y relación con el ciclo de subducción. PhD Thesis (Unpublished), Universidad Católica del Norte - Université Paul Sabatier Toulouse III: 346.

Cortés-Aranda., J., González., G., Remy., D., Martinod, J. (2014). Normal upper plate fault reactivation in northern Chile and the subduction earthquake cycle: From geological observations and static Coulomb Failure Stress (CFS) change. Tectonophysics 639: 118–131.

Costa, C. (2004). Microtectónica en el Cuaternario? Métodos y aplicaciones de la Paleosismología. Revista Asociación Geológica Argentina, Publicación Especial 7: 9-19.

Costa, C., Audemard, F., Audin, L., Benavente, C. (2010). Geomorphology as a Tool for Analysis of Seismogenic Sources in Latin America and the Caribbean. In Natural Hazards and Human-Exacerbated Disasters in Latin America. Special Volumes of Geomorphology. Developments in Earth Surface Processes (Latrubesse, E. Ed.). Elsevier 13: 29-47. Amsterdam.

Costa, C., Smalley, R., Schwartz, D., Stenner, H., Ellis, M., Ahumada, E., Velasco, M. (2006b. Paleoseismic observations of an onshore transform boundary: The Magallanes–Fagnano fault, Tierra del Fuego, Argentina. Revista de la Asociación Geológica Argentina, 61 (4): 647-657.

Costa, C.H., Audemard M, F.A., Bezerra, F.H.R., Lavenu, A., Machette, M.N., París, G. (2006a. An overview of the main Quaternary deformation of South America. Revista de la Asociación Geológica Argentina, 61: 461–479.

Das, S., Watts, A.B. (2009). Effect of subducting seafloor topography on the rupture characteristics of great subduction zone earthquakes. In: Lallemand, S., Funiceillo, F. (Eds.), Subduction Zone Geodynamics. Springer-Verlag, Berlin–Heidelberg, pp.103–118.

David, C. (2007). Comportamiento actual del ante-arco y del arco del codo de Arica en la orogénesis de los Andes centrales. PhD Thesis (Unpublished), Universidad de Chile-Université Paul Sabatier: 291.

David, C., Martinod, J., Comte, D., Haessler, H., Dorbath, L. (2002). Intracontinental Seismicity and Neogene Deformation of the Andean Forearc in the region of Arica (18,5°-19,5°S). In 5th International Symposium on Andean Geodynamics ISAG. Toulouse, France.

DeLouis, B., Philip, H., Dorbath, L. Cisternas, A. (1998). Recent crustal deformation in the Antofagasta Region (northern Chile) and the subduction process. Geophys. J. Int. (132: 302-338.

DeMets, C., Gordon, R.G., Argus, D.F. (2010). Geologically current plate motions. Geophys. J. Int. (181: 1–80.

DeMets, C., Gordon, R.G., Argus, D.F., Stein, S. (1990). Current plate motions. Geophys. J. Int. (10: 425–478.

DeMets, C., Gordon, R.G., Argus, F., Stein, S. (1994). Effect of recent revisions of the geomagnetic timescale on estimates of current plate motions. Geophys. Res. Lett. (21: 2191–2194.

De Pascale, G. P., Penna, I., Hermanns, R.L., Froude, M., Sepulveda, S.A. (2016). First steps towards a fast slip rate along the Liquine-Ofqui Fault Zone in Chilean Patagonia. American Geophysical Union, Fall Meeting 2016, abstract #T41B-2911.

De Pascale, G.P., Froude, M., Penna, I., Hermanns, R., Moncada, D., Sepulveda, S., Persico, M., Petley, D., Vargas, G., Murphy, W., Pairoa, S. (2018). Preliminary geologic slip rates along Andes fastest slipping crustal fault, the Liquiñe-Ofqui Fault Zone (LOFZ), Patagonia. (2018 SCEC Annual Meeting, SCEC Contribution #8265, Poster #222.

Dewey, J.W., Choy, G., Presgrave, B., Sipkin, S., Tarr, A. C., Benz, H., Earle, P., Wald, D. 2007). Seismicity associated with the Sumatra–Andaman Islands earthquake of 26 December 2004. Bull. Seismol. Soc. Am., 97(1A), S25–S42.

Dunai, T.J., González López, G.A., Juez-Larré, J. (2005, Oligocene–Miocene age of aridity in the Atacama Desert revealed by exposure dating of erosion-sensitive landforms. Geology 33: 321–324.

Espinoza, R. (2013). Sistemas de fallas Caleta Herradura: Evolución, Cinemática y Geometría. Península de Mejillones, Norte de Chile. Memoria de Título (Inédito). Universidad Católica del Norte.

Estay, N.P., Yáñez, G., Carretier, S., Lira, E., Maringue, J. (2016). Seismic hazard in low slip rate crustal faults, estimating the characteristic event and the most hazardous zone: study case San Ramón fault, in central Andes. Natural Hazards Earth System Sciences 16: 2511-2528.

Fairbridge, R. (1981). The concept of neotectonics: An introduction. Zeitschrift Geomorphologischen Beilband 40: 7-12.

Farías, M. (2007). Tectónica y erosión en la evolución del relieve de los Andes de Chile Central durante el Neógeno. Tesis de PhD (Inédito), Universidad de Chile, Departamento de Geología: 191.

Farías, M., Charier, R. Comte, D. Martinod, J. Hérail, G. (2005). Late Cenozoic deformation and uplift of the western flank of the Altiplano: Evidence from the

depositional, tectonic, and geomorphologic evolution and shallow seismic activity (northern Chile at 19◦30'S). Tectonics 24 (TC4001).

Farías, M., Comte, D., Charrier, R., Martinod, J., David, C., Tassara, A., Tapia, F., Fock, A. (2010). Crustal-scale structural architecture in central Chile based on seismicity and surface geology: implications for Andean mountain building. Tectonics 29 (3) TC3006.

Farías, M., D. Comte, S. Roecker, D. Carrizo, y M. Pardo. (2011). Crustal extensional faulting triggered by the 2010 Chilean earthquake: The Pichilemu Seismic Sequence. Tectonics 30 (TC6010).

Fock, A.. (2005). Cronología y tectónica de la exhumación en el neógeno de los Andes de Chile central entre los 33º y los 34ºS. Tesis de Magister (Inédito), Universidad de Chile: 235.

Forsythe, R.D., Nelson, E. (1985). Geological manifestation of ridge collision: Evidence for the Golfo de Penas, Taitao basin, southern Chile. Tectonics 4: 477–495.

Gerbault, M., Cembrano, J., Mpodozis, C., Farías, M., Pardo, M. (2009). Continental margin deformation along the Andean subduction zone: Thermo-mechanical models. Physics of the Earth and Planetary Interiors 177: 180–205.

Giocoli, A., Galli, P., Giaccio, B., Lapenna, V., Messina, P., Peronace, E., Romano, G., Piscitelli, S. (2011). Electrical Resistivity Tomography across the Paga-nica-San Demetrio fault system (L'Aquila 2009 earthquake). Bollettino di Geofisica Teorica ed Applicata, v.52 (3), pp. 457-469.

González -Bonorino, G., Rinaldi, V., del Valle, L., Alvarado, P., Bujalesky, G.G., Güell, A. (2012). Paleoseismicity and seismic hazard in southern Patagonia (Argentina-Chile, 50–55S) and the role of the Magallanes-Fagnano transform fault. Nat. Hazards 61: 337–349

González, A. (2008). Análisis estructural entre los valles del río Tinguiririca y Teno, Cordillera Principal de Chile Central: Microsismicidad y Geología Superficial. Memoria de Título (Inédito), Universidad de Chile 90.

González, G. Cembrano J. Carrizo D. Macci, A. Schneider, H. (2003). Link between forearc tectonics and Pliocene-Quaternary deformation of the Coastal Cordillera, Northern Chile. Journal of South American Earth Sciences 16: 321-342.

González, G., Dunai, T., Carrizo, D., Allmendinger, R. (2006). Young displacements on the Atacama Fault System, northern Chile from field observations and cosmogenic 21Ne concentrations. Tectonics 25 (TC3006).

González, G., Gerbault, M., Martinod, J., Cembrano, J., Allmendinger, R., Carrizo, D., Espina, J. (2008). Crack formation on top of propagating reverse faults of the Chuculay Fault System northern Chile: insights from field data and numerical modeling. Journal of Structural Geology 30: 791–808.

González, G., Salazar, P., Loveless, J.P., Allmendinger, R.W., Aron, F., Shrivastava, M. (2015). Upper plate reverse fault reactivation and the unclamping of the megathrust during the 2014 northern Chile earthquake sequence. Geology G36703.1.

Grant, L. (2002). Paleoseismology. In International Handbook of Earthquake and Engineering Seismology, (Lee, W.H.K., Kanamori, H., Jennings, P., Kisslinger, C. Eds.). Academic Press: Vol. 81A (30) 475-489. London.

Gutscher, M., Spakman, W., Bijwaard, H., Engdahl, E. (2000). Geodynamics of flat subduction: seismicity and tomographic constraints from the Andean margin. Tectonics 19: 814–833.

Haberland, C., Rietbrock, A., Lange, D., Bataille, K., Hofmann, S. (2006). Interaction between forearc and oceanic plate at the south-central Chilean margin as seen in local seismic data. Geophys. Res. Lett. 33: 1–5.

Hamilton, S., Shennan, I. (2005). Late Holocene great earthquakes and relative sea-level change at Kenai, southern Alaska. Journal of Quaternary Science, 20(2), 95–111.

Hampel, A., Kukowski, N., Bialas, J. (2004). Ridge subduction at an erosive margin: the collision zone of the Nazca Ridge in southern Peru. J. Geophys. Res. (109, B02101.

Hancock, P. (1988). Neotectonics. Geology Today 4: 57-61.

Hancock, P.L., Williams, G.D. (1986). Neotectonics. Journal of the Geological Society 143 (2): 325-326.

Hanks, T.C., Bakun, W.H. (2008). M-logA Observations for Recent Large Earthquakes. Bulletin of the Seismological Society of America 98: 490-494.

Hanks, T.C., Kanamori, H. (1979). A Moment Magnitude Scale. Journal of Geophysical Research 84: 2348-2350.

Hardebeck, J. L. (2012). Coseismic and postseismic stress rotations due to great subduction zone earthquakes. Geophys. Res. Lett., 39, L21313.

Hayes, G. P., Wald, D. J., Johnson, R. L. (2012). Slab1.0: A three-dimensional model of global subduction zone geometries. J. Geophys. Res., 117, B01302.

Hervé, F., Araya, E., Fuenzalida, J.L., Solano, A. (1979). Edades radiométricas y tectónica neógena en el sector costero de Chiloé continental, X Región. In II Congreso Geológico Chileno 1: FI-F8.

Hervé, M. (1976). Estudio geológico de la falla Liquiñe-Reloncaví en el área de Liquiñe, antecedentes de un movimiento transcurrente (Provincia de Valdivia). In I Congreso Geológico Chileno l: B39-B56.

Hervé, M. (1987). Movimiento normal de la falla Paposo, Zona de Falla de Atacama, en el Mioceno, Chile. Revista Geológica de Chile 31: 31-36.

Hoffmann-Rothe, A., Kukowski, N., Dresen, G., Echtler, H., Oncken, O., Klotz, J., Scheuber, E., Kellner, A. (2006). Oblique convergence along the Chilean margin:

partitioning, margin-parallel faulting and force interaction at the plate interface. In: The Andes – Active Subduction Orogeny. Frontiers in Earth Science Series Part II (Oncken, O., Chong, G., Franz, G., Giese, P., Götze, H-J., Ramos, V.A., Strecker, M.R., Wigger, P. Eds.). Springer-Verlag: (6), 125–146. Berlin.

Hoke, G.D. (2006). The influence of climate and tectonics on the geomorphology of the western slope of the Central Andes, Chile and Peru. PhD Thesis (Unpublished), Cornell University: 283.

Hyndman, R. D., Wang, K. (1993). Thermal constraints on the zone of major thrust earthquake failure: The Cascadia Subduction Zone. J. Geophys. Res. 98, 2039–2060.

Isacks, B., Barazangi, M. (1977). Geometry of Benioff zones: lateral segmentation and downwards bending of the subducted lithosphere. In Island Arcs, Deep Sea Trenches and Back Arc Basins (Talwani M., Pitman W., Eds.). American Geophysical Union, Ewing Series (1): 99–114. Washington.

Isacks, B.L.. (1988). Uplift of the central Andean plateau and bending of the Bolivian orocline. J. Geophys. Res. 93 (B4): 3211–3231.

Iturrieta, P.C., Hurtado, D.E., Cembrano, J., Stanton-Yonge, A. (2017). States of stress and slip partitioning in a continental scale strike-slip duplex: Tectonic and magmatic implications by means of finite element modeling. Earth and Planetary Science Letters, 473: 71–82.

Jarrard, R.D. (1986). Relations among subduction parameters. Rev. Geophys. (24 (2): 217–284.

Jordan, T. E., Burns, W. M., Veiga, R., Pangaro, F., Copeland, P., Kelley, S., Mpodozis, C. (2001). Extension and basin formation in the southern Andes caused by increases convergence rate: a Mid-Cenozoic trigger for the Andes. Tectonics 20: 308–324.

Jordan, T. E., Isacks, B. L. Ramos, V. & Allmendinger, R. W. (1983b. Mountain building in the Central Andes. Episodes 3: 20–26.

Jordan, T. E., Isacks, B. L., Allmendinger, R. W., Brewer, J.A., Ramos, V.A., Ando, C.J. (1983a. Andean tectonics related to geometry of subducted Nazca plate. GSA Bulletin 94: 341-361.

Jordan, T.E., Kirk-Lawlor, N., Blanco, N., Nester, P., Rech, J. (2014, Landscape modification in response to repeated onset of hyperarid paleoclimate states since 14 Ma, Atacama Desert, Chile. Geological Society of America Bulletin 126: B30978-B30971.

Kagan, Y. (2002). Seismic moment distribution revisited: I. Statistical results. Geophys. J. Int. (148: 520–541.

Kagan, Y.Y. (1993). Statistics of characteristic earthquakes. Bull. Seism. Soc. Am., 83, 7–24.

Kilb, D., Gomberg, J., Bodin, P. (2000). Triggering of earthquake aftershocks by dynamic stresses. Nature 408, 570–574.

King, G.C.P., Stein, R.S., Lin, J. (1994). Static stress changes and the triggering of earthquakes. Bull. Seismol. Soc. Am., 84(3), 935–953.

Kley, J., Monaldi, C.R., Salfity, J.A. (1999). Along-strike segmentation of the Andean foreland: causes and consequences. Tectonophysics 301: 75–94.

Kober, F., Ivy-Ochs, S., Schlunegger, F., Baur, H., Kubik, P.W., Wieler, R. (2007). Denudation rates and a topography-driven rainfall threshold in northern Chile: Multiple cosmogenic nuclide data and sediment yield budgets: Geomorphology 83: 97–120.

Lamb, S. (2011). Did shortening in thick crust cause rapid Late Cenozoic uplift in the northern Bolivian Andes? J. Geol. Soc. (168 (5): 1079–1092.

Lamb, S. (2016). Cenozoic uplift of the Central Andes in northern Chile and Bolivia—reconciling paleoaltimetry with the geological evolution. Canadian Journal of Earth Sciences 53: 1227-1245.

Lamb, S., Davis, P. (2003). Cenozoic climate change as a possible cause for the rise of the Andes. Nature 425: 792–797.

Lange, D., Cembrano, J., Rietbrock, A., Haberland, C., Dahm, T., Bataille, K. 2008). First seismic record for intra-arc strike-slip tectonics along the Liquiñe-Ofqui fault zone at the obliquely convergent plate margin of the southern Andes. Tectonophysics 455: 14–24.

Lara, L., Lavenu, A., Cembrano, J., Rodriguez, C. (2006). Structural controls of volcanism in transversal chains: resheared faults and neotectonics in the Cordón Caulle–Puyehue area (40.5°S), Southern Andes. J. Volcanol. Geotherm. Res. (158: 70–86.

Lara, L., Naranjo, J., Moreno, H. (2004). Rhyodacitic fissure eruption in Southern Andes (Cordón Caulle, 40.5°S) after the 1960 (Mw: 9.5) Chilean earthquake: a structural interpretation. J. Volcanol. Geotherm. Res. (138: 127–138.

Lavenu, A. (2005). Fallas Cuaternarias de Chile. Servicio Nacional de Geología y Minería, Boletín N° 62: 71p.

Lavenu, A. Cembrano, J.. (1999). Compressional and transpressional-stress pattern for Pliocene and quaternary brittle deformation in fore arc and intra-arc zones (Andes of central and southern Chile). J. Struct. Geol. (21: 1669–1691.

Lavenu, A., Thiele, R., Machette, M., Dart, R., Bradley, L.-A., Haller, K. (2000). Maps and database of quaternary faults in Bolivia and Chile. USGS Open File Report 00-283: 46p.

Legrand, D., DeLouis, B., Dorbath, L., David, C., Campos, J., Marquez, L., Thompson, J., Comte, D. (2007). Source parameters of the Mw = 6.3 Aroma crustal earthquake

of July 24, 2001 (northern Chile), and its aftershock sequence. Journal of South American Earth Sciences 24: 58–68.

Legrand, D., S. Barrientos, K. Bataille, J. Cembrano, J. (2011). The fluid-driven tectonic swarm of Fjordo Aysén, Chile. (2007) associated with two earthquakes (Mw=6.1 and Mw=6.2) within the Liquiñe-Ofqui Fault Zone, Continental Shelf Research 31: 154-161.

Leyton, F., Ruiz, S., Sepúlveda, S. (2010). Reevaluación del peligro sísmico probabilístico en Chile Central. Andean Geology 37 (2): 455-472.

Li, Y-G., De Pascale, G., Quigley, M., Gravley, D. (2014). Fault damage zones of the M7.1 Darfield and M6.3 Christchurch earthquakes characterized by fault-zone trapped waves. Tectonophysics 618: 79–101

Lin, J., Stein, R.S. (2004). Stress triggering in thrust and subduction earthquakes and stress interaction between the southern San Andreas and nearby thrust and strike-slip faults. J. Geophys. Res., 109, B02303.

Lindquist, K.G., Engle, K., Stahlke, D., Price, E. (2004). Global topography and bathymetry grid improves research efforts. EOS 85 (19),186.

Lindsay, D., Zentilli, M., Rivera, A. (1995). Evolution of an active ductile to brittle shear system controlling mineralization at Chuquicamata porphyry copper deposit, northern Chile, International Geology Review 37: 945–958.

Lockner, D.A., Beeler, N.M. (2002). Rock Failure and Earthquakes. In International Handbook of Earthquake and Engineering Seismology, (Lee, W.H.K., Kanamori, H., Jennings, P., Kisslinger, C. Eds.). Academic Press Vol. 81A (32): 505-538. London.

Lodolo, E., Menichetti, M., Bartole, R., Ben-Avraham, Z., Tassone, A., Lippai, H. (2003). Magallanes-Fagnano continental transform fault (Tierra del Fuego, southernmost South America). Tectonics 22 (6).

Lodolo, E., Menichetti, M., Tassone, A., Geletti, R., Sterzai, P., Lippai, H., Hormaechea, H.L. (2002). Researchers target a continental transform fault in Tierra del Fuego. Eos Trans. AGU, 83, 5 - 61.

Lomnitz, C. (1960). A study of the Maipo Valley earthquakes of September 4, 1958. Instituto de Geofísica y Sismología, Universidad de Chile, Publication N° 10.

Lomnitz, C. (1970). Major earthquakes and tsunamis in Chile during the period 1535 to 1955. Geologische Rundschau. 59: 938-960.

Lomnitz, C. (2004). Major earthquakes of Chile: A historical survey, 1535–1960. Seismology Research Letters 75: 368–378.

Loveless, J.P., Allmendinger, R.W., Hoke, G.D., González, G., Isacks, B.L., Carrizo, D.A. (2005). Pervasive cracking of the northern Chilean Coastal Cordillera: New evidence for forearc extension. Geology, 33(12), 973 – 976.

Loveless, J.P., Allmendinger, R.W., Pritchard, M.E., González, G. (2010). Normal and reverse faulting driven by the subduction zone earthquake cycle in the northern Chilean fore arc: Tectonics, 29, TC2001.

Loveless, J.P., Hoke, G.D., Allmendinger, R.W., Pritchard, M.E., Garroway, J.L., González, G. (2009). Surface cracks record long-term seismic segmentation of the Andean margin. Geology, 37 (1), 23 – 26.

Machare, J., Fenton, C., Machette, M.N., Levenu, A., Costa, C., Dart, R. (2003, Database and map of Quaternary faults and folds in Peru and its offshore region, U.S. Geological Survey Open File Report 03-451. International Lithosphere Program's Task Group II-2 "World Map of Major Active Faults." accompanied by database http://pubs.usgs.gov/of/2000/ofr-03-451/.

Machare, J., Ortlieb, L. (1992). Plio–Quaternary vertical motions and the subduction of the Nazca Ridge, central coast of Peru. Tectonophysics 205 (1–3): 97–108.

Machette, M. (2000). Active, Capable and Potentially Active Faults- A paleoseismic perspective. Journal of Geodynamics 29: 387-392.

Maksymowicz, A., Trhu, A. M., Contreras-Reyes, E., Ruiz, S. (2015). Density depth model of the continental wedge at the maximum slip segment of the Maule Mw 8.8 megathrust earthquake. Earth and Planetary Science Letters, 409, 265 – 277.

Marquardt C., Lavenu, A., Ortlieb, L., Godoy, E., Comte, D. (2004). Coastal Neotectonics in Southern Central Andes: Uplift Rates and Strain Patterns in the Caldera Area, Northern Chile (27ºS). Tectonophysics 394 (3-4): 193-219.

Marquardt, C. (2005). Deformations Néogènes le long de la Côte Nord du Chile (23°–27°S), avant-arc des Andes Centrales. PhD Thesis (Unpublished), Universite Toulouse III Paul Sabatier: 212 p.

Marquardt, C., Lavenu, A., Ortlieb, L. (2000). Tectónica compresiva Neógena en el dominio costero del área de Caldera y Mejillones. In Congreso Geológico Chileno, No. 9, 2: 583-587. Puerto Varas.

Masana, E., Santanach, P., Pallás, R., Calvet, J., Chong, G. (2005). Active tectonics and kinematics of the Chomache fault (Salar Grande, northern Chile). In 6th International Symposium on Andean Geodynamics ISAG: 493-496. Barcelona.

Matmon, A., Simhai, O., Amit, R., Haviv, I., Porat, N., Mc-Donald, E., Benedetti, L., Finkel, R. (2009, Desert pavement–coated surfaces in extreme deserts present the longest-lived landforms on Earth. Geological Society of America Bulletin 121: 688–697.

McCalpin, J. (2009). Paleoseismology (Second Edition). Academic Press (Elsevier): 613 p. Burlington, Massachusetts.

McQuarrie, N., Horton, B.K., Zandt, G., Beck, S., DeCelles, P.G. (2005). Lithospheric evolution of the Andean fold-thrust belt, Bolivia, and the origin of the central Andean plateau. Tectonophysics 399 (1–4): 15–37.

Melnick, D., Bookhagen, B., Strecker, M.R., Echtler, H.P. (2009). Segmentation of megathrust rupture zones from forearc deformation patterns over hundreds to millions of years, Arauco peninsula, Chile. J. Geophys. Res. (114: B01407.

Melnick, D., Folguera, A., Ramos, V. (2006). Structural control on arc volcanism: The Caviahue–Copahue complex, Central to Patagonian Andes transition (38°S). J. S. Am. Earth Sci. (22: 66–88.

Mercier, J. (1976). La néotectonique: Ses méthodes et ses buts. Revue Geographie Physique et Geologie Dynámique 18 (2): 323-346.

Metcalf, K., Kapp, P. (2015, Along-strike variations in crustal seismicity and modern lithospheric structure of the central Andean forearc. In Geodynamics of a Cordilleran Orogenic System: The Central Andes of Argentina and Northern Chile (DeCelles, P.G., Ducea, M.N., Carrapa, B., Kapp, P.A., Eds.). Geological Society of America Memoir: (212) 61–78.

Miyakawa, A., Otsubo, M. (2015). Effect of a change in the state of stress on the likelihood of inland fault failure during the Mw 6.6 Iwaki earthquake resulting from the Mw 9.0 2011 Tohoku earthquake, Japan. Tectonophysics, 661, 112.

Mora, C., Comte, D., Russo, R., Gallego, A. & Mocanu, V. (2010). Aysén seismic swarm (January 2007) in southern Chile: analysis using joint hypocentral determination. J. Seismol. (14 (4): 683–691.

Moreno, H., Parada, M.A. (1976). Esquema geológico de la Cordillera de los Andes entre los paralelos 39° y 41°30'S. In I Congreso Geológico Chileno: 213–A226. Santiago.

Mörner, N. (1994). Neotectonics in new perspectives. Bulletin INQUA Neotectonics Commission 18: 63-65.

Mpodozis, C., Cornejo, P. (2012). Cenozoic Tectonics and Porphyry Copper Systems of the Chilean Andes. Society of Economic Geologists, Inc. Special Publication 16: 329–360.

Mpodozis, C., Ramos, V.A. (1989). The Andes of Chile and Argentina. In Geology of the Andes and its Relation to Hydrocarbon and Mineral Resources (Ericksen, G.E., Cañas, M.T., Reinemud, J.A. Eds). Circumpacific Council for Energy and Mineral Resources. Earth Sciences Series 11: 59–90. Houston, Texas.

Mpodozis, C., Ramos, V.A. (2008). Tectónica jurásica en Argentina y Chile: extensión, subducción oblicua, rifting, deriva y colisiones? Revista de la Asociación Geológica Argentina 63: 481–497.

Müller, R.D., Landgrebe, T.C.W. (2012). The link between giant earthquakes and the subduction of oceanic fracture zones. J. Geophys. Res., Solid Earth3, 447–465.

Müller, R.D., Roest, W.R.: Royer, J.Y., Gahagan, L.M., Sclater, J.G. (1997). Digital isochrons of the world's ocean floor. J. Geophys. Res. (102(B2): 3211–3214.

Muñoz, J., Stern, C.R.R. (1988). The quaternary volcanic belt of the southern continental margin of South America: transverse structural and petrochemical variations across the segment between 38°S and 39°S. J. S. Am. Earth. Sci. (1: 147–161.

Muñoz, N., R. Charrier. (1996). Uplift of the western border of the Altiplano on a west-vergent thrust system, Northern Chile, J. South Amer. Earth Sci. 9: 171–181.

Naranjo, J.A. (1987). Interpretación de la actividad cenozoica superior a lo largo de la Zona de Falla Atacama, Norte de Chile. Revista Geológica de Chile 31: 43-55.

Nelson, A. R., Manley, W. F. (1992). Holocene coseismic and aseismic uplift of Isla Mocha, south-central Chile. In Impacts of Tectonics on Quaternary Coastal Evolution (Y. Ota, A. R. Nelson, and K. Berryman, Eds.), Quat. Int., vol. (15/16, pp. 61–76.

Nelson, A. R., Shennan, I., Long, A. J. (1996). Identifying coseismic subsidence in tidal wetland stratigraphic sequences at the Cascadia subduction zone of western North America. J. Geophys. Res. (101(B3), 6115–6135.

Nelson, A.R. (1992). Lithofacies analysis of colluvial sediments -- An aid in interpreting the recent history of quaternary normal faults in the Basin and Range Province, Western United States. Journal of Sedimentary Petrology. 62 (4): 607-621.

Nettles, M., Ekström, G., Koss, H.C. (2011). Centroid-moment-tensor analysis of the 2011 off the Pacific coast of Tohoku earthquake and its larger foreshocks and aftershocks. Earth Planets Space, 63(7), 519–523.

New, M., Lister, D., Hulme, M., Makin, I. (2002). A high-resolution data set of surface climate over global land areas. Climate Res. (21, 1–25.

Okada, A. (1971). On the neotectonics of the Atacama Fault Zone region. Preliminary notes on late Cenozoic faulting and geomorphic development of Coast Range of northern Chile. Bulletin of the Department of Geography Kyoto University 3: 47-65.

Órdenes, T. (2002). Petrología de los Intrusivos de la Cordillera entre las Coordenadas 23°08'-23°17'S y 70°15'-70°22'O, Región de Antofagasta, Chile. Memoria de Título (Inédito), Departamento de Ciencias Geológicas, Universidad Católica del Norte: 117 p.

Ostenaa, D.A. (1984). Relationships affecting estimates of surface fault displacements based on scarp-derived colluvial deposits. Geol. Soc. Am., Abtsr. Prog. (16 (5), 327.

Pankhurst, R., Hervé, F. (2007). Introduction and overview Earthquakes in Chile. In The Geology of Chile (Moreno, T., Gibbons, W. Eds.). Geological Society: 263-287. London.

Pankhurst, R., Hervé, F., Rojas, L., Cembrano, J. (1992). Magmatism and tectonics in continental Chiloe´, Chile (42° and 42°30'S). Tectonophysics 205: 283–294.

Pardo, M., Comte, D., Monfret, T. (2002). Seismotectonic and stress distribution in the central Chile subduction zone. Journal of South American Earth Sciences 15: 11-22.

Paris, G., Machette, M.N., Dart, R.L., Haller, K.M. (2000, Database and map of Quaternary faults and folds in Colombia and its offshore region, U.S. Geological Survey Open File Report 00-0284. PDF file of map of Quaternary faults and folds in Columbia prepared as part of the World Map of Major Active Faults with locations, ages, and activity rates of major earthquake-related features accompanied by database of description and activity: http://pubs.usgs.gov/of/2000/ofr-00-0284./

Pavlides, S. (1989). Looking for a definition of Neotectonics. Terra Nova 1: 233-235.

Pelayo, A., Wiens, D. (1989). Seismotectonics and relative plate motions in the Scotia sea region. J. Geophys. Res. 94: 7293–7320

Pérez, A., Ruiz, J.A., Vargas, G., Rauld, R., Rebolledo, S., Campos J. (2014, Improving seismotectonics and seismic hazard assessment along the San Ramon Fault at the eastern border of Santiago city, Chile. Natural Hazards 71: 243-274.

Pérez-Flores, P., Cembrano, J., Sánchez-Alfaro, P., Veloso, E., Arancibia, G., Roquer, T. (2016). Tectonics, magmatism and paleo-fluid distribution in a strike-slip setting: Insights from the northern termination of the Liquiñe Ofqui Fault System, Chile. Tectonophysics 680: 192–210.

Proyecto Multinacional Andino (PMA): Geociencia para las Comunidades Andinas. (2009). Atlas de deformaciones cuaternarias de los Andes. Servicio Nacional de Geología y Minería, Publicación Geológica Multinacional No. 7: 320 p., 1 mapa en CD. Santiago.

Radic, J.P. (2010). Las cuencas cenozoicas y su control en el volcanismo de los Complejos Nevados de Chillán y Copahue–Callaqui (Andes del Sur, 36–39 ° S). Andean Geol. 37: 220–246.

Ramos, V.A. (2009a. The tectonic regime along the Andes: Present-day and Mesozoic regimes. Geological Journal 45 (1): 2-25.

Ramos, V.A. (2009b. Anatomy and global context of the Andes: Main geologic features and the Andean orogenic cycle. In Backbone of the Americas: Shallow Subduction, Plateau Uplift, and Ridge and Terrane Collision (Kay, S.M., Ramos, V.A., Dickinson, W.R., Eds.). Geological Society of America Memoir 204: 31–65.

Rauld, R. (2002). Análisis morfoestructural del frente cordillerano de Santiago oriente, entre el río Mapocho y la quebrada de Macul. Memoria de Título (Inédito), Universidad de Chile: 57 p.

Rauld, R. (2011). Deformación cortical y peligro sísmico asociado a la Falla San Ramón en el frente cordillerano de Santiago, Chile central (33ºS). Tesis de PhD (Inédito), Universidad de Chile, Departamento de Geología: 311 p.

Rehak, K., Strecker, M., Echtler, H. (2008). Morphotectonic segmentation of an active forearc, 37°-41°S, Chile. Geomorphology 94 (1-2): 98—116.

Reutter, K.-J., Scheuber, E., Chong, G. (1996). The Precordilleran fault system of Chuquicamata, Northern Chile: evidence for reversals along arc parallel strike-slip faults. Tectonophysics 259: 213–228.

Reutter, K.-J., Scheuber, E., Helmcke, D. (1991). Structural evidence of orogen-parallel strike slip displacements in the Precordillera of northern Chile. Geologische Rundschau 80: 135–153.

Riquelme, R., Hérail, G., Martinod, J., Charrier, R., Darrozes, J. (2007). Late Cenozoic geomorphologic signal of Andean forearc deformation and tilting associated with the uplift and climate changes of the Southern Atacama Desert (26°S–28°S). Geomorphology 86, 283–306.

Riquelme, R., Martinod, J., Hérail, G., Darrozes, J., Charrier, R. (2003). A geomorphological approach to determining the Neogene to Recent tectonic deformation in the Coastal Cordillera of northern Chile (Atacama). Tectonophysics 361: 255–275.

Rosenau, M. (2004). Tectonic and geomorphic evolution of the southern Andean intra-arc zone between latitudes 38° and 42°S. PhD Thesis (Unpublished), Freie Universität: 156 p.

Rosenau, M., Melnick, D., Echtler, H. (2006). Kinematic constraints on intra-arc shear and strain partitioning in the Southern Andes between 38°S and 42°S latitude. Tectonics 25: (TC4013).

Ruiz, J.A., Hayes, G.P., Carrizo, D., Kanamori, H., Socquet, A., Comte, D. (2014 Seismological analyses of the 2010 March 11, Pichilemu, Chile Mw 7.0 and Mw 6.9 coastal intraplate earthquakes. Geophysical Journal International 197: 414–434.

Ryder, I., Rietbrock, A., Kelson, K., Bürgmann, R., Floyd, M., Socquet, A., Vigny, C., Carrizo, D. 2012). Large extensional aftershocks in the continental forearc triggered by the 2010 Maule earthquake, Chile. Geophysical Journal International 188: 879–890.

Salazar, P. (2011). The upper crustal microseismicity image from the north Chilean subduction zone: implication for tectonics and fluid migration. PhD Thesis (Unpublished), Freie Universität, Berlin: 145 p.

Sánchez, P., Pérez-Flores, P., Arancibia, G., Cembrano, J., Reich, M. (2013). Crustal deformation effects on the chemical evolution of geothermal systems: the intra-arc Liquiñe–Ofqui Fault System, Southern Andes. Int. Geol. Rev.: 37–41.

Scheuber, E., Andriessen, A. M. (1990). The kinematics and geodynamic significance of the Atacama Fault Zone, northern Chile. Journal of Structural Geology 12 (2): 243-257.

Scheuber, E., González, G. (1999). Tectonics of the Jurassic–Early Cretaceous magmatic arc of the north Chilean Coastal Cordillera (228–268S): a story of crustal deformation along a convergent plate boundary. Tectonics 18: 895– 910.

Scholz, C. H. (1998). Earthquakes and friction laws. Nature 391 (6662), 37.

Scholz, C. H., Campos, J. (2012). The seismic coupling of subduction zones revisited. J. Geophys. Res., 117, B05310.

Scholz, C.H. (1980). The Mechanics of Earthquakes and Faulting. Cambridge University Press.Cambridge, UK.

Scholz, C.H. (1988). The brittle-plastic transition and the depth of seismic faulting. Geol. Rundschau 77: 319-328.

Schwartz, D. P., & Coppersmith, K. J. (1984). Fault behavior and characteristic earthquakes - examples form the Wasatch and San18 Andreas fault zones. Journal of Geophysical Research, 89(NB7), pp. 5681–5698.

Schwartz, D. P., Coppersmith, K. J. (1984). Fault behavior and characteristic earthquakes—Examples from the Wasatch and San Andreas fault zones. J. Geophys. Res. 89, 5681–5698.

Schwartz, D.P., Coppersmith, K.J. (1986). Seismic hazard: new trends in analysis using geologic data. In: Active Tectonics, Studies in Geophysics (Wallace, R.E. Ed.). National Academy Press: 215–230. Washington, D.C.

Seeber, L., Armbruster, J.G. (2000). Earthquakes as beacons of stress change. Nature 407, 69–72.

Sepúlveda, S., Astroza, M., Kausel, E., Campos, J., Casas, E., Rebolledo, S., Verdugo, R. (2008). Newfindings on the 1958 Las Melosas earthquake sequence, Central Chile: implications for seismic hazard related to shallow crustal earthquake in subduction zones. J. Earthquake Eng. (12, 432–455.

SERNAGEOMIN. (2003). Mapa Geológico de Chile: versión digital. Servicio Nacional de Geología y Minería, Publicación Geológica Digital, No. 4 (CD-ROM, versión1.0. (2003). Santiago.

Shimazaki, K., Nakata, T. (1980). Time-predictable recurrence model for large earthquakes. Geophys. Res. Lett. 7, 279–282.

Shrivastava, M., González, G., Moreno, M., Soto, H., Schurr, B., Salazar, P., Báez, J.C. (2019). Earthquake segmentation in northern Chile correlates with curved plate geometry. Scientific Reports 9, Article number: 4403.

Sibson, R.H. (1984). Roughness at the base of the seismogenic zone: contributing factors. J. Geophys. Res. 89, 5791-5799.

Sibson, R.H. (1992). Implications of fault-valve behaviour for rupture nucleation and recurrence. Tectonophysics 211, 283-293.

Sibson, R.H. (1994). Crustal stress, faulting, and fluid flow. In: "Geofluids: Origin, Migration and Evolution of Fluids in Sedimentary Basins" (J. Parnell, Ed.), Geol. Soc. Land. Spec. Publ. 78, 69-84.

Sibson, R.H. (2002). Geology of the Crustal Earthquake Source. In International Handbook of Earthquake and Engineering Seismology, (Lee, W.H.K., Kanamori, H., Jennings, P., Kisslinger, C. Eds.). Academic Press Vol. 81A (29): 455-473. London.

Sielfeld, G., Lange, D., Cembrano, J. (2017). Intra-arc Seismicity: Geometry and Kinematic Constraints of Active Faulting along Northern Liquiñe-Ofqui and Andean Transverse Fault Systems [38º and 40ºS, Southern Andes]. AGU 2017, New Orleans.

Silva, N. (2008). Caracterización y Determinación del Peligro Sísmico en la Región Metropolitana. Memoria de Título (Inédito), Universidad de Chile, Departamento de Ingeniería Civil: 148p.

Slemmons, D. B. (1977). State-of-the-Art for Assessing Earthquake Hazards in the US. Rep. No. 6, Misc. Pap. S-73-1. U.S. Army Corps of Engineers, Waterways Experiment Station, Vicksburg, MS.

Slemmons, D.B. (1995). Complications in making paleoseismic evaluations in the Basin and Range province, western United States. In Perspectives in Paleoseismology (Serva, L., Slemmons, D. B., Eds.). Assoc. Eng. Geol. Spec. Publ.: (6) 19–34.

Slemmons, D.B., DePolo, C. M. (1986). Evaluation of active faulting and related hazards. In: Active Tectonics, Studies in Geophysics (Wallace, R.E. Ed.). National Academic Press: 45–62. Washington, DC.

Smalley, R.Jr., Kendrick, E., Bevis, M., Dalziel, I., Taylor, F., Lauria, E., Barriga, R., Casassa, G., Olivero, E., Piana, E. (2003). Geodetic determination of relative plate motion and crustal deformation across the Scotia-South America plate boundary in eastern Tierra del Fuego. Geochem Geophy. Geosyst. 4 (9): 1-19.

Smith, R.B., Bruhn, R.L. (1984). Intraplate extensional tectonics of the eastern Basin-Range: inferences on structural style from seismic reflection data, regional tectonics, and thermo- mechanical models of brittle-ductile deformation. J. Geophys. Res. 89, 5733-5762.

Sobolev, S.V., Babeyko, A.Y. (2005). What drives orogeny in the Andes? Geology 33 (8): 617–620.

South America Risk Assessment (SARA) Project. (2016). Research Topic 2 (RT2): Building a harmonised database of 'hazardous' crustal faults. https://sara.openquake.org/hazard_rt2.

Sparkes, R., Tilmann, F., Hovius, N., Hillier, J. (2010). Subducted seafloor relief stops rupture in South American great earthquakes: implications for rupture behavior in the 2010 Maule, Chile earthquake. Earth Planet. Sci. Lett. (298 (1–2), 89–94.

Stanton-Yonge, A., Griffith, W.A., Cembrano, J., St. Julien, R., Iturrieta, P. 2016). Tectonic role of margin-parallel and margin-transverse faults during oblique subduction in the Southern Volcanic Zone of the Andes: Insights from Boundary Element Modeling. Tectonics 35: 1990–2013.

Stein, C.A. (2003). Heat flow and flexure at subduction zones. Geophys. Res. Lett. 30, 23.

Stein, R. S., King, G. C., Rundle, J. B. (1988). The growth of geological structures by repeated earthquakes: 2 Field examples of continental dip-slip faults. J. Geophys. Res. 93, 13319–13331.

Stein, R.S. (1999). The role of stress transfer in earthquake occurrence. Nature, 402(6762), 605–609.

Stein, R.S., King, G.C.P., Lin, J. (1994). Stress triggering of the 1994 M= 6.7 Northridge, California, earthquake by its predecessors. Science, 265(5177), 1432–1435.

Stewart, I.S., Hancock, P.L. (1994). Neotectonics. In Continental deformation, Hancock, P.L., Pergamon Press: 370–409. New York.

Stirling, M., Goded, T., Berryman, K., Litchfield, N. (2013). Selection of Earthquake Scaling Relationships for Seismic-Hazard Analysis. Bulletin of the Seismological Society of America 103 (6): 2993-3011.

Suarez, G., Comte, D. (1993). Comment on "Seismic coupling along the Chilean Subduction Zone" by B. W. Tichelaar and L. R. Ruff. J. Geophys. Res., 98 (B9): 15825–15828.

Tardani, D., Reich, M., Roulleau, E., Takahata, N., Sano, Y., Peréz-Flores, P., Sánchez, P., Cembrano, J., Arancibia, G. (2016). Exploring the structural controls on helium, nitrogen and carbon isotope signatures in hydrothermal fluids along an intra-arc fault system. Geochimica et Cosmochimica Acta 184:193-211

Tassara, A., Swain, C., Hackney, R., Kirby, J. (2007). Elastic thickness structure of South America estimated using wavelets and satellite-derived gravity data. Earth and Planetary Science Letters 253: 17–36.

Tassara, A., Yáñez, G. (1996). Thermomechanic segmentation of the Andes (158–508S): a flexural analysis approach. In 3rd International Symposium on Andean Geodynamics ISAG: 115– 118. St. Malo, France.

Tassara, A., Yáñez, G. (2003). Relación entre el espesor elástico de la litosfera y la segmentación tectónica del margen andino (15–47°S). Revista Geológica de Chile 30 (2): 159–186.

Telford, W. M., Geldart, L. P., & Sheriff, R. E. (1990). Applied Geophysics. Cambridge University Press, UK.

Thatcher, W. (1986). Cyclic deformation related to great earthquakes at plate boundaries. In Recent Crustal Movements of the Pacific Region (W. I. Reilly, and B. E. Harford, Eds.), Bull. R. Soc. N. Z., vol. (24, pp. (245–272.

Thomas, T., Livermore, R.A., Pollitz, F. (2003). Motion of the Scotia Sea plates. Geophys. J. Int. (155: 789–804.

Thomson, S. N. (2002). Late Cenozoic geomorphic and tectonic evolution of the Patagonian Andes between latitudes 42° and 46°S: An appraisal based on fission-track results from the transpressional intra-arc Liquine-Ofqui fault zone. Geol. Soc. Am. Bull. (114 (9): 1159–1173.

Tibaldi, A., Lagmay, A.M.F.A., Ponomareva, V.V. (2005). Effects of basement structural and stratigraphic heritages on volcano behaviour and implications for human activities (The UNESCO/IUGS/IGCP project 455). Episodes 28: 158–170.

Tichelaar, B. W., Ruff, L. J. (1993). Depth of seismic coupling along subduction zones. J. Geophys. Res., 98 (B2): 2017–2037.

Toda, S.R., Lin, J., Stein, S. (2011a. Using the 2011 Mw 9.0 off the Pacific coast of Tohoku earthquake to test the Coulomb stress triggering hypothesis and to calculate faults brought closer to failure. Earth, Planets and Space, 63(7), 725–730.

Toda, S.R., Stein, S., Lin, J. (2011b. Widespread seismicity excitation throughout central Japan following the 2011M= 9.0 Tohoku earthquake and its interpretation by Coulomb stress transfer. Geophys. Res. Lett., 38, L00G03.

Tomlinson, A., Blanco, N. (1997a. Structural evolution and displacement history of the west fault system, Precordillera, Chile: Part 1, synmineral history. In VIII Congreso Geológico Chileno 3: 1883–1887. Antofagasta.

Tomlinson, A., Blanco, N. (1997b. Structural evolution and displacement history of the west fault system, Precordillera, Chile: Part 2, postmineral history. In VIII Congreso Geológico Chileno 3: 1878–1882. Antofagasta.

USGS. (2018a. ANSS (Advanced National Seismic System) Comprehensive Earthquake Catalog (ComCat) Documentation. https://earthquake.usgs.gov/earthquakes/search.

USGS. (2018b. Earthquake Glossary. Earthquake Hazards Program. http://earthquake.usgs.gov/learn/glossary/?term=active%20fault.

Uyeda, S., Kanamori, H. (1979). Back-arc opening and the mode of subduction. Journal Geophysical Research 84: 1049–1061.

Valdenegro, P., Muñoz, M., Yáñez, G., Parada, M.A., Morata, D. (2019). A model for thermal gradient and heat flow in central Chile: The role of thermal properties. Journal of South American Earth Sciences.

Vargas, G., C. Palacios, M. Reich, S. Luo, C. Shen, and G. González. (2011). U-series dating of co-seismic gypsum and submarine paleoseismology of active faults in Northern Chile (23ºS). Tectonophysics 497, 34-44.

Vargas, G., Klinger Y., Rockwell T., Forman S.L., Rebolledo S., Baize S., Lacassin R., Armijo R. (2014). Probing large intra-plate earthquakes at the west flank of the Andes. Geology 42: 1083–1086.

Vargas, G., Rebolledo, S., Sepúlveda, S.A., Lahsen, A., Thiele, R., Townley, B., Padilla, C., Rauld, R. Herrera, M.J., Lara, M. (2013). Submarine earthquake rupture, active faulting and volcanism along the major Liquiñe-Ofqui Fault Zone and implications for seismic hazard assessment in the Patagonian Andes. Andean Geology 40 (1): 141-171.

Villalobos-Claramunt, A., Vargas, G., Maksymowicz, A., Lastras, G. (2015). Evidencias paleosismológicas del origen cortical de la Crisis Sísmica del año 2007 en la región de Aysén. In XIV Congreso Geológico Chileno: 306-309. La Serena.

Vita-Finzi, C. (1987). Recent Earth Movements. Academic Press, 226 p. London.

Wallace, R.E. (panel chairman). (1986). Active Tectonics, Studies in Geophysics. National Academy Press. Washington, D.C.

Wallace, R.E. (1981). Active faults, paleoseismology and earthquake hazards in the Western United States. In Earthquake Prediction (Simpson, D., Richards, P., Eds). American Geophysical Union, M. Ewing Series: (4) 209–216.

Wang, K., Hu, Y., Bevis, M., Kendrick, E., Smalley Jr., R., Vargas, R.B., Lauria, E. (2007). Crustal motion in the zone of the 1960 Chile earthquake: Detangling earthquake-cycle deformation and forearc-sliver translation. Geochem. Geophys. Geosyst. 8 (10): 1-14.

Wells, C., Coppersmith, K. (1994). New empirical relationships among Magnitude, Rupture Length, Rupture Width, Rupture Area and Surface Displacement. Bulletin of the Seismological Society of America 84: 974–1002.

Wesnousky, S.G. (2008). Displacement and geometrical characteristics of earthquake surface ruptures: Issues and implications for seismic hazard analysis and the process of earthquake rupture. Bull. Seismol. Soc. Am. 98 (4) 1609–1632.

Yáñez, G., Cembrano, J. (2004). Role of viscous plate coupling in the late Tertiary Andean tectonics. J. Geophys. Res. (109 (B02407): 1-21.

Yáñez, G., Gana, P., Fernández, R. (1998). Origen y significado geológico de la Anomalía Melipilla, Chile central. Rev. Geol. Chile 25: 174–198.

Yáñez, G., Ranero, C., Von Huene, R., Diaz, J. (2001). Magnetic anomaly interpretation across the southern Central Andes (328–33.58S): the role of the Juan Fernandez ridge in the late Tertiary evolution of the margin. Journal of Geophysical Research 106: 6325–6345.

Yeats, R., Sieh, K., Allen, C. (1997). The Geology of Earthquakes. Oxford University Press: 568p. Oxford.

Yepes, H., Audin, L., Alvarado, A., Beauval, C., Aguilar, J., Font, Y., Cotton, F. (2016). A new view for the geodynamics of Ecuador: Implication in seismogenic source definition and seismic hazard assessment. Tectonics 35 (5): 1249–1279.